Karlsruher Institut für Technologie

Characterization of microtubule organizing center associated proteins in *Aspergillus nidulans*

Zur Erlangung des akademischen Grades eines

DOKTORS DER NATURWISSENSCHAFTEN

(Dr. rer. nat.)

Fakultät für Chemie und Biowissenschaften

Karlsruher Institut für Technologie (KIT) - Universitätsbereich

genehmigte

DISSERTATION

von

Ying Zhang

aus

Weifang, China

Dekan: Prof. Dr. Peter Roesky

Referent: Prof. Dr. Reinhard Fischer

Korreferent: Prof. Dr. Peter Nick

Tag der mündlichen Prüfung: 18.12.2015

Erklärung

Ich erkläre, dass ich die Doktorarbeit selbständig angefertigt und keine anderen als die angegebenen Quellen und Hilfsmittel benutzt sowie die wörtlich oder inhaltlich übernommenen Stellen als solche kenntlich gemacht und die Satzung des Karlsruher Institut für Technologie (KIT) zur Sicherung guter wissenschaftlicher Praxis in der jeweils gültigen Fassung beachtet hat.

Karlsruhe, den 3.11.2015

_____

Ying Zhang

Publikationsliste

Im Rahmen dieser Arbeit konnten folgende Publikationen angefertigt oder vorbereitet werden:

Zhang, Y., Teichert, I., Kück, U. & Fischer, R. (2015). Laser capture microdissection to identify septum-associated proteins in *Aspergillus nidulans*. *Mycologia*, in revision.

Zhang, Y., Schmid, M., Osmani, S. & Fischer, R. (2015). Functional analysis of a microtubule organizing center associated protein SPA18 and characterization of the different MTOCs in *Aspergillus nidulans.* In preparation.

Weitere Publikationen, die nicht direkt mit dem Thema dieser Arbeit verknüpft sind:

Cai M.*, Zhang Y.*, Hu W., Shen W., Yu Z., Zhou W., Jiang T., Zhou X. & Zhang Y. (2014). Genetically shaping morphology of the filamentous fungus *Aspergillus glaucus* for production of antitumor polyketide aspergiolide A. *Microb Cell Fact* **13**, 73-83.

Fang Z., Zhang Y., Cai M., Zhang J., Zhang Y. & Zhou X. (2012). Improved gene targeting frequency in marine-derived filamentous fungus *Aspergillus glaucus* by disrupting *ligD*. *J Appl Genet* **53**, 355-362.

Yu Z., Cai M., Hu W., Zhang Y., Zhou J., Zhou X. & Zhang Y. (2014). A cyclin-like protein, ClgA, regulates development in *Aspergillus nidulans*. *Res Microbiol* **165**, 462-467.

* Autoren haben in gleichem Maße zu der Arbeit beigetragen.

Contents

I Abbreviations

alcA(p)	Alcohol dehydrogenase promoter
BiFC	Bimolecular Flourescence Complementation
CBD	Calmodulin binding domain
CM1	Centrosomin Motif 1
gpd(p)	Glycerinaldehyde-3-phosphate-dehydrogenase promoter
IDP	Intrinsically disordered protein
LCM	Laser capture microdissection
MS	Mass spectrometry
MT	Microtubule
MTOC	Microtubule organizing center
NCP	Nuclear pore complex
NE	Nuclear envelope
PCM	Pericentriolar material
PTS	Peroxisomal Targeting Sequence
SIN	Septation initiation network
sMTOC	Septal microtubule organizing centre
SPA protein	Septal pore associated protein
SPB	Spindle pole body
γ-TuRC	γ-Tubulin ring complex
γ-TuSC	γ-Tubulin small complex
WT	Wild type

II Summary

Microtubule polymerization starts in fungal and animal cells from large multi-subunit protein complexes, the microtubule-organizing centers (MTOC). In *Aspergillus nidulans*, microtubule polymerization is initiated at septal MTOCs (sMTOC) and not only from nuclear spindle pole bodies (SPB). ApsB is a component of both sMTOC and SPB, and is important for nucleation of cytoplasmic MTs and astral MTs, as well as nuclear migration and conidiospore production. The N-terminal 523 aa are important for sporulation but not required for localization.

A novel MTOC associated protein SPA18 was characterized, which was first identified as a septal pore associated (SPA) protein. SPA18 directly binds to ApsB at SPBs and sMTOCs, forming an ApsB/SPA18 complex which is required for recruitment of γ-TuRCs. The ApsB/SPA18 complex is the sole anchor of γ-TuRC at septa. SPA18 is also crucial for cytoplasmic MTs nucleation, as well as the activity of sMTOCs and SPBs, whereas it is not required for astral MTs organization or nuclear migration. This is a big distinction from ApsB. Localization of SPA18 to different MTOCs does not depend on ApsB.

Three domains: Centrosomin motif 1 (CM1), MASC (Mto1 and Spc72p C-terminus) and SMB (sMTOC binding) were identified in ApsB. CM1 is responsible for recruitment of γ-TuRCs. SMB is required but not sufficient for ApsB targeting to septa. In this process, MASC is also needed and plays a more important role. Besides, MASC domain is also responsible for SPB localization. The localization of ApsB partially depends on SPA18, which plays a minor role.

Furthermore, ApsB and SPA18 are targeted to sMTOCs and SPBs by different anchors. Another SPA protein SPA10, which is a potential septation suppresser, is required for both ApsB and SPA18 targeting to septa. ApsB is targeted to the outer plaque of SPBs by SepK.

By BLASTP analysis with the known SPB associated proteins in *Saccharomyces cerevisiae* or *Schizosaccharomyces pombe*, potential SPB components of *A. nidulans* were identified or further characterized, such as PcpA, SepK, Cdc31, SfiA, MztA, Nud1, Ndc1 and Calmodulin. MztA (AN1361) is a very tiny but conserved compoment of γ-TuRC. PcpA is the γ-TuRC receptor at the inner plaque of SPB. SfiA (AN0704) and Cdc31 are essential for SPB duplication, localizing at SPBs but not to septa. All of these findings suggest only the outer plaque of SPB locates at the sMTOC.

In addition to homologous alignment, laser capture microdissection (LCM) combined

with mass spectrometry (MS) was performed to identify septum associated proteins. With the collected 3000 septa, we identified AlpA, which was visualized at the plus-end of the microtubules nucleated from sMTOCs. AlpA may also play other roles in sMTOC.

Peroxisomes are found to play a role in microtubule organization, whose absence will cause reduced activity of MTOCs and number of cytoplasmic MTs and astral MTs, as well as partially defective nuclear migration. However, it is still not clear whether these influences are direct or not.

II Zusammenfassung

Mikrotubuli-Polymerisation beginnt in Pilz- und Tierzellen an großen Proteinkomplexen, den Mikrotubuli-Organisationszentren (MTOC). In *Aspergillus nidulans* findet die Mikrotubuli-Polymerisation auch an septalen MTOCs (sMTOC) statt und nicht nur an nuklearen Spindelpolkörpern (SPB). ApsB ist eine Komponente von sowohl sMTOC als auch SPB und ist wichtig für die Bildung von zytoplasmatischen MTs und astralen MTs, sowie für die Kernwanderung und die Bildung von Konidiosporen. Die N-terminalen 523 aa sind wichtig für die Sporulation, sind aber nicht für die richtige Lokalisierung des Proteins erforderlich.

Ein weiteres Protein, das in dieser Arbeit untersucht wurde, ist das MTOC assoziierte Protein SPA18, das zuerst als ein Septum-Poren assoziiertes (SPA) Protein identifiziert wurde. SPA18 bindet an SPBs und sMTOCs direkt an ApsB, wodurch ein ApsB / SPA18 Komplex gebildet wird, der für die Rekrutierung von γ-TuRCs erforderlich ist. Der ApsB / SPA18 Komplex ist der einzige Anker der γ-TuRCs an Septen. SPA18 ist sowohl für die Bildung zytoplasmatischer MTs sowie für die Aktivität der sMTOCs und SPBs äußerst wichtig,, während es für die Organisation astraler MTs und die Zellkernwanderung nicht erforderlich ist. Dies ist ein großer Unterschied zu ApsB. Die Lokalisierung von SPA18 an unterschiedlichen MTOCs ist nicht von ApsB abhängen.

Drei Domänen: Centrosomin Motiv 1 (CM1), MASC (Mto1 and Spc72p C-Terminus) und SMB (sMTOC binding) wurden in ApsB identifiziert. CM1 ist für die Rekrutierung von γ-TuRCs verantwortlich. SMB ist für die Lokalisierung an den Septen erforderlich, aber nicht ausreichend. Hierfür wird zusätzlich die MASC-Domäne benötigt. Außerdem ist die MASC-Domäne für die Lokalisierung von ApsB am SPB verantwortlich. Zusätzlich ist die Lokalisierung von ApsB teilweise von SPA18 abhängig, das eine untergeordnete Rolle spielt.

Außerdem werden ApsB und SPA18 durch verschiedene Proteine an sMTOCs und SPBs verankert. Ein anderes SPA Protein, SPA10, ein möglicher Inhibitor der Septierung , ist sowohl für die Lokalisierung von ApsB als auch von SPA18 an Septen erforderlich. ApsB wird durch SepK zur äußeren Platte der SPBs geleitet.

Durch BLASTP-Analyse mit den bekannten SPB assoziierten Proteinen in *Saccharomyces cerevisiae* oder *Schizosaccharomyces pombe* wurden potentielle SPB Komponenten von *A. nidulans* identifiziert oder bereits bekannte genauer charakterisiert. Hierbei handelt es sich um PcpA, SepK, Cdc31, SfiA, MztA, Nud1, Ndc1 und Calmodulin.

MztA (AN1361) ist eine sehr kleine, aber konserviert Komponente von γ-TuRC. PcpA ist der γ-TuRC Rezeptor an der Innenseite der SPB. SfiA und Cdc31 sind essentiell für die SPB Vervielfältigung/Verdopplung, lokalisieren an SPBs aber nicht an Septen. All diese Ergebnisse deuten darauf hin, dass nur die äußere Seite des SPB am sMTOC lokalisiert.

Neben der BLAST-Analyse, wurde eine Laser Mikrodissektion (LCM) in Kombination mit Massenspektrometrie (MS) durchgeführt, um Septen assoziierte Proteine zu identifizieren. Mit Hilfe von 3000 gesammelten Septen wurde AlpA identifiziert, das an den Plus-Enden von sMTOCs nukleierten Mikrotubuli,lokalisiert, und das vermutlich auch eine Rolle bei der sMTOC Funktionalität spielt.

Peroxisomen spielen eine Rolle bei der Mikrotubuli-Organisation; ihr Fehlen führt zu einer reduzierten Anzahl von zytoplasmatischen und astralen MTs, eingeschränkter Aktivität von MTOCs, sowie einem Defekt in der Kernmigration. Allerdings ist nicht bekannt, ob diese Einflüsse direkt oder indirekt sind.

III Introduction

Aspergillus nidulans (also called *Emericella nidulans* when referring to its sexual form, or teleomorph) is one of many species of filamentous fungi in the phylum Ascomycota. It has been an important research organism for studying eukaryotic cell biology for over 70 years (Martinelli & Kinghorn, 1994; Osmani & Mirabito, 2004) in varieties of subjects including cell cycle, cytoskeleton, recombination, DNA repair, metabolism, evolution, and so on (Nierman *et al*., 2005; Schoustra *et al*., 2005). *A. nidulans* is able to form sexual spores during meiosis, thus allowing crossing of strains in the laboratory. It is also a homothallic fungus, which means it is able to self-fertilize and form fruiting bodies without a mating partner. The mycelia of *A. nidulans* are white with a woolly colony texture and the hyphae are separated by a specific structure called septa. The wild type colonies take on green colour because of pigmentation of the spores, while mutations in the pigmentation pathway will bring other spore colours, such as white and yellow. The *A. nidulans* genome was sequenced and publicly released in 2003. It is 30 million base pairs in size and predicted to contain approximately 9,500 protein-coding genes on eight chromosomes (Galagan, 2005). *A. nidulans* has several nuclei in each compartment of the vegetative hyphae and the nuclei are haploid during interphase (Swart, 1996). In case of septation, the first septum usually forms after three rounds of nuclear division and contains a central septal pore 50 nm in diameter. The left side (subapical) cellular compartment is removed from the cell cycle until it forms a new axis of growth like branching. The right (apical) compartment remains in the cell cycle due to the growing apical tip (Osmani *et al*., 2014). In my Ph.D. thesis, I studied the microtubule cytoskeleton and in particular the microtubule organizing centers (MTOC) in *A. nidulans.*

1 The microtubule cytoskeleton

In eukaryotes, the cytoskeletons (including microtubules and actin) together with their corresponding motor proteins (kinesin, dynein and myosin), are involved in establishing and maintaining cell polarity. The organization of microtubules and actin depend on each other, and positive feedback loops ensure robust polar growth (Fischer *et al.*, 2008; Manck *et al*., 2015; Xiang & Plamann, 2003).

1.1 On the role of the microtubule cytoskeleton in polar growth

In the budding yeast *Saccharomyces cerevisiae* and fission yeast *Schizosaccharomyces pombe*, polarized growth is restricted to certain times during the cell cycle, while in filamentous fungi, such as *A. nidulans* or *Neurospora crassa*, cell extension is a continuous and indefinite process (Snell & Nurse, 1994; Pringle *et al.*, 1995; Riquelme *et*

al., 2003). In filamentous fungi, the continuous flow of secretion vesicles from the hyphal cell body to the growing hyphal tip is crucial for cell wall and membrane extension. Microtubules provide the tracks for long-distance vesicle movement **(Figure 1, A)**. Before fusion with the cell membrane, the secretion vesicles accumulate at the apical dome of the hyphae in "Spitzenkörper (SPK)" **(Figure 1, B)**, a special structure which determines growth direction of the hyphae in filamentous fungi (Girbardt, 1957; Harris *et al.*, 2005; Takeshita *et al.*, 2014). Microtubules also play roles in signalling polarity information to the hyphal tips (Konzack *et al.*, 2005; Takeshita *et al.*, 2008), as well as nuclear migration and positioning (Fischer & Timberlake, 1995; Suelmann *et al.*, 1998; Veith *et al.*, 2005).

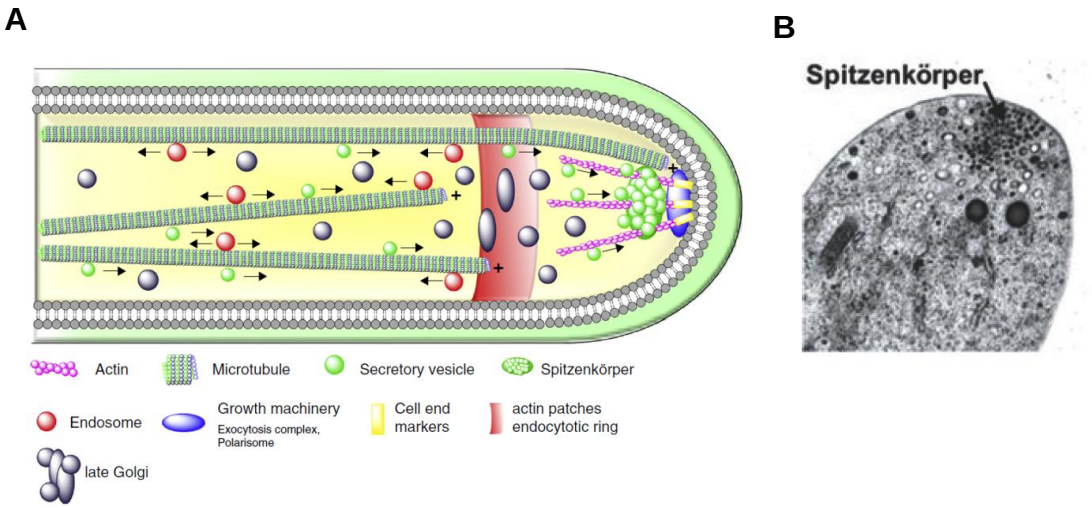

Figure 1. Polar growth in *A. nidulans*. (A) Scheme of an *A. nidulans* hyphal tip showing organelles, cytoskeletons and polarity factors (Takeshita *et al.,* 2014). **(B)** Transmission electron micrograph of a hyphal tip. The small vesicles accumulate in the Spitzenkörper. The picture was provided by B. Richardson (Athens, GA).

1.2 Microtubule nucleation

Microtubules are hollow, cylindrical tubes assembled by the polymerization of heterodimeric α/β-tubulin in a GTP-dependent manner (Job *et al*., 2003; Kollman *et al.*, 2011). They are 25 nm in outer diameter with a 17 nm interior space diameter (Hawkins *et al.*, 2009). There are two proposed models for microtubule nucleation from α/β-tubulin subunits **(Figure 2)**. Longitudinal contacts run the length of forming protofilaments, and lateral contacts between protofilaments form the circumference of the microtubule (Nogales *et al.*, 1998; Nogales *et al.*, 1999). *In vitro*, the more-flexible lateral contacts can accommodate between 11 and 16 protofilaments from purified tubulin, yielding microtubules of different diameter (Chretien & Wade, 1991; Sui & Downing, 2010). *In vivo*, almost all microtubules have 13 protofilaments to establish unique microtubule geometry (Evans *et al.*, 1985; Ledbetter & Porter, 1964; Tilney *et al.*, 1973).

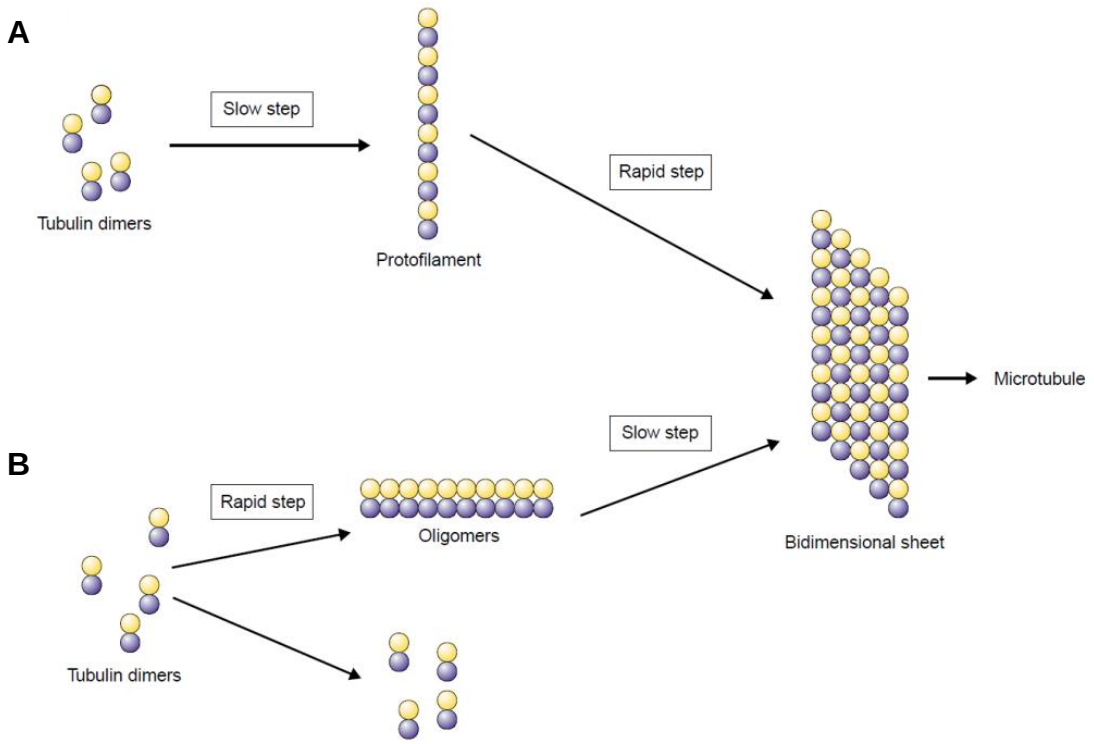

Figure 2. Two models for microtubule nucleation. (A) Aggregation of α/β tubulin dimers to form a protofilament. This step is slow and determines the nucleation exponent. Tubulin sheet and microtubule formation from protofilaments is rapid. **(B)** Tubulin dimers rapidly assemble oligomers, which are combined slowly to form a microtubule start (Job et al., 2013).

All tubulin genes were first identified in *A. nidulans*, including two α-tubulin genes (*tubA*, *tubB*) (Morris *et al.*, 1979; Doshi *et al.*, 1991; Kirk & Morris, 1991; Kirk & Morris, 1993; Oakley *et al.*, 1987), two β-tubulin genes (*benA*, *tubC*) (May *et al.*, 1985; Sheir-Neiss *et al.*, 1976; Sheir-Neiss *et al.*, 1978; Weatherbee *et al.*, 1985) and one γ-tubulin gene (*mipA*) (Weil *et al*., 1986)**.** γ-tubulin was first identified by suppressor analysis of the *benA33* mutation (Weil *et al.*, 1986), which defines a completely new class of tubulin (Oakley & Oakley, 1989). Subsequently, γ-tubulin was reported to be crucial for microtubule organization, including initiation of microtubule assembly and establishing microtubule polarity, as well as assembly of mitotic spindle microtubules (Martin *et al.*, 1997; Oakley *et al.*, 1990; Oakley, 1992; Prigozhina *et al*., 2004). Indeed, γ-tubulin is conservative from yeast to mammalian cells, as one important component of MTOC, where it forms a high molecular weight complex known as the γ-tubulin complex which can provide a template for MT assembly (Horio *et al.*, 1991; Joshi *et al.*, 1992; Liang *et al.*, 1996; Stearns *et al.*, 1991).

2 Microtubule organizing center

More than a century ago, the centrosome was identified as the primary MTOC in animal

cells (Wilson, 1925; Bornes, 2012). The centrosome is composed of a pair of centrioles, defining a polar microtubule array as the central anchor point for microtubules (Azimzadeh & Bornens, 2007). In fungi, the functional analogue of the centrosome is the spindle pole body (SPB), which is a large multi-layered structure embedded in the nuclear envelope (NE) that nucleates microtubules on both cytoplasmic and nuclear faces (Jaspersen & Winey, 2004; Kilmartin, 2014; Snyder, 1994). Plants, however, have no centrosome equivalent. Instead, they have highly organized acentrosomal and cortical microtubule arrays (Shaw *et al*., 2003; Wasteneys, 2002; Wasteneys & Ambrose, 2009). Interestingly, γ-tubulin is also involved in microtubule nucleation and organization in plant cells (Eckardt, 2006; Murata *et al*., 2005).

2.1 The γ-tubulin complex

When γ-tubulin was purified from *Drosophila melanogaster* embryos or *Xenopus laevis* eggs, it was found to be part of a ~2.2 MDa complex with at least five other proteins: γ-Tubulin complex protein 2 (GCP2), GCP3, GCP4, GCP5, GCP6 (Moritz *et al.*, 1998; Murphy *et al.*, 1998; Murphy *et al.*, 2001; Oegema *et al.*, 1999; Zheng *et al.*, 1995). The complex has a ring or lockwasher shape with 25 nm in diameter, resulting in the name γ-tubulin ring complex (γ-TuRC, Zheng *et al.*, 1995). Subsequent electron microscopic (EM) reconstructions of the γ-TuRC indicated that the lockwasher had an asymmetrical cap **(Figure 3)** (Keating & Borisy, 2000; Moritz *et al*., 2000). The γ-TuRC dissociated under high salt conditions to yield a stable 300 kDa sub-complex of γ-tubulin associated with GCP2 and GCP3, named γ-tubulin small complex (γ-TuSC). Importantly, purified γ-TuSC had a much lower microtubule-nucleating activity than intact γ-TuRC, suggesting that the assembly state of γ-tubulin is important for determining its activity (Oegema *et al.*, 1999). *S. cerevisiae* appears to have lost all of the γ-TuRC-specific components, retaining only the γ-TuSC (Geissler *et al.*, 1996; Knop *et al.*, 1997; Vinh *et al.*, 2002). The γ-TuRC is composed of multiple copies of the γ-TuSC plus GCP4, GCP5 and GCP6. The γ-TuSC consists of two copies of γ-tubulin and one each of GCP2 and GCP3. GCP2 and GCP3 are found in almost all eukaryotes and are essential for proper microtubule organization, suggesting that they form the core of the nucleating machinery. Most eukaryotes also possess GCP4 and GCP5, whereas GCP6 appears to be a recent addition in animal and fungal lineages. The components of γ-tubulin complex in different species are listed in **table 1** (Masuda *et al.*, 2013). Although GCPs constitute a unique family of homologous proteins, the overall sequence identity between them is quite low. Homology has only been confidently predicted in two short segments, the GRIP1 and GRIP2 motifs. Almost nothing is known about the specific functions of these motifs, although it was speculated that they might participate in conserved protein–protein interactions (Gunawardane *et al*., 2000; Murphy *et al*., 2001).

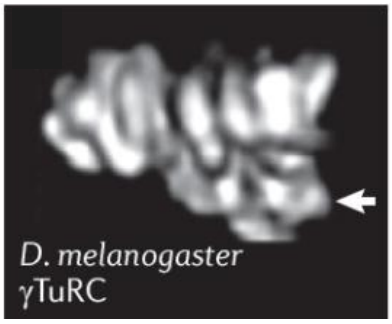

Figure 3. The low-resolution negative-stain EM reconstruction of a single *Drosophila melanogaster* γTuRC. The cap is indicated with an arrow (Zheng *et al.,* 1995).

Table 1. Comparison of γ-Tubulin complex components in different species.

H. sapiens[#]	*X. laevis*	*D. melanogaster*	*A. nidulans*	*S. pombe*	*S. cerevisiae*
GCP1	TUBG1, 2	γ-Tub23C, CD	MIPA	Gtb1/Tug1	Tub4
GCP2	Xgrip110	Dgrip84	GCPB	Alp4	Spc97
GCP3	Xgrip109	Dgrip91	GCPC	Alp6	Spc98
GCP4	Xgrip75	Dgrip75	GCPD	Gfh1	-
GCP5	Xgrip133	Dgrip128	GCPE	Mod21	-
GCP6	Xgrip210	Dgrip163	GCPF	Alp16	-
MOZART1	MOZART1	MOZART1	MztA	Mzt1	-

[#]In humans, MOZART2A and MOZART2B were identified as new components of γ-TuRC (Hutchins *et al.,* 2010). However, these homologues are found only in the deuterostome lineage.

The functions of γ-TuRC-specific proteins GCPD-F have been investigated in different organisms. In *A. nidulans*, depletion of GCPD, GCPE and GCPF in cells - either singly or all three simultaneously - is still able to nucleate microtubules from SPBs, indicating that γ-TuSC can still assemble ring structures without GCPD-F. γ-TuRC-specific proteins are also suggested to function in reducing the frequency of chromosome mis-segregation (Xiong & Oakley, 2009). In fission yeast *S. pombe*, although single or simultaneous disruption of *alp16*, *mbo1* and *gfh1* is still viable for cells, the MTOC activity or microtubule nucleation in these mutants presents aberrant behaviors (Anders *et al*., 2006). *alp16* deletion displays abnormally long cytoplasmic microtubules, which curve around the cell tip. Furthermore, *alp16*-deleted mutants are hypersensitive to microtubule-depolymerizing drugs and synthetically lethal with temperature-sensitive *alp4-225*, *alp4-1891*, or *alp6-719* mutants. Overproduction of

Alp16 is lethal, with defective phenotypes very similar to loss of Alp4 or Alp6 (Venkatram *et al*., 2004). Deletion of *mbo1* or *gfh1* exhibits a number of defects associated with altered microtubule function such as defects in cell polarity, nuclear positioning, spindle orientation, and cleavage site specification. In addition, *mbo1* and *gfh1* cells exhibit defects in astral microtubule formation and anchoring, suggesting that these proteins have specific roles in astral MT function (Fujita *et al.*, 2002). *D. melanogaster* γ-TuRCs are able to localize along interphase cytoplasmic microtubules in a GCP4-6-dependent manner. However, these γ-TuRCs do not nucleate MTs but act as points where rescue can occur (Bouissou *et al*., 2009). Interestingly, GCP4 and GCP5 are essential for *D. melanogaster* germline development (Vogt *et al*., 2006), indicating a more important role for γ-TuRC in meiosis. In human cells, γ-TuRC is required for centrosomal microtubule nucleation and mitotic spindle formation. Depletion of either GCP5 or GCP6 prevents γ-TuRC assembly and dramatically reduces γ-tubulin recruitment to spindle poles, leading to frequent mitotic failure with monopolar spindles (Bahtz *et al*., 2012; Izumi *et al*., 2008). GCP6 is also important for the apical distribution of γ-tubulin in interphase epithelial cells (Oriolo *et al*., 2007).

γ-TuRC interacts specifically with microtubule minus ends, at where it functions as a cap to prevent microtubule growth in the minus direction (Wiese & Zheng, 2000). Two proposed models were assumed for γ-TuRC nucleating microtubules **(Figure 4)**: Template model (Keating & Borisy, 2000; Moritz *et al*., 2000; Oakley, 1992; Zheng *et al*., 1995) and protofilament model (Erickson & Stoffler, 1996; Erickson, 2000). In the template model, γ-TuRCs act as a seed onto which microtubules assemble. γ-Tubulin can make lateral contacts with each other around the ring and longitudinal contacts with α-tubulin. While in the protofilament model, γ-tubulins make longitudinal contacts with each other. This seems reasonable, since longitudinal contacts are much stronger than lateral contacts. Moreover, electron micrographs of γ-TuRCs indicated that the structure might be quite flexible, suggesting that it could potentially unfurl to present a single protofilament of γ-tubulins that would nucleate through lateral contacts with α-tubulin and β-tubulin. However, most evidences now strongly support the template model (Job *et al.*, 2003).

The stoichiometry of γ-TuRC components is a very important aspect for characterizing the assembly of γ-TuRC. A study in human cells showed that the complex contained multiple copies of the γ-TuSC components and GCP4, but only a single copy of GCP5, and no determination could be made about the copy number of GCP6 (Murphy *et al*., 2001). A more-recent study quantified the ratio of components in the human γ-TuRC, and estimated the stoichiometry of the complex to be 14 copies of γ-tubulin, 12 copies of GCP2 or GCP3, 2-3 copies of GCP4 and a single copy of GCP5. Interestingly,

the stoichiometry implied by this study has more γ-tubulins than GCP2 and GCP3, suggesting that a small portion of γ-tubulin is incorporated into the γ-TuRC independently of the γ-TuSC (Kollman *et al*., 2011).

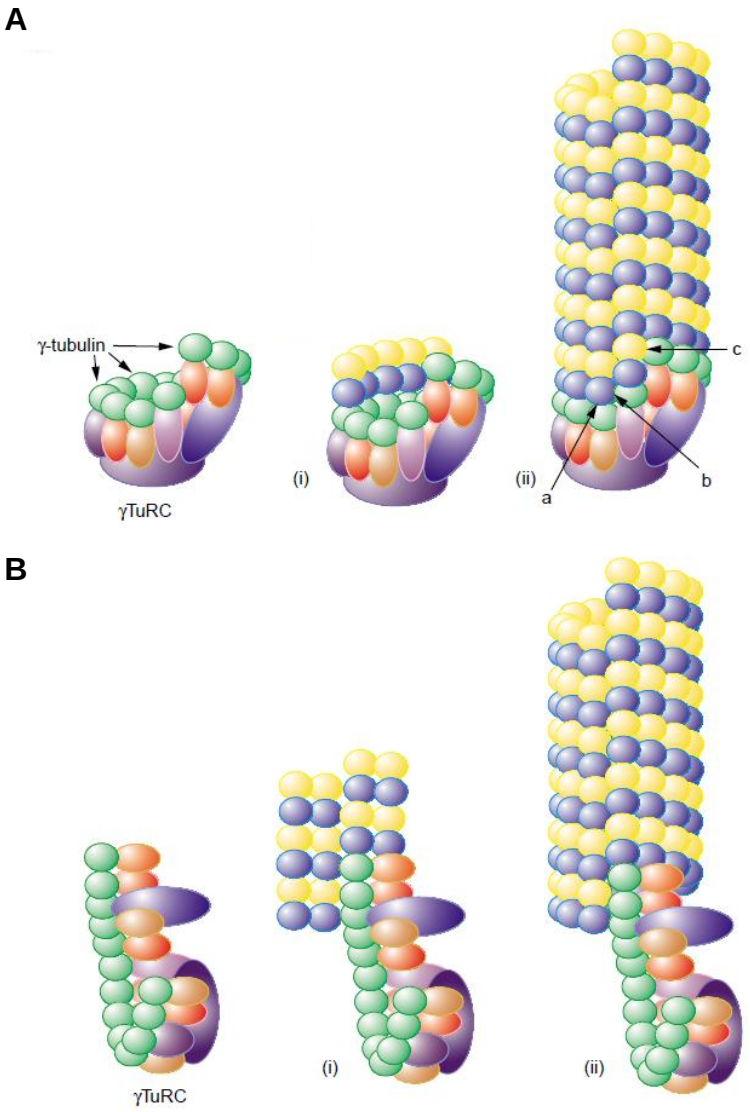

Figure 4. Two proposed models for microtubule nucleation by γ-TuRC: The template model (A) and the protofilament model (B) (Job *et al.,* 2003)**.**

However, the accurate assembly of γ-TuRC remains unclear. To our knowledge, all of the GCPs directly bind to γ-tubulin (Gunawardane *et al*., 2003; Kollman *et al*., 2011), which is in agreement with the stoichiometry of γ-TuRC components that partial γ-tubulins are incorporated into the γ-TuRC dependent on γ-TuRC-specific proteins GCP4-6. What's more, GCP4-6 directly interact with each other (Anders *et al*., 2006), and exhibit a hierarchy of localization to the SPB in *A. nidulans*. Deletion of GCPF eliminates GCPD and GCPE localization to the SPB, and deletion of GCPD prevents GCPE (but not GCPF) localization. All GCPs localize normally in a GCPE deletion (Xiong

& Oakley, 2009). In (Kollman *et al.*, 2011), it was suggested that the best place to position GCP4, GCP5 and GCP6 would be at the ends of the ring, where the half-γ-TuSC overlap occurs **(Figure 5)**. In this location, they could efficiently initiate or terminate γ-TuSC assembly and stabilize the ring by interacting with each other across the overlap.

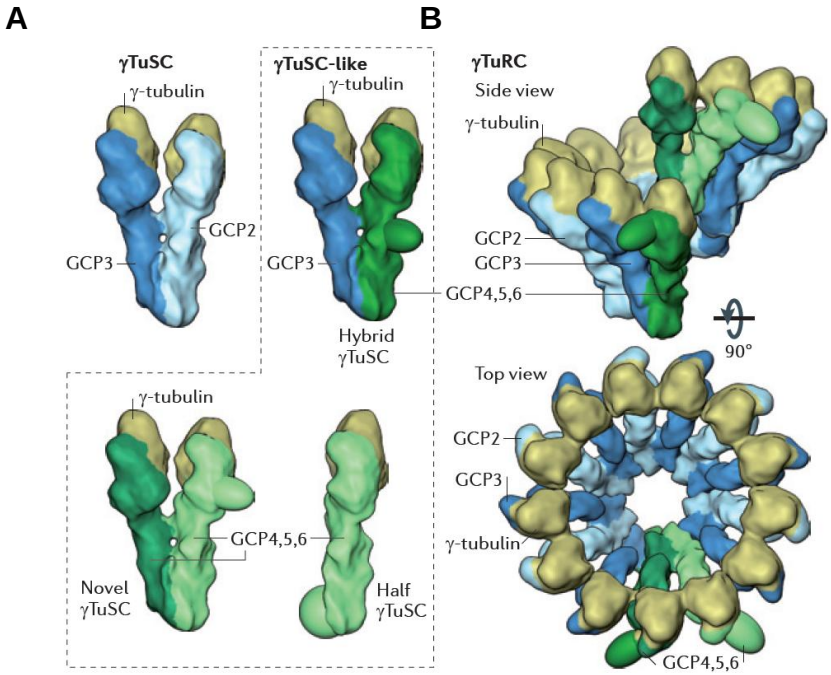

Figure 5. A proposed model of γ-TuRC assembly (Kollman *et al.,* 2011)**. (A)** All GCP family members are able to act as γ-TuSC-like components. The γ-TuRC-specific GCPs (GCP4, GCP5 and GCP6, all shown in green) may function in one of three γ-TuSC-like complexes: As hybrid γ-TuSCs with GCP2 or GCP3 (blue); interacting with each other to form novel γ-TuSC-like complexes; or as γ-tubulin-binding half γ-TuSCs. **(B)** GCP4, GCP5 and GCP6 incorporate at the ends of the ring, where they might function to initiate or terminate ring formation and to stabilize the ring at the overlap.

MOZART1, MOZART2A and MOZART2B, although shared no homolog to the GCPs family, are three new discovered γ-TuRC components in human lineage (Hutchins *et al.*, 2010; Teixidó-Travesa *et al*., 2010). It appears that, owing to their small size, these proteins were overlooked in earlier γ-TuRC pull-down experiments. MOZART1 is conservative in most eukaryotes, such as *S. pombe* (Dhani *et al.*, 2013; Masuda *et al.*, 2013) and *A. nidulans* (this work), but not in *S. cerevisiae*. In *S. pombe*, Mzt1 was identified to localize to all the MTOCs and directly interact with Alp6 (GCP3), with the approximately equal stoichiometry with Alp4 (GCP2) and essential for cell viability (Dhani *et al*., 2013; Masuda *et al.*, 2013)**.** MOZART1 was also suggested to play a role in γ-TuRC recruitment to MTOCs in human and *S. pombe* (Masuda *et al.*, 2013; Teixidó-Travesa *et al*., 2010). MOZART2A and MOZART2B, which are found only in the deuterostome lineage, are specifically involved in γ-TuRC recruitment to interphase centrosomes but do not seem to play a part in γ-TuRC assembly (Teixidó-Travesa *et al.*,

2010). Due to the recent experience with MOZART proteins, it would not be surprising to find that our list of γ-TuRC components is incomplete, and additional integral γ-TuRC components might be identified in the future.

2.2 Targeting of γ-Tubulin complexes to multiple distinct cellular locations

γ-Tubulin complexes are regulated by various factors that recruit them to different cellular locations, spatially controlling microtubule nucleation activity. Such sites include the canonical MTOCs SPB and centrosome, the Golgi apparatus, the lateral side of existing MTs, and some other non-centrosomal MTOCs. Depending on the complexity and diversity of γ-Tubulin complex from yeast to human, the recruiting proteins of them would present conservation and divergence as well, which will be described here **(Table 2)**.

2.2.1 The basic MT organization system in budding yeast

The budding yeast *S. cerevisiae* represents the simplest microtubule nucleation system: Self-oligomerization of γ-TuSCs promoted by γ-TuSC receptors Spc110 and Spc72, which target γ-TuSCs to the nuclear and cytoplasmic sides of the SPB respectively (Kilmartin & Goh, 1996; Knop & Schiebel, 1997; Chen *et al*., 1998; Knop & Schiebel, 1998; Soues & Adams, 1998). The N-terminal region of Spc110 directly interacts with Spc97 and Spc98 to recruit γ-TuSCs to the SPB towards nuclear face (Knop & Schiebel, 1997; Nguyen *et al.*, 1998). Subsequently, two highly conserved domains - centrosomin (Cnn) motif 1 (CM1) and Spc110–Pcp1 motif (SPM) at N-terminus were identified and considered to be required for targeting γ-TuRCs to SPB. (Samejima *et al*., 2008; Zhang *et al*., 2007). Spc110 is conserved in eukaryotes, homologous to *S. pombe* Pcp1, *A. nidulans* PcpA and human Pericentrin (Chen *et al*., 2012; Flory *et al*., 2000; Flory *et al*., 2002).

Nearly all (17 of 18) SPB associated proteins were modulated by phosphoralation in cell cycle, including γ-TuSC components, linkers, half-bridge proteins and so on. The phosphorylation is dynamic during cell cycle and is enriched in mitosis (Keck *et al.*, 2011). Spc110 phosphorylated by kinases Mps1 and Cdk1 activates γ-TuSC oligomerization and microtubule nucleation in a cell cycle dependent manner. Phosphorylation of Spc110-N by S-phase Cdk1-Clb5 and Mps1 at SPBs promotes γ-TuSC oligomerization to initiate microtubule nucleation. However, subsequent phosphorylation of T18 by mitotic Cdk1-Clb2 dominantly counteracts the promoting activity of the S-phase phosphorylation sites. The activating phosphosites of Spc110 locate in the putative disordered linker that connects SPM and CM1 domain, while the inactivating phosphosite T18 resides within the SPM. It is assumed that the SPM and CM1 constitute a bipartite docking site for the γ-TuSC in which CM1 binding to the N-Spc98 is complemented by SPM binding to the

stem region of the core body of Spc98 (Lin *et al.*, 2015).

By contrast, Spc72, a conservative eukaryotic protein (*S. pombe* Mto1, *A. nidulans* ApsB) which is required to target γ-TuSCs to the cytoplamic side of the SPBs, only contains the CM1 domain but not the SPM, indicating a different manner for Spc72 recritment of γ-TuSC. Like Spc110, the deletion of Spc72 is also lethal for cells. Besides, Spc72 also directly interact with Spc97 and Spc98 at the N-terminus. Notably, Spc72 directly interact with Stu2 to anchor astral MTs at the cytoplasmic side of the SPB and to regulate astral MT dynamics (Chen *et al*., 1998; Usui *et al.*, 2003).

Stu2 belongs to a big microtubule-associated proteins (MAPs) family**,** including *A. nidulans* AlpA, *S. pombe* Dis1 and Alp14, *X. laevis* XMAP215 and human TOG etc.. They localize along microtubule and at MT plus ends as well as SPBs, involved in various microtubule and spindle functions, including MT polymerization, spindle formation, kinetochore function and cell morphogenesis (Brouhard *et al*., 2008; Enke *et al.*, 2007; Ohkura *et al.*, 2001; Takeshita *et al.*, 2013). In *A. nidulans*, AlpA also interacts with the cell end marker TeaA at the hyphal tip cortex, contributing to microtubule guidance and polarity maintenance (Takeshita *et al.*, 2013). During anaphase, AlpA migrates to the kinetochores and moves to the poles together with them. The role of AlpA might be related to microtubule dynamics, promoting anaphase depolymerization of the spindle microtubules, and not to the checkpoint activity like Alp14 in fission yeast (Garcia *et al.*, 2001). It might be the kinetochore components that switch AlpA from a microtubule-stabilizing proteinto a depolymerase at the end of metaphase, as reported in *X. laevis* XMAP215 as well (Herrero *et al*., 2010; Brouhard *et al*., 2008**).**

2.2.2 Increased complexity of MT nucleation in fission yeast

In contrast to the sole MTOC SPB in *S. cerevisiae*, there are four different types of MTOCs in fission yeast *S. pombe* (Hoog *et al*., 2007). During interphase, besides SPBs (iSPBs), microtubules are also nucleated from MTOCs distributed in the cytoplasm, on the cytoplasmic MT lattice, and on the nuclear surface. These MT nucleation sites are collectively termed interphase MTOCs (iMTOCs) (Drummond *et al*., 2000; Sawin *et al.*, 2006). During mitosis, the astral microtubules and nuclear MTs are nucleated from SPBs, named mSPBs. And in post-anaphase, MTs are nucleated by equatorial MTOCs (eMTOCs) at the cell division site for the initiation of interphase MT arrays in daughter cells (Heitz *et al.*, 2001). All of the MTOCs were shown in a scheme **(Figure 6).**

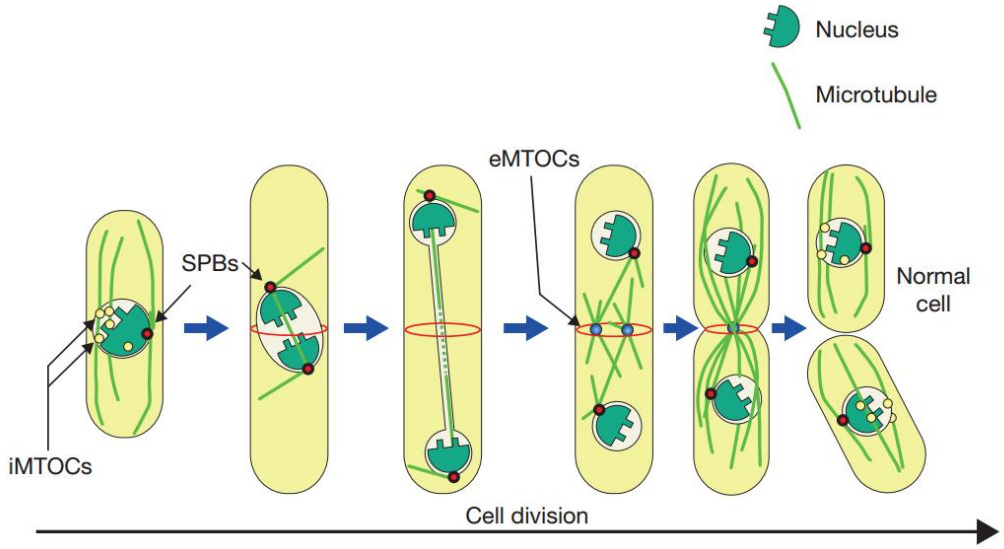

Figure 6. MTOCs in *S. pombe* during cell cycle. iMTOCs, iSPBs/mSPBs and eMTOCs during cell cycle were illustrated (Horio & Toda *et al.,* 2006).

In *S. pombe*, Pcp1 only localized to the SPBs, not to the non-SPB MTOCs (iMTOCs and eMTOCs) (Flory *et al.*, 2002). Pcp1 also possesses the CM1 and SPM motifs for recruiting γ-TuRC (Lin *et al*., 2015), in addition to another C-terminal Calmodulin-binding domain (CBD) (Flory *et al*., 2002). The CBD motif is also conserved in all Pcp1 family proteins, which is required for Pcp1 targeting to SPBs via binding with Calmodulin. Moreover, the CBD motif is included in another conserved region called PACT domain at the C-terminus (Gillingham & Munro, 2000). PACT is responsible for cellular localization of Pcp1.

Mto1 is the *S. cerevisiae* Spc72 ortholog in *S. pombe* (Sawin er al., 2004; Samejima *et al*., 2005). Mto1 and Spc72 share the conserved MASC domain at C-terminus, required for anchorage Mto1 to multiple different MTOCs through different regions of MASC motif (Samejima *et al*., 2010). Unlike in *S. cerevisiae*, Mto1 has a crucial interaction partner Mto2 in *S. pombe*, forming a Mto1/Mto2 complex for recruiting γ-TuRCs to MTOCs (Jason *et al*., 2005; Lynch *et al.*, 2014**)**. Mto1 is required for Mto2 targeting to different MTOCs, while the proper localization of Mto1 only partially depends on Mto2, especially for non-SPB MTOCs (Samejima *et al*., 2005; Venkatram *et al*., 2005). Both Mto1 and Mto2 are indispensable for non-SPB derived MTs nucleation, although Mto1 is also required for astral MT formation during mitosis. Mto2 binds to Mto1 via a 89 aa region in the middle part (461-549 aa) of Mto1 (Samejima *et al*., 2008).

2.2.3 Emergence of paralogs in higher eukaryotes

In vertebrates, additional members of the same type of γ-TuRC recruiting factor are likely

to have evolved as paralogs. These putative paralogs do not only share main structural and functional features but also have evolved specialized functions (Lin *et al*., 2015). One example is the expansion of the Spc110/Pcp1 family orthologs pericentrin and CG-NAP (AKAP450/AKAP9), which recruit γ-TuRC to the pericentriolar material (PCM) during mitosis (Takahashi *et al*., 2002; Zimmerman *et al*., 2004). Both pericentrin and CG-NAP share internal coiled-coil regions that mediate dimerization and a conserved C-terminal PACT domain for centrosomal localization. Despite a direct interaction with the γ-TuC, the SPM and CM1 elements in pericentrin and CG-NAP are degenerated. CG-NAP is also localized and required for MT nucleation at the Golgi apparatus and maintenance of the interphase centrosome-Golgi nexus (Hurtado *et al*., 2011; Kim *et al*., 2007; Rivero *et al*., 2009; Takahashi *et al*., 1999), indicating the acquirement of novel functions for this paralog.

The Spc72/Mto1 orthologs myomegalin and CDK5RAP2 in human share the N-terminal CM1 for binding to the γ-TuRC and the C-terminal CM2 for proper self-localization (Roubin *et al.*, 2013). CDK5RAP2 accumulates both in the PCM and along the spindles of metaphase cells, and at the Golgi apparatus (Barrera *et al*., 2010; Bond *et al.*, 2005; Fong *et al*., 2008; Wang *et al*., 2010). Via association with EB1, CDK5RAP2 tracks cytoplasmic MT plus ends and regulates the dynamics of growing MT tips (Fong *et al*., 2009). Interestingly, the localization of CDK5RAP2 and myomegalin to centrosomes and the Golgi apparatus appears to depend on its interaction with pericentrin and CG-NAP (Wang *et al*., 2010; Wang *et al*., 2014).

NEDD1/GCP-WD is a specific γ-TuRC targeting factor which exists in most species of the two largest subphyla of metazoans, the Chordata (including vertebrates) and the Arthropoda, with no homology to γ-TuSC receptors. NEDD1 was also recoganized as one component of γ-TuRC, since it was co-purified with the other γ-TuRC compoments in *D. melanogaster*. But NEDD1 shares no sequence homology with other GCPs, without GRIP1 or GRIP2, and thus normally considered as a localization factor of γ-TuRC (Kollmann *et al.*, 2011). The N-terminal WD40 repeats of NEDD1 are responsible for its cellular localization while C-terminal region is required for γ-TuRC docking (Haren *et al*., 2006; Luders *et al*., 2006; Manning *et al*., 2010). Instead of the role of γ-TuSC receptors in forming ring-like MT nucleation templates, NEDD1 is not responsible for γ-TuRC formation. Rather, γ-TuRC formation is a prerequisite for NEDD1 targeting γ-tubulin properly (Liu *et al*, 2008; Luders *et al*, 2006; Verollet *et al*., 2006). Differential phosphorylation is likely to regulate the sites to which NEDD1 recruits γ-TuRC (Pinyol *et al*., 2013; Sdelci *et al*., 2012), Notably, species of the subphyla Nematoda and Platyhelminthes such as *Caenorhabditis elegans* and the flatworm *Macrostomum lignano* appear to lack genes homologous to those encoding GCP4–6 and NEDD1, suggesting

that NEDD1 specifically interacts with γ-TuRC but not γ-TuSC (Lin *et al*., 2015).

2.2.4 MTOC associated proteins in *A. nidulans*

Compared to the well-analyzed MTOCs as well as their associated proteins in *S. cerevisiae*, *S. pombe* and human, the MTOCs in *A. nidulans* is less studied. Recently, septal MTOC (sMTOC) was discovered as a novel microtubule nucleation site besides SPB by an MT plus-end marker KipA. sMTOC localized constantly at septa, unlike the transiently residing eMTOC in *S. pombe* (Konzack *et al*., 2005). γ-Tubulin and GCPs could also be observed at sMTOCs besides SPBs, which confirmes the existence of sMTOC (Xiong & Oakley, 2009; Zekert *et al*., 2010). ApsB is a component of both sMTOC and SPB, playing a more important role in sMTOC MT nucleation than SPB (Veith *et al.*, 2005). PcpA was analyzed as an essential SPB component (Chen *et al*., 2012). However, the characterization of ApsB or PcpA was quite limited. Our work is based on those findings and will further characterize ApsB and PcpA, as well as a novel Mto2 ortholog SPA18.

Table 2. The γ-Tubulin complex recruiting factors in different organisms.

	degSPM-degCM1-PACT	**SPM-CM1-PACT**	**CM1-CM2**	**CM1-MASC**	**other receptors**
H. sapiens	pericentrin, AKAP450/AKAP9	-	CDK5RAP2, myomegalin	-	-
A. nidulans	-	PcpA	-	ApsB	SPA18
S. pombe	-	Pcp1	-	Mto1	Mto2
S. cerevisiae	-	Spc110	-	Spc72	-

2.3 Non-centrosomal MTOCs

In eukaryotes, centrosomes or SPBs are the main microtubule nucleation apparatus in cell cycle. But recent work revealed that microtubules were also able to generate from membranous organelles, chromosomes and other sites in the cell, in a γ-tubulin dependent manner. Here we will briefly describe some of the known non-centrosomal MT nucleation processes in eukaryotes.

2.3.1 Golgi apparatus

The Golgi apparatus is part of the cellular endomembrane system, packaging proteins

into membrane-bound vesicles inside the cell before the vesicles are sent to their destination (Pavelk & Mironov，2008). MTs nucleated at the Golgi have been suggested to be indispensable for the Golgi organization, post-Golgi trafficking and cell polarity (Miller *et al.*, 2009; Zhu & Kaverina, 2013). Nucleating of MTs from the Golgi also depends on the γ-tubulin. In some of the interphase cells, like RPE-1 cells, half of their microtubules are generated from Golgi MTOCs (Chabin-Brion *et al.*, 2001; Efimov *et al.*, 2007). Besides, myomegalin, the anchor of γ-TuRC to PCM also co-localize with the *cis*-Golgi (Roubin *et al*., 2013). What's more, the *cis*-Golgi-specific protein GM130 can recruit mitotic-γ-TuRC-targeting factor AKAP450, which in turn recruits CDK5RAP2. CDK5RAP2 is responsible for anchoring γ-TuRC to PCM as well (Rivero *et al*., 2009; Wang *et al*., 2010). GM130 might be a key regulatory factor of the Golgi MTOC (Petry & Vale, 2015).

2.3.2 Nuclear membrane

The phenomenon of microtubule nucleation at the nuclear membrane is very common in eukaryotes. In skeletal muscle cells, γ-Tubulin and the centrosomal proteins pericentrin and ninein are redistributed to the nuclear envelope (NE) during skeletal muscle differentiation (Bugnard *et al*., 2005), and the nuclei of non-muscle cells are able to bind centrosomal proteins when fused to differentiating myoblasts (Fant *et al*., 2009). In plant cells, γ-tubulin and GCP2/3 also target to the surface of nuclei to nucleate microtubules (Seltzer *et al*., 2007; Erhardt *et al.*, 2002). In *Arabidopsis thaliana*, microtubules generated at the nuclear membrane are suggested to play a role in establishing nuclear shape and positioning nuclear pore complexes. Moreover, GCP9 is important for γ-tubulin localization to the NE (Batzenschlager *et al*., 2013). In *S. pombe*, during interphase, MTOCs distribute at nuclear surface besides SPBs, cytoplasm and cytoplasmic MT lattice. The γ-TuRC receptor Mto1 and Mto2 were also identified at MTOCs at nuclear envelope. The N-terminal 130 aa of Mto1 are specifically required for targeting to NE (Lynch *et al*., 2014).

2.3.3 Chromatin and kinetochores

In open mitosis organism metazoan cells like *Xenopus* egg extracts, most kinetochore MTs nucleated from poles are guided by a gradient of RanGTP that extends over a long range (20 μm) (Kalab *et al*., 2006). Many spindle assembly factors, such as hepatoma upregulated protein (HURP) and targeting protein for Xklp2 (TPX2), were also found to be regulated in a RanGTP-dependent manner (Gruss *et al*, 2002). The chromosomal passenger complex (CPC) can compensate for the Ran-GTP gradient under certain conditions by generating MTs from centromeric chromatin (Maresca *et al*., 2009). Moreover, it has been suggested that the nuclear pore complex (NCP) Nup107-160 and

ELYS/Mel-28 are interacting partners of γ-TuRCs (Mishra *et al.*, 2010; Yokoyama; 2014), along with the Ran-GTP and CPC pathways, contribute to microtubule formation at kinetochores, possibly assisting in kinetochore capture (Tulu *et al.*, 2006). By contrast, in cells undergoing closed mitosis such as *S. cerevisiae* and *S. pombe*, a RanGTP gradient is not available. The RanGTP concentration is uniformly high throughout the nucleus due to rapid RanGTP diffusion (Lin *et al*., 2015). Nevertheless, in *S. pombe*, RanGTP together with Cdk1 can still play an essential role in nuclear accumulation of the TACC-TOG complex (Alp7-Alp14), interacting with Ndc80 complex at kinetochores (Okada *et al*., 2014; Sato *et al*., 2007; Tang *et al*., 2013). In *S. cerevisiae*, during early mitosis, kinetochores can nucleate MTs with distal plus ends, depending on the TOG protein (Stu2). These kinetochore-derived MTs can interact with SPB-derived MTs to facilitate kinetochore loading onto the lateral surface of SPB-derived MTs (Kitamura *et al*., 2010).

2.3.4 Microtubules branching on pre-existing MTs

New microtubules branching from pre-existing MTs were initially found in interphase plant and yeast cells. In plant cells, microtubules branched on existing MTs at the cell cortex with a characteristic angle of ~45° or 0°, in a γ-tubulin-dependent manner (Chan *et al*., 2009; Murata *et al*., 2005). Whereas in *S. pombe*, the new generated daughter MTs are anti-parallel to the mother MT (at a 180° angle) (Jason *et al*., 2005). Besides, microtubules are observed to be generated within the body of spindles, not only at centrosomes and kinetochores as we described before (Brugues *et al*., 2012; Mahoney *et al*., 2006). Recently, microtubule nucleation from the sides of existing microtubules was demonstrated in cell-free meiotic *Xenopus* egg extracts (Petry *et al*., 2013). The branch angle between the daughter and mother MT is usually low, or even in parallel, resulting in the same polarity of them. The γ-TuRC is required for branching microtubule nucleation. In *Drosophila* and human cells, an 8-subunit complex called augmin complex was found to specifically target γ-tubulin to spindle MTs but not to centrosomes. Depletion of augmin causes spindle defects in animal cells and a reduction in microtubule density within the spindle (Goshima *et al*., 2007; Goshima *et al*., 2008; Lawo *et al*., 2009; Uehara *et al*., 2009). Although not found in *S. pombe* and *S. cerevisiae*, augmin exists in plants and plays an important role in the formation of the plant spindle and the microtubule-rich phragmoplast and triggering MT-dependent microtubule nucleation at the plant cortex (Ho *et al*., 2011; Hotta *et al*., 2012; Liu *et al*., 2014; Nakaoka *et al.*, 2012). The branching microtubule nucleation is also stimulated by factors previously implicated in chromatin-stimulated nucleation, Ran-GTP and its effector, TPX2 (the targeting factor of Xlkp2) (Petry *et al*., 2013).

2.4 The spindle pole body in budding yeast

The SPB is the sole microtubule organization in the budding yeast *S. cerevisiae*. SPBs are embedded in the nuclear envelope throughout the life cycle and are thus able to nucleate both nuclear and cytoplasmic microtubules. It makes a big challenge that nearly all genes involved in SPB functions are essential. Nevertheless, the budding yeast SPB is perhaps the best-characterized MTOC of all, serving us a model for characterizing MTOCs in other organisms like *A. nidulans*.

In *S. cerevisiae*, the molecular mass of a diploid SPB, including microtubules and MT associated proteins, is estimated to be 1-1.5 GDa, while a core SPB is 0.3-0.5 GDa (Adams & Kilmartin, 1999, Bullitt *et al*., 1997). This is approximately 20 times the size of a nuclear pore complex (NPC), which contains at least 30 different proteins (Jaspersen & Winey, 2004). In haploid cells, the SPB grows of diameter from 80 nm in G1 to 110 nm in mitosis, although the height of the SPB (the inner plaque to outer plaque distance) remains constant at approximately 150 nm (Byers & Goetsch, 1974). A larger SPB diameter increases the capacity of the SPB for microtubule nucleation, thus facilitating chromosome segregation. However, the whole structure of SPB is not always constant. SPB components exchange in and out of the organelle during most of the mitotic cell cycle (Byers & Goetsch, 1975; Moens & Rapport, 1971; Peterson *et al*., 1972; Yoder *et al*., 2003; Zickler & Olson, 1975). For instance, in meiosis II, the outer plaque protein Spc72 is replaced by two meiotic SPB proteins, Mpc54 and Spo21/Mpc70, which form the new meiotic plaque (Knop & Strasser, 2000).

Analyzed by electron microscopy (EM), the SPB was found to be a cylindrical organelle that appears to consist of three disks or plaques **(Figure 7)**: An outer plaque (OP) that faces the cytoplasm and is associated with cytoplasmic MTs or astral MTs, an inner plaque (IP) that faces the nucleoplasm and is associated with nuclear MTs, and a central plaque (CP) that spans the nuclear membrane (Byers & Goetsch, 1974; Byers & Goetsch, 1975; Moens & Rapport, 1971; Robinow & Marak, 1966). One side of the CP is associated with an electron-dense region of the nuclear envelope termed the half-bridge (HB). Afterwards, with cryo-EM (Bullitt *et al.*, 1997) and electron tomography (O'Toole *et al.*, 1999), two additional layers termed the first and second intermediate layers (IL1 and IL2) were observed between the outer and central plaque besides the three known plaque layers **(Figure 8)**. Tomographic studies show that the half-bridge is also a multi-layered structure consisting of two continuous layers that mirror the membrane bilayers and an additional layer lying on the cytoplasmic side of the half-bridge, which is associated with the CP and IL2 at the edge of the SPB. Two hook-like appendages emanating from the central plaque that probably anchor the SPB to the nuclear

membrane were also visualized by tomography.

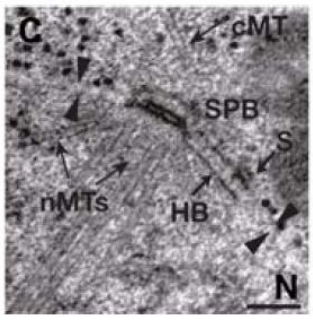

Figure 7. The layered SPB structure by electron micrograph in *S. cerevisiae* (Jaspersen & Winey, 2004)**.** The SPB is embedded in the NE (arrowheads), which separates the nuclear (N) and cytoplasmic (C) sides. HB, half bridge; S, satellite.

Until now, 17 of 30 components of the mitotic SPB have been identified (Jaspersen & Winey, 2004). Spc42 is an essential coiled-coil protein that forms the central core of the SPB (Donaldson & Kilmartin, 1996). Approximately 1000 Spc42 molecules assemble into trimers of Spc42 dimers to form the hexagonal lattice, which was visualized by cryo-EM in IL2 (Bullitt *et al.*, 1997). Overexpression of Spc42 caused lateral expansion of the hexagonal lattice within the plane of the membrane to be a superplaque structure (Donaldson & Kilmartin, 1996). The N-terminus of Spc42 binds to Spc110 and Spc29, two other essential coiled-coil proteins that localize to the nuclear face of the SPB (Adams & Kilmartin, 1999; Elliott *et al.*, 1999). C-terminal Spc110 localizes to center plaque and is estimated to bind to Calmodulin (Cmd1) and Spc29 through overlapping binding sites (Elliott *et al.*, 1999, Kilmartin & Goh, 1996; Spang *et al*. 1996; Stirling *et al*., 1994; Sundberg *et al.*, 1996). In yeast, Calmodulin is involved in several cellular processes, one of which is an essential function to regulate binding of Spc110 to Spc29 at the SPB (Elliott *et al.*, 1999; Geiser *et al*., 1991, 1993). Spc29 directly binds with both Spc42 and Spc110, indicating that it might be a linker between the inner plaque and central plaque, although it was also reported that Spc110 could directly interact with Spc42 (Adams & Kilmartin, 1999; Vinh *et al.*, 2002). Dimerization of the long coiled-coiled domains in the central region of Spc110 forms striated struts, which was seen between the central and inner plaques by tomography. The length of Spc110 coiled-coils determines the distance between the central plaque and inner plaque (Kilmartin *et al*., 1993; O'Toole *et al*., 1999). The N-terminus of Spc110 localizes to the inner plaque and binds directly to Spc 97 and Spc98, which form the γ-TuSC with γ-tubulin (Kilmartin & Goh, 1996; Knop & Schiebel, 1997; Nguyen *et al*., 1998; Sundberg & Davis, 1997; Vinh *et al*., 2002). On the other direction, the C-terminus of Spc42 binds to the C-Cnm67, towards the cytoplasmic face. (Adams & Kilmartin, 1999). Similar to Spc110, a Cnm67 coiled-coil region facilitates its dimerization and acts as a spacer between IL1 and IL2 (Schaerer *et al*., 2001). The N-terminus of Cnm67 binds to the outer plaque protein Nud1, which is required for exit from mitosis (Adams & Kilmartin, 1999; Elliott *et al*., 1999).

Another coiled-coil protein, Spc72 (Chen *et al*., 1998; Wigge *et al*., 1998), binds to the C-Nud1 via its C-terminus (Gruneberg *et al*., 2000) and recruits γ-TuSCs via its N-terminus, through interacting with Spc97 and Spc98 (Knop & Schiebel, 1998). All components are presented in the model **(Figure 8)**.

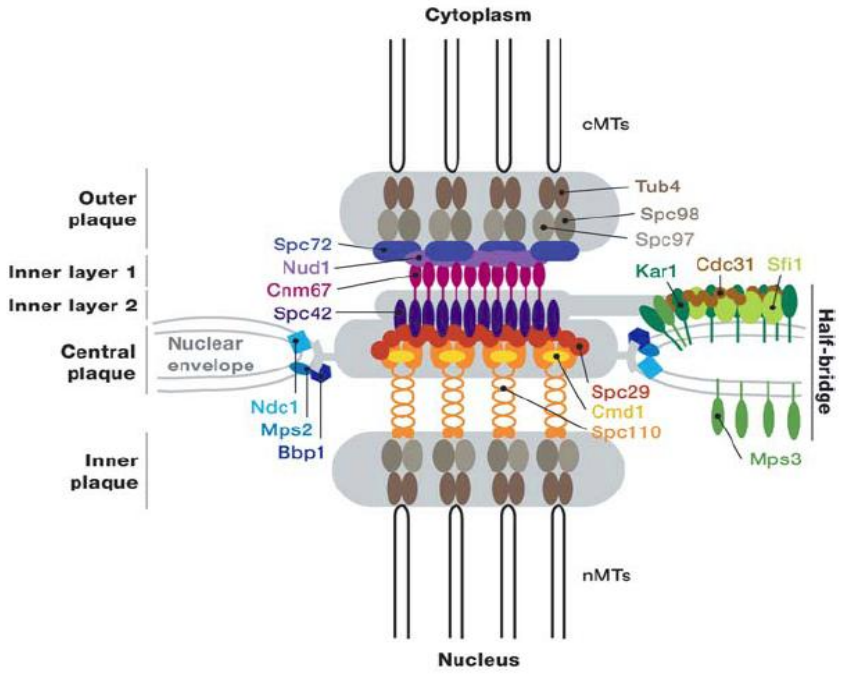

Figure 8. The structure of SPB in *S. cerevisiae*. SPB contains five layers (outer plaque, inner layer 1, inner layer 2, central plaque and inner plaque), which can be found in the scheme. The components of core SPB and HB are also illustrated (Jaspersen & Winey, 2004).

Since none of the core SPB components contains a trans-membrane domain, how SPB is inserted and anchored in the nuclear envelope becomes a mistery. It is reported that Mps2 and Ndc1 are two membrane proteins that localize to the SPB periphery at the junction between the central plaque and the nuclear envelope, thus anchoring SPBs to nuclear membrane (Chial *et al*., 1998; Munoz-Centeno *et al*., 1999; Winey *et al*., 1993). In addition, Mps2 binds to a third protein required for membrane insertion, Bbp1 (Schramm *et al*., 2000), which in turn binds to Spc29 as well as the half-bridge protein Kar1. It is proposed that Bbp1 and Mps2 form the hook structure visualized by tomography between the central plaque and nuclear envelope. Ndc1 may also be part of this structure, but its role in SPB function is less clear since no Ndc1 interacting proteins have been identified (O'Toole *et al*., 1999).

The half-bridge, together with the proteins on it, is responsible for SPB duplication. The membrane-anchored protein Kar1 is accompanied by Sfi1 on the cytoplasmic side of the half-bridge (Rose & Fink, 1987; Spang *et al*., 1995). The yeast centrin Cdc31, a

conserved Ca^{2+}-binding protein like Calmodulin, directly interacts with both Sfi1 and Kar1 **(Figure 9)** (Spang *et al*., 1993; Biggins & Rose, 1994; Wiech *et al*., 1996; Kilmartin, 2003). The SUN domain protein Mps3 is the sole component at the nuclear half-bridge side (Jaspersen *et al*., 2002, 2006). Sfi1 is a long, α-helical protein that longitudinally spans the entire length of the half-bridge (Kilmartin, 2003). All Sfi1 molecules are aligned with the same orientation in the half-bridge, with the N-terminus embedded in the SPB's central plaque and the C-terminus (CT) marking the distal end of the half-bridge. By CT-to-CT interaction of Sfi1 molecules, half-bridge-into-bridge extension occurs (Kilmartin, 2003; Li *et al*., 2006; Elserafy *et al*., 2014). In S phase, Sfi1-CT becomes phosphorylated by kinase Cdk1 to separate the bridge after SPB duplication and to restrict this event to once per cell cycle (Avena *et al*., 2014; Elserafy *et al*., 2014). In yeast, Kar1 harbors a single Cdc31-binding site, whereas Sfi1 contains 20-21 binding sites in its center (Li *et al*., 2006). The function of Kar1 is to tether Sfi1 to the NE (Seybold *et al*., 2015). In higher eukaryotes, centrin forms complexes with multi-centrin binding proteins named hSfi1 and Poc5 in the lumen of centrioles (Kilmartin, 2003; Azimzadeh *et al*., 2009).

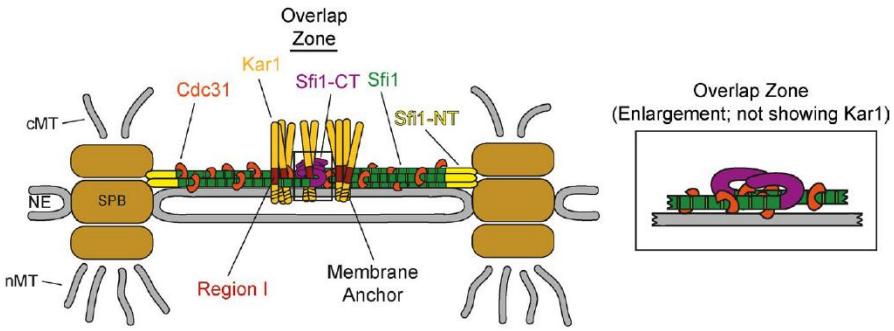

Figure 9. Model for the SPB bridge in *S. cerevisiae*. CT-CT interaction of Sfi1 extends the half-bridge into bridge, while N-terminus is embedded in the SPB. Cdc31 binds to both Sfi1 and Kar1. Kar1 tethers Sfi1 to the half-bridge (Seybold *et al*., 2015).

In addition, Kar1 also plays a role in re-organization of the SPB during G1 and karyogamy. In response to mating factor α-factor, Spc72 can relocalize from the outer plaque to the cytoplasmic side of the half-bridge by binding to N-terminal Kar1. As a result, cytoplasmic MTs originate from the half-bridge instead of the outer plaque. Kar1-dependent re-organization of the SPB is not essential for normal vegetative growth but is required for mating (Pereira *et al*., 1999).

3 Aim of this work

In comparison to the well-characterized microtubule organization centers in budding yeast, fission yeast and human, the MTOCs in *A. nidulans* are less known, especially for the septal MTOC (sMTOC). In this work, our aim is to identify new components of sMTOC as well as SPB in *A. nidulans.* Afterwards, the structural and functional difference between different MTOCs will be investigated. Several strategies were performed to discover new MTOC components, such as laser capture microdissection (LCM), affinity purification and homology alignment. We are also interested in how the MTOCs are targeted to different locations. Here we have identified a novel sMTOC/SPB component SPA18, an ApsB interaction partner. The role of SPA18 will be analyzed in this work. The constitution of sMTOC and SPB will also be primarily described based on the new components we found, such as MztA and SfiA. Besides, the recruitment of γ-TuRC to different MTOCs by ApsB/SPA18 or PcpA, as well as targeting of the γ-TuRC receptors by SepK or SPA10, will be characterized as well. Detailed domain analysis can help us to understand these interaction processes. Further characterization of the sMTOC and SPB in *A. nidulans* is still in progress.

IV Results

1 Characterization of the role of ApsB at septal MTOCs

ApsB, an important component of SPBs and sMTOCs, was first identified as a 1051 aa protein in 1998, cloned by functional complementation of the developmental defect using the genomic cosmid library (Suelmann *et al*., 1998). However, this 1051 aa protein (named ApsB$^{3.2}$ in this work) was not found in our RNA-seq library (created by Julio Rodríguez-Romero). Alternatively, a 4773 bp gene *apsB*$^{4.7}$, with additional 1569 bp upstream of *apsB*$^{3.2}$, was found in the RNA-seq library. *apsB* encodes a 1574 aa (MW 177 kDa) protein, with an intron at 2051-2098 bp. ApsB is the ortholog of Spc72 (*S. cerevisiae*) and Mto1 (*S. pombe*).

1.1 Deletion of *apsB*$^{4.7}$

Because in previous studies only a part of *apsB* was deleted or even only disrupted, it could be that part of ApsB was still produced and thus the observed phenotypes were not the phenotypes of a complete null mutant. Therefore, we constructed a complete *apsB*-deletion strain and analyzed the cell-biological phenotypes. The *apsB* open reading frame (ORF) was deleted in the wild type (WT) strain TN02A3 with *pyroA* as selection marker. The deletion event was confirmed by diagnostic PCR and Southern blot (SB). The flanking regions of *ApsB* were amplified by PCR with genomic DNA as template, as well as primers apsB-LB_fwd/apsB-LB-linker_rev for the upstream region of *apsB* and apsB-RB-linker_fwd/apsB-RB_rev for the downstream region. *pyroA* was amplified with pyroA-linker_fwd/pyroA-linker_rev. Then the left border (LB), *pyroA* and right border (RB) were fused together by fusion PCR with nested primers apsB-LB-N_fwd and apsB-RB-N_rev. The construct was ligated to pJET1.2 /blunt, yielding vector pYZ11. After transformation of pYZ11 to TN02A3 and selection by diagnostic PCR and Southern blot **(Figure 10)**, *apsB*-deletion strain SYZ3 was created.

1.2 Localization of ApsB$^{4.7}$

In order to create an N-terminal fusion of ApsB with GFP, 1.0 kb *apsB*$^{4.7}$ from the start codon was amplified with primers apsB_AscI_fwd and apsB-1_PacI_rev (*Asc*I and *Pac*I restriction sites are used and in italics on the list), cloned into the pMCB17apx vector, resulting in pYZ6. It was subsequently transformed into TN02A3, yielding SYZ2 in which N-terminal ApsB$^{4.7}$ was tagged with GFP by homologous integration. Germlings of a corresponding strain were observed in the fluorescence microscope. As a result, ApsB localized at SPBs and sMTOCs **(Figure 11)**, which is in agreement with ApsB$^{3.2}$. In interphase, a single dot was visualized at

each SPB, while during mitosis, two dots at the spindle poles were observed. ApsB localized to septa constantly during the cell cycle as two dots **(Figure 11)**, and we supposed it to be a disk-like (ring-like) structure around the septal pore.

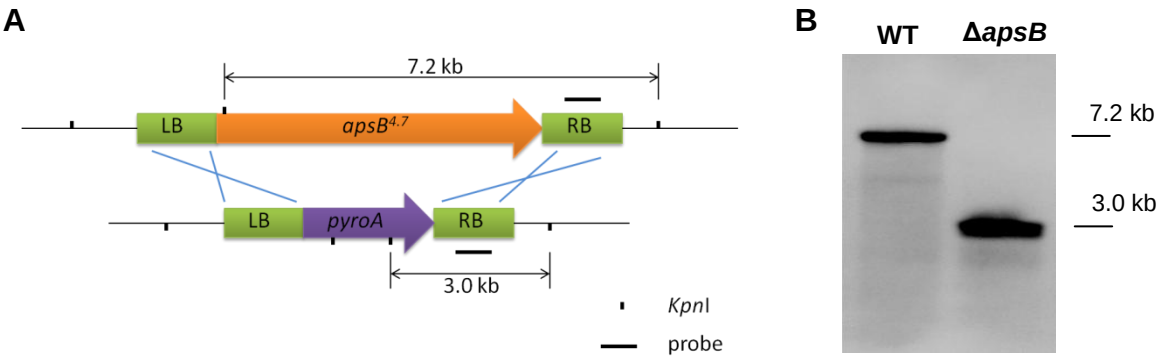

Figure 10. Deletion of *apsB*. **(A)** Scheme of the *apsB*-deletion construct. LB and RB are in the flanking regions of the *apsB* ORF. By homologous integration at the LB and the RB, the deletion cassette (lower) was integrated into the genome. **(B)** Southern blot with the probe illustrated in **(A)**. Genomic DNA was digested with *Kpn*I. The mutant and wild type strains got blotting bands at 3.0 kb and 7.2 kb, respectively.

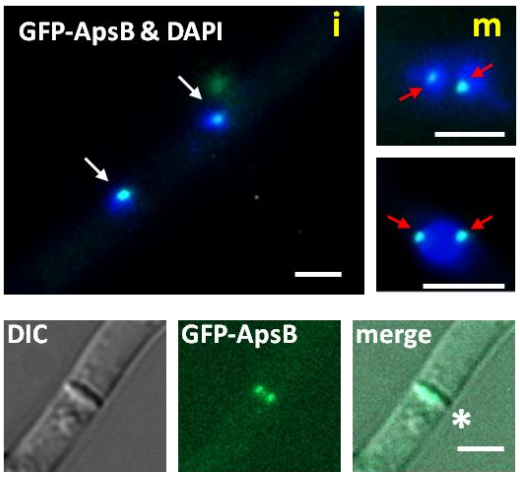

Figure 11. Localization of ApsB. The white arrows, red arrows and asterisk indicate ApsB localization at interphase SPBs, mitotic SPBs and septum respectively. SYZ2 was observed. The strain was grown in MM (2% glycerol) with pyridoxin overnight at 28°C. Bar, 5 µm; i, interphase; m, mitosis.

1.3 The N-terminal 523 aa are functionally important

In contrast to wild type TN02A3, Δ*apsB*$^{4.7}$ (SYZ3) produced scarce spores after 3 days, similar to Δ*apsB*$^{3.2}$ (SRS31) **(Figure 12, A)**. Nevertheless, when we used *apsB*$^{3.2}$ expressed from the *alcA* promoter to re-complement SYZ3, the resulting SYZ6 produced only 12% spores compared with SYZ7, in which SYZ3 was re-complemented with the full-length ApsB protein **(Figure 12, A & B)**. As a result, Δ*apsB*$^{4.7}$ was not completely re-complemented by *apsB*$^{3.2}$, indicating that the missing 523 aa are functionally important, although no predicted domain was found within that region. The function of this region will be discussed in **V 3.3**..

2 Characterization of SPA18

SPA18 was first identified as a septal pore-associated (SPA) protein in *N. crassa* by using a combination of mass spectrometry (MS) of Woronin body associated proteins and a bioinformatics approach that identifies related proteins based on composition and character. 17 intrinsically disordered proteins (IDP) were identified to localize to the septal pore in rings and pore-centered foci (Lai *et al*., 2012). SPA18, one of these IDPs, was also found in *A. nidulans* by BLASTP analysis (Stephen Osmani, Ohio University, US). In addition to septa, SPA18 (AN4545) was also visualized at SPBs. Thus we anticipated that SPA18 might be an MTOC-associated protein.

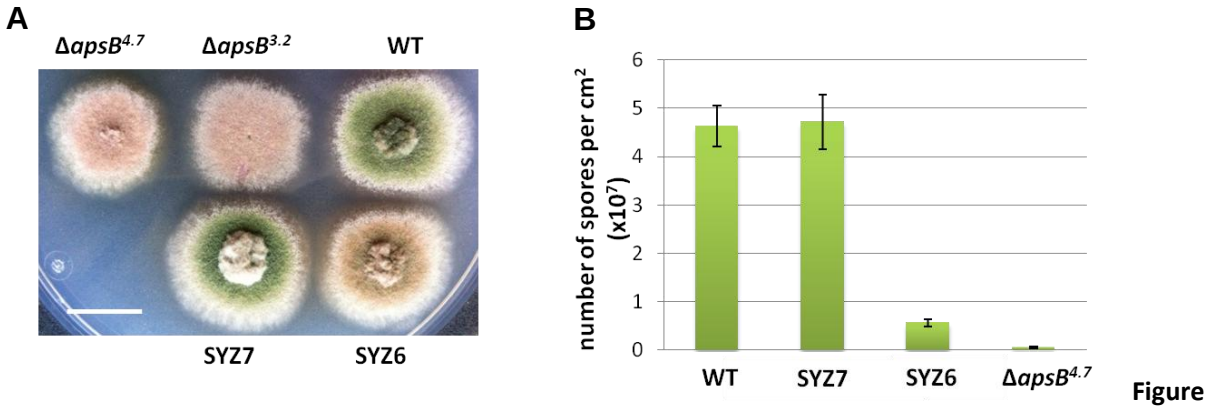

Figure 12. Comparison of ApsB$^{4.7}$ and ApsB$^{3.2}$. (A) Comparison of colony growth of WT and different *apsB*-mutant strains. The strains were grown on an MM (2% glycerol) agar plate with uridin, uracil and pyridoxin at 37°C for 3 days. **(B)** Number of spores in the strains. Equivalent number of spores were spread on MM (2% glycerol) agar plates with appropriate selection markers. After 3 days at 37°C, the number of spores was counted from 5 cut pieces with the back of a 1 ml pipette tip. Spores were washed off and counted in a Neubauer chamber. Bar, 1 cm.

On the other hand, in *S. pombe*, Mto2 is a Mto1 (*A. nidulans* ApsB) interaction partner, forming a complex for recruiting the γ-TuRCs to non-SPB MTOCs (Lynch *et al*., 2014; Samejima *et al*., 2005; Venkatram *et al*., 2005). We were expecting that the orthologue of Mto2 would exist in *A. nidulans*. By contrast, if we blasted Mto2 in *A. nidulans* (NCBI), we were unable to find any homologous candidate. However, when we blasted Mto2 in other organisms, we found a *Penicillium rubens* protein (XP_ 002562312) homologous to Mto2. Using the *P. rubens* XP_ 002562312 protein we were able to identify an orthologue in *A. nidulans*, SPA18 (ANID_4545).

2.1 Bioinformatic analysis of SPA18

SPA18 is a 2591 bp gene residing on chromosome III with an intron at 1075-1172 bp, encoding a 950 aa (MW 102.5 kDa) protein. SPA18 sequence revealed 85% homology with *A.*

niger (56% identity), 81% with *A. terreus* (57% identity), 86% with *A. oryzae* (55% identity), 86% with *A. fumigatus* (50% identity), 70% with *P. rubens* (48% identity) and only 29% with *N. crassa* (40% identity). The alignment between SPA18 and its homologues was done with GeneDoc **(Figure S1)**.) A phylogenetic tree **(Figure 13)** was constructed using ClustalX 2.1 and MEGA5.2 (Tamura *et al.*, 2011.

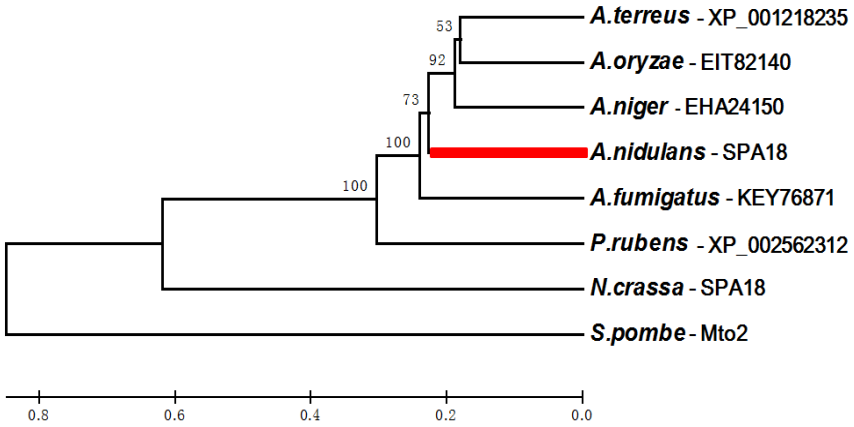

Figure 13. Phylogenetic analysis of SPA18 using Neighbor-Joining method. Values indicate the number of times (in percentages) that each branch topology was found in 2,000 replicates of a bootstrap analysis, assuming gamma-distributed rates for amino acid substitutions. The distance between branch points shows the relatedness of the sequences. The branches of *A. nidulans* SPA18 are highlighted.

2.2 Localization of SPA18

A strain in which SPA18 was tagged with GFP at the C-terminus was provided by Stephen Osmani. *GFP* and the selection marker *pyrG* from *A. fumigatus were* inserted by fusion PCR in between the last 1 kb of SPA18 ORF and 1 kb following the ORF. The whole fragment was transformed in wild type SO451, yielding *SPA18*::*GFP* strain SO1312. The fluorescence was also visualized at SPBs during interphase and mitosis, as well as to septa (two spots, disk-like), similar to ApsB (**Figure 14)**. The same localization patterns were obtained with N-terminal GFP tagging of SPA18 strain SYZ75, which was constructed by transforming pYZ66 (pMCB17apx vector with 1.0 kb N-terminal SPA18 insertion) into TN02A3.

2.3 Double deletion of *apsB* and *SPA18*

The Δ*SPA18* strain SO1334 was also kindly provided by Stephen Osmani. They used *AfpyrG* as selection marker, and the construction was similar to the Δ*apsB* strain. In case of the colony, Δ*SPA18* appeared the same as the wild type strain SO451 **(Figure 15)**. SO1334 was crossed with RMS011, yielding a para-aminobenzoic acid (*pabaA*) and pyridoxine auxotrophic (*pyroA*) mutant strain SYZ33, an arginin (*argB*) auxotrophic mutant strain SYZ32 and a

pyridoxine and arginin auxotrophic mutant strain SYZ31. Subsequently, we crossed SYZ33 with SYZ3 (Δ*apsB*). After selection, *SPA18* and *apsB* double deletion strain SYZ45 was created with the *pabaA* auxotrophic selection marker. The colony of SYZ45 produced less conidiospores like Δ*apsB* as compared to wild type, without any significant defect on the growth rate as well (**Figure 15)**. We also created an *apsB* and *SPA18* double deletion strain SYZ35 (*argB* auxotrophic*)* by crossing SYZ31 with SYZ3.

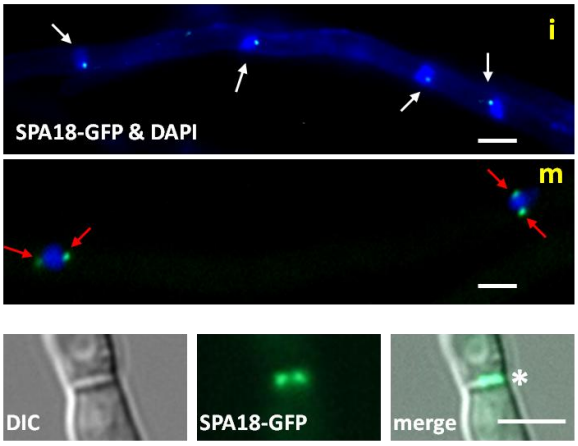

Figure 14. Localization of SPA18. The white arrows, red arrows and asterisk indicate SPA18 localization at interphase SPBs, mitotic SPBs and septum respectively. SO1312 was observed. The strain was grown in MMurea with pyridoxin overnight at 28°C. Bar, 5 μm; i, interphase; m, mitosis.

Figure 15. The colony of *ΔapsB* (SYZ3), *ΔSPA18* (SO1334) and the double mutant (SYZ45). The strains were grown on a MM agar plate with appropriate markers at 37°C for 3 days. Bar, 1 cm.

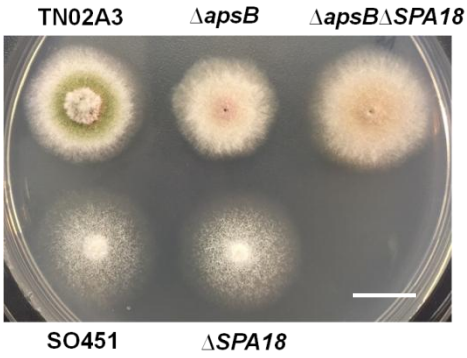

3 The interaction and interdependence between ApsB and SPA18

Since ApsB and SPA18 both localized at MTOCs, we attempted to investigate whether ApsB and SPA18 interacted with each other and localized interdependently in *A. nidulans*. In this part, co-localization analysis, Bimolecular Fluorescence Complementation (BiFC) assay and Yeast two Hybrid (Y2H) was carried out.

3.1 Co-localization of ApsB and SPA18

The N-terminal 1.0 kb of the ApsB ORF was digested with *Asc*I and *Pac*I from pYZ6, and ligated into the pMCB17apx-*mCherry* vector in which *GFP* was instead by *mCherry*. The resulting plasmid pYZ27 was transformed into SO1312. After screening, we got SYZ47 in

which ApsB was tagged with mCherry at the N-terminus and SPA18 was C-terminally tagged with GFP. In this strain, mCherry-ApsB was visualized to co-localize with SPA18-GFP at SPBs and sMTOCs **(Figure 16).**

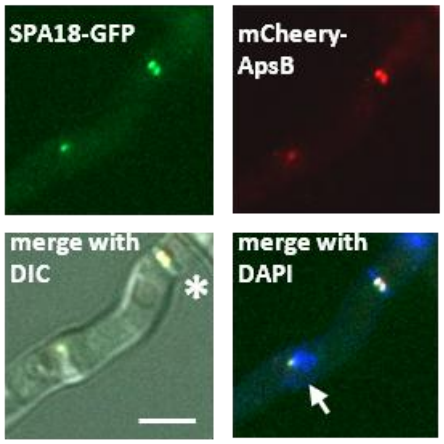

Figure 16. Co-localization of ApsB and SPA18. The arrowhead indicates the co-localization signals at SPB, and the asterisk indicates the septal co-localization signals. Strain SYZ47 was incubated in MMurea (2% glycerol) at 28°C overnight and observed. Bar, 5 µm.

3.2 Bimolecular Fluorescence Complementation assay

To analyze the interaction of ApsB and SPA18, a Bimolecular Fluorescence Complementation assay (BiFC or Split YFP) was performed. Full-length ApsB was amplified with primers apsB_AscI_fwd and apsB-4.7_PacI_rev, cloned into pMCB17apx-*YFP*^{C} vector in which *GFP* was instead by *YFP*^{C}, yielding pYZ47. Similarly, the full-length SPA18 was amplified with primers SPA18_AscI_fwd and SPA18-f_PacI_rev, cloned into pMCB17apx-*YFP*^{N} vector, giving pYZ56. Then pYZ56 and pYZ47 were co-transformed into TN02A3. After screening, the resulting strain SYZ61 was observed for YFP signals. As a result, YFP^{N}-SPA18 and YFP^{C}-ApsB interacted at SPBs and sMTOCs **(Figure 17)**. *Ancdc31*^{f}

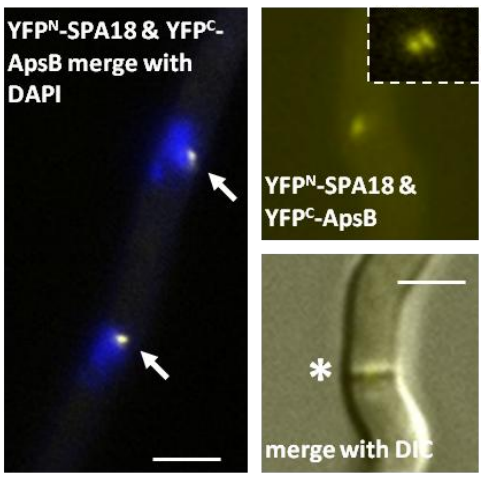

Figure 17. BiFC of ApsB and SPA18. The arrowheads and asterisk indicate the YFP signals at SPBs and sMTOC separately. Strain SYZ61 was incubated in MM (2% glycerol) overnight at 28°C and observed. Bar, 5 µm.

3.3 Yeast two Hybrid

In order to verify the observed protein-protein interaction in the BiFC assay, a Yeast two

Hybrid (Y2H) assay was performed. To this end full-length SPA18 cDNA was amplified with primers Y2H_SPA18_NdeI_F and Y2H_SPA18_BamHI_R using the total cDNA from TN02A3 as template, cloned into vector pGBKT7, yielding pYZ51. Similarly, the full-length ApsB cDNA was amplified with primers Y2H_ApsB_NdeI_F and Y2H_ApsB_BamHI_R, cloned into vector pGADT7-Rec, giving pYZ61. pYZ51 and pYZ61 were transformed separately into *S. cerevisiae* Y187 and AH109, yielding YSYZ1 and YSYZ2. After mating with them, we got strain YSYZ3. YSY3 can grow on SD-LW and SD-LWHA, with phenocopy as positive control **(Figure 18)**, indicating that SPA18 and ApsB can interact with each other and bind directly.

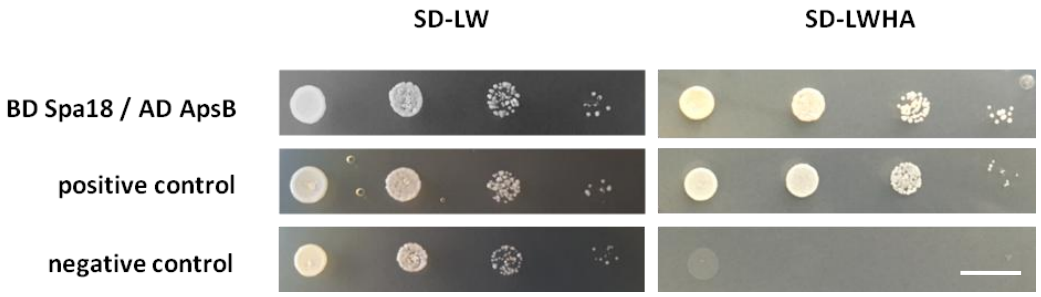

Figure 18. Y2H assay with ApsB and SPA18. Positive and negative controls were provided in the Matchmaker™ Gold Yeast Two-Hybrid System by Clontech Laboratories, Inc.. Dilution series of respective strains were grown on SD-LW and SD-LWHA at 30°C for 3 days. Bar, 1 cm.

3.4 Localization of ApsB and SPA18 to different MTOCs do not completely depend on each other

To answer the question whether SPA18 still localized to different MTOCs without ApsB, we crossed SYZ3 (Δ*apsB*) with SO1312(SPA18-GFP), giving SYZ38 with SPA18-GFP in the absence of ApsB. In this strain, SPA18-GFP was still seen at SPBs and septa with the same signal intensity as in SO1312 **(Figure 19, A)**, suggesting that SPA18 localized to SPBs and sMTOCs do not completely depend on ApsB. This is dramatically different from Mto2 and Mto1 in *S. pombe*, that Mto2 localizes to all MTOCs in an Mto1 dependent manner. On the other hand, whether localization of ApsB to different MTOCs depends on SPA18 was also investigated in a similar manner. SYZ32 was crossed with SYZ2 (GFP-ApsB), giving SYZ46 (GFP-ApsB, Δ*SPA18*). In this strain, GFP-AspB was also visualized at SPBs and septa in the same patterns as SYZ2 **(Figure 19, B)**, indicating the localization of ApsB is also not completely depending on SPA18. However, further analysis demonstrated that ApsB targeting to different MTOCs partially depend on SPA18 (see **IV 5.2**), this is consistent with *S. pombe* to some extent (also see **V 1.3**). The interdependence between ApsB and SPA18 still needs to be investigated deeply.

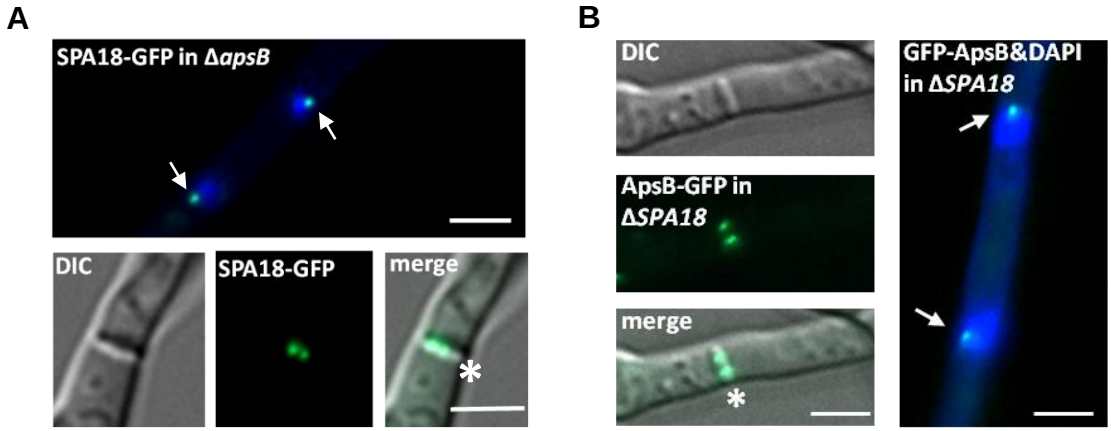

Figure 19. Interdependence of ApsB and SPA18 to different MTOCs. (A) SPA18 localization to SPBs and septa was not affected in the absence of ApsB. Strain SYZ38 was grown in MM overnight at 28°C and observed. **(B)** Localization of ApsB to different MTOCs doesn't completely depend on SPA18. Strain SYZ46 was grown in MM (2% glycerol) overnight at 28°C. Arrowheads indicate the signals at SPBs and asterisks indicate the septal localization. Bar, 5 μm.

4 The role of ApsB and SPA18 on microtubule organization

In *A. nidulans*, ApsB was found to be important for cytoplasmic MTs, astral MTs, nuclear migration and the activity of the MTOCs (Veith *et al.*, 2005). In the part, we compared the role of SPA18 in microtubule organization with ApsB.

4.1 The ApsB/SPA18 complex is essential for sMTOC formation

GCPC is an essential component of γ-TuRC (Xiong & Oakley, 2009). GCPC localized to both SPBs and sMTOCs in SNZ-SH80, in which GCPC was C-terminally tagged with GFP. SNZ-SH80 was crossed with SYZ3 (Δ*apsB*), SYZ31 (Δ*SPA18*) and SYZ35 (Δ*apsB*Δ*SPA18*) separately, yielding strains SYZ39 (GCPC-GFP in Δ*apsB*), SYZ42 (GCPC-GFP in Δ*SPA18*) and SYZ44 (GCPC-GFP in Δ*apsB*Δ*SPA18*). In all of these three strains, we didn't see any GCPC localizing at sMTOCs, and only to SPBs **(Figure 20)**. As a conclusion, ApsB and SPA18 are both indispensable for recruiting γ-TuRCs to septa, but not necessary for SPBs.

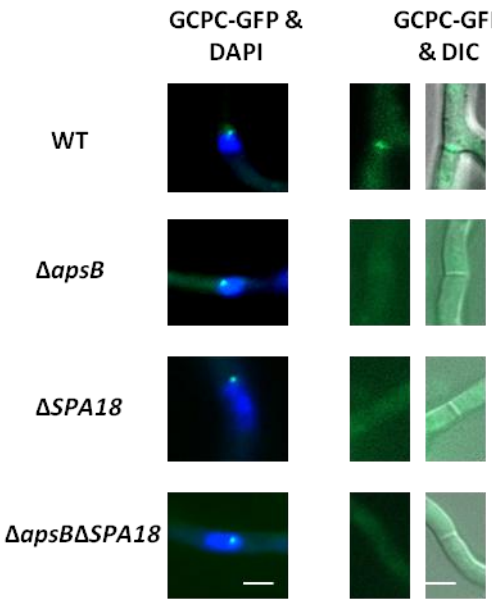

Figure 20. Localization of GCPC to septa depends on ApsB and SPA18. GCPC was still able to localize at SPBs in the absence of ApsB or SPA18 (left), by contrast, not to septa any more (right). Strains SNZ-SH80, SYZ39, SYZ42 and SYZ44 were grown in MM with appropriate selection markers at 28°C overnight and observed. Bar, 5 µm.

4.2 The activity of SPBs and sMTOCs in the absence of ApsB or SPA18

The kinesin-like motor protein KipA is an MT plus-end marker which can demonstrate the number of MTs emerging from MTOCs and determine the activity of MTOCs (Konzack *et al*., 2005; Veith *et al*., 2005). Strain SSH27 in which KipA was N-terminally tagged with GFP was crossed with SYZ33 (Δ*SPA18*) and SYZ45(Δ*apsB*Δ*SPA18*) separately, yielding SYZ43 (GFP-KipA in Δ*SPA18*) and SYZ51 (GFP-KipA in Δ*apsB*Δ*SPA18*). SSK92 (GFP-KipA, pyroA$^-$) was crossed with SYZ3, giving strain SYZ9 (GFP-KipA in Δ*apsB*). As a result, in the absence of SPA18 (SYZ43), ApsB (SYZ9) or both of them (SYZ51), nearly no GFP-KipA signal was detected to emerge from sMTOCs, while in SSH27, an average of 5.6 was detected per 100 s **(Figure 21)**. However, the number of GFP-KipA signals from SPBs was reduced by only 18.2%, 21.7% and 18.8% in Δ*SPA18*, Δ*apsB* and the double mutant, indicating a not severe effect in these three strains **(Figure 21)**. The comparison of the effect of ApsB/SPA18 on these two MTOCs will be discussed in **V 2**.

4.3 The number of cytoplasmic MT bundles and astral MTs in the absence of ApsB or SPA18

In order to investigate the microtubules in the absence of ApsB or SPA18, we crossed GFP-TubA strain SJW02 with SYZ3 (Δ*apsB*), SO1334 (Δ*SPA18*) and SYZ45 (Δ*apsB*Δ*SPA18*)

separately, giving SYZ11 (GFP-TubA in Δ*apsB*), SYZ34 (GFP-TubA in Δ*SPA18*) and SYZ49 (GFP-TubA in Δ*apsB*Δ*SPA18*). The number of cytoplasmic MT bundles was counted during interphase. Compared to SJW02, the number of cytoplasmic MT bundles respectively decreased by 31%, 36.2%, and 34.5% in Δ*SPA18*, Δ*apsB* and the double mutant **(Figure 22, A & B)**. During mitosis, the astral MTs in Δ*SPA18* (SYZ34) did not show any significant aberrance (only 1.6% reduction), unlike in Δ*apsB* (SYZ11) and the double mutant (SYZ49), which respectively decreased by 61.0% and 65.2% **(Figure 22, C & D)**. Time-lapse analyses of mitosis revealed that the duration of mitosis was unaltered in mutants. As a conclusion, the absence of SPA18 or ApsB influenced the cytoplasmic microtubules nucleation, which might be caused by the defect of sMTOCs as well as the SPBs. Astral MTs formation only requires ApsB.

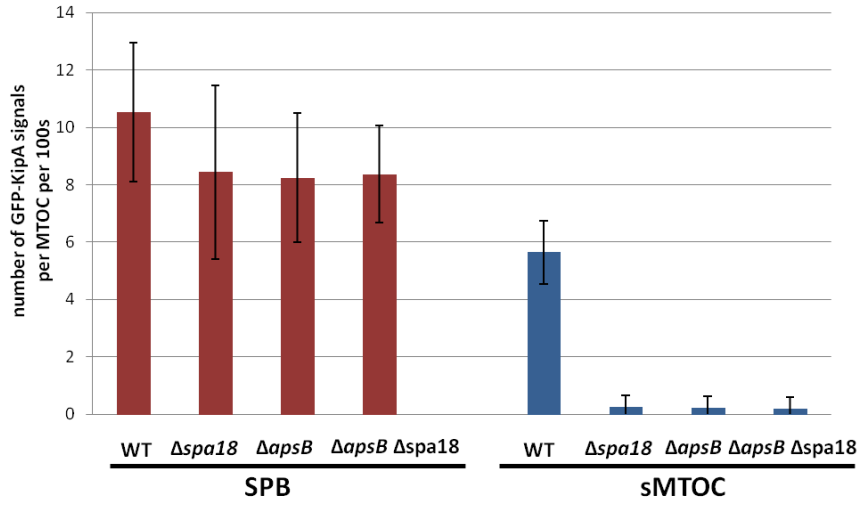

Figure 21. The activity of SPBs and sMTOCs in WT, Δ*apsB*, Δ*SPA18* and the double mutant. Time-lapse analyses were performed for counting the number of GFP-KipA signals from MTOCs. Strains SSH27, SYZ43, SYZ9 and SYZ51 were grown in MM (2% glycerol) with appropriate selection markers at 28°C overnight and observed. 50 SPBs and 50 sMTOCs were counted for each strain.

4.4 Nuclear migration in the absence of ApsB or SPA18

Since the astral MTs during mitosis were not significantly affected in Δ*SPA18*, the nuclear migration of hyphae and conidiospore formation were also quite regular in Δ*SPA18* (SO1334) **(Figure 23, A & B)**. By contrast, nuclear migration in Δ*apsB* (SYZ3) and Δ*apsB*Δ*SPA18* (SYZ45) was seriously affected **(Figure 23, A & B)**, which might be caused by the aberrance of the astral microtubules. This finding can help us to explain the sporulation of these stains, as presented in **Figure 15.**

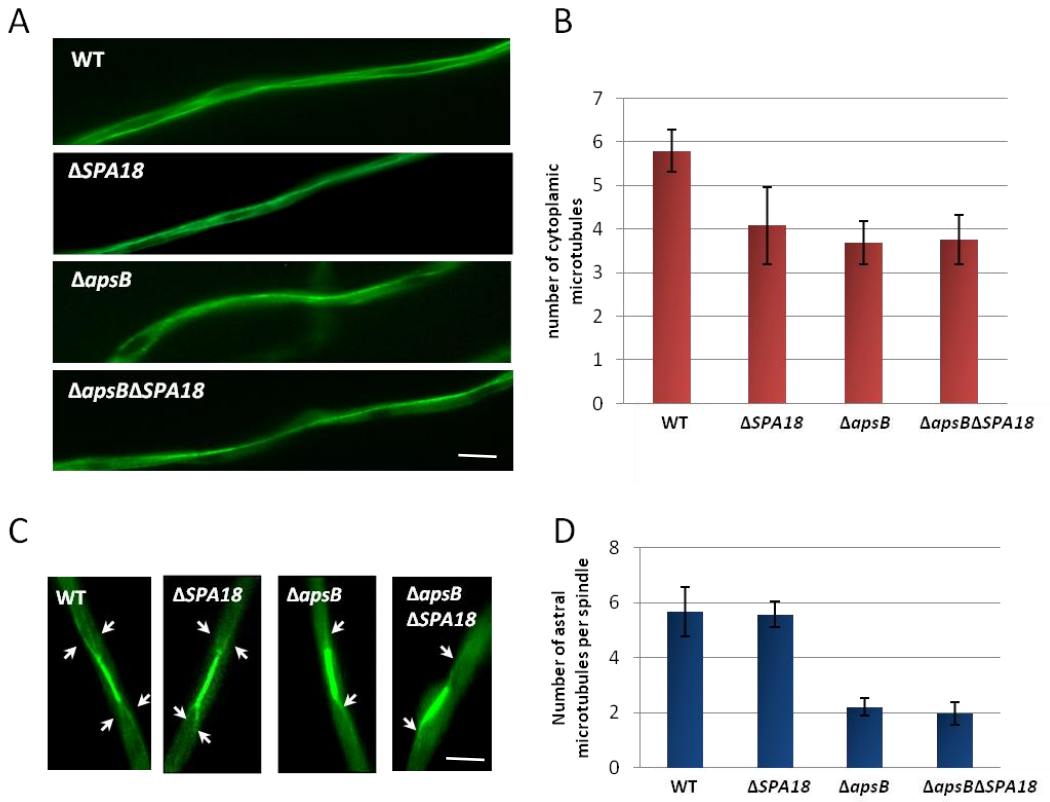

Figure 22. The cytoplasmic MTs and the astral MTs in WT, Δ*apsB*, Δ*SPA18* and double mutant. (A) and **(B)**, the cytoplasmic MTs during interphase. 100 hyphae were counted for each strain. **(C)** and **(D)**, the astral MTs in mitosis, which are indicated with arrowheads. 50 spindles were counted for each strain. Strains SJW02, SYZ34, SYZ11 and SYZ49 were grown in MM (2% glycerol) with appropriate selection markers at 28°C overnight and observed. Bar, 5 µm.

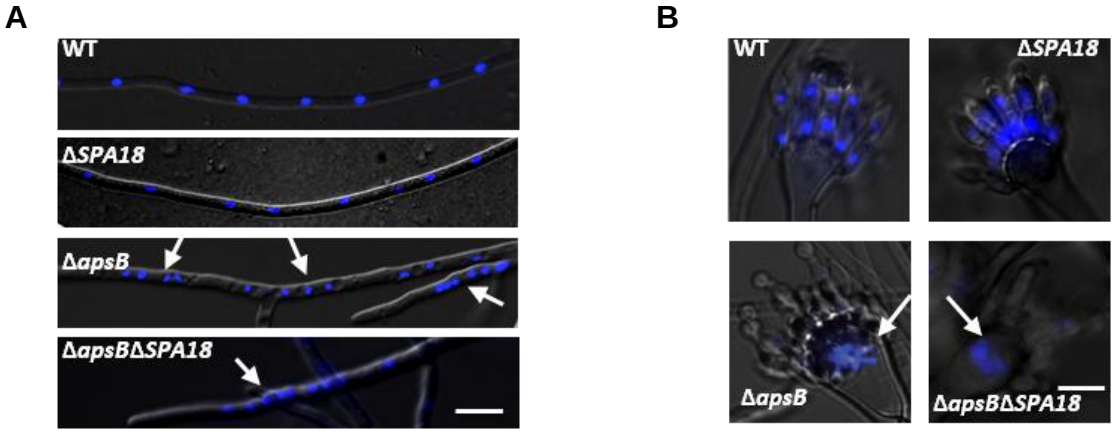

Figure 23. Nuclear migration in WT, Δ*apsB*, Δ*SPA18* and the double mutant. (A) Nuclear migration in hyphae. Strains TN02A3, SO1334, SYZ3 and SYZ45 were grown in MM with appropriate selection markers at 28°C overnight and observed. **(B)** Nuclear migration in conidiophores. The same strains as in **(A)** were incubated on glass slides with a thin layer of solid MM with 1.5% agarose and the appropriate selection markers at 37°C for 2-3 days and observed. The nuclei were stained with DAPI. Arrowheads indicate the nuclear migration defect. Bar, 5 µm.

5 Domain analysis of ApsB

5.1 The CM1 motif is responsible for recruitment of γ-TuRCs to MTOCs

The Centrosomin Motif 1 (CM1) domain, required for proper recruitment of γ-TuRC to MTOCs, is conservative in eukaryotes such as *S. pombe* Mto1 and Pcp1, *S. cerevisiae* Spc110 and Spc72 (Samejima *et al*., 2008). The CM1 domain of ApsB was predicted to be at 525 to 599 aa (pfam07989). To investigate whether this predicted domain is required for recruitment of γ-TuRC, we deleted this domain in ApsB by transforming into Δ*apsB* with a fragment in which CM1 coding region was removed from *apsB*. In case of constructing the fragment, the left part was amplified with apsB_AscI_fwd and ΔCM1_L_linker_R, and right part was amplified with ΔCM1_R_F and apsB-4.7_PacI_rev. The two parts were fused together by fusion PCR, followed by digestion with restriction enzymes *Asc*I and *Pac*I and ligation to a pMCB17apx-*mCherry* vector, yielding pYZ65. The GCPC (also called AlpB) C-terminal tagging GFP cassette *alpB*::*GFP*::*AfpyrG*::RB-*alpB* was amplified with Alp6_Nprimer_fwd and Alp6_Nprimer_rev (Zekert *et al.*, 2010) using genomic DNA from strain SNZ-SH80 (*AlpA*::*GFP*) as the template. The PCR product and pYZ65 were co-transformed into SYZ3 (Δ*apsB*), yielding strain SYZ56 with *mCherry*::*apsB* and *GCPC*::*GFP*. In this strain, ApsB still localized to SPBs and sMTOCs **(Figure 24, A, 3rd column)**, indicating that CM1 is not required for ApsB targeting to MTOCs. However, the γ-TuRC marker GCPC was only detected at SPBs but not at septa **(Figure 24, A, 2nd column)**. Therefore, we proposed CM1 domain is required for the recruitment of γ-TuRC. At septa, ApsB, as well as its CM1 domain, is an indispensable receptor for γ-TuRCs. Besides, SYZ56 (CM1 depletion) presented almost the same conidiospore formation as SYZ3 (Δ*apsB*) **(Figure 24, B)**, indicating that ApsB plays an important role on sporulation by recruiting γ-TuRC.

5.2 ApsB targeting to multiple distinct MTOCs via the MASC domain and the SMB domain

In *A. nidulans*, two domains responsible for ApsB targeting to different MTOCs were identified. One of them is the conserved MASC domain, which was first characterized in *S. pombe* Mto1 and found to be important for targeting Mto1 to multiple distinct MTOCs (Samejima *et al.*, 2010). This domain was identified in ApsB at 1476 to 1524 aa by BLASTP analysis. In addition, the sequence following the MASC domain at the C-terminal end of the protein (1525 to 1574 aa), termed sMTOC binding (SMB) domain, was also identified to play a very important role in ApsB targeting **(Figure 25, A)**.

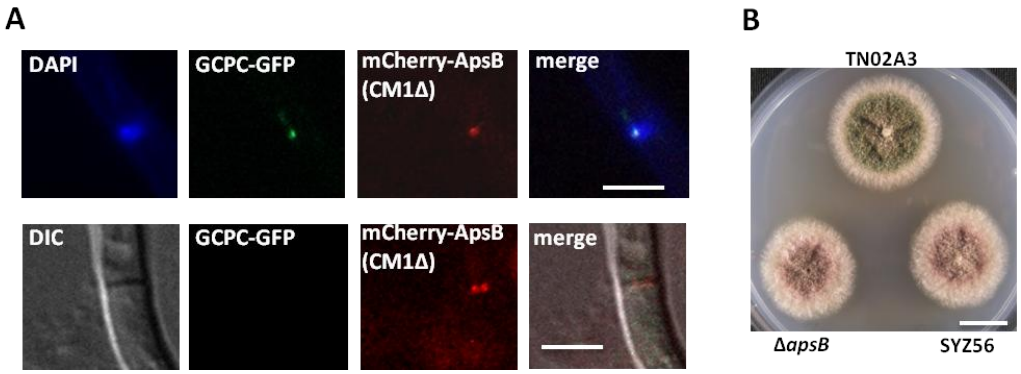

Figure 24. The role of ApsB CM1 domain. (A) In the absence of CM1, γ-TuRCs were not able to target to sMTOCs, only to SPBs. Strain SYZ56 was incubated in MM (2% glycerol) overnight at 28°C. Bar, 5 µm. **(B)** The strain lack of CM1 domain of ApsB (SYZ56) is with phenocopy to *ΔapsB* (SYZ3). The strains were grown on an MM (2% glycerol) agar plate with uridin, uracil and pyridoxin at 37°C for 3 days. Bar, 1 cm.

The fragment of ApsB without the SMB domain was amplified with primers apsB_AscI_fwd and apsB_ΔSMB_PacI_rev, and cloned into pMCB17apx-*pyroA* vector, giving plasmid pYZ29. pYZ29 was co-transformed into SYZ3 (Δ*apsB*) with pAB4-1 (with *A. niger pyrG* ORF), yielding strain SYZ40. pYZ29 was also co-transformed with pCK17 (with *A. nidulans pabaA* ORF) into SYZ45 (Δ*apsB*Δ*SPA18*), yielding SYZ53. Without the SMB domain, ApsB still localized to both SPBs and sMTOCs (SYZ40), while in the absence of SPA18, we were not able to see ApsB localizing to sMTOCs any more but only to SPBs (SYZ53) **(Figure 25, B)**, suggesting SPA18 is required for ApsB localizing to septa when the SMB domain is absent, and ApsB targeting to SPBs doesn't require the SMB domain.

Similarly, the fragment of ApsB without MASC and SMB domains was amplified with primers apsB_AscI_fwd and apsB_ΔMASCΔSMB_PacI_rev, cloned into pMCB17apx-*pyroA* vector, giving plasmid pYZ28. The resulting pYZ28 was co-transformed into SYZ3 (Δ*apsB*) with pAB4-1, yielding strain SYZ41. By co-transformation with pYZ28 and pCK17 into SYZ45 (Δ*apsB*Δ*SPA18*), SYZ52 was yielded. Without the MASC domain and the SMB domain, ApsB was only visualized with very weak signal at SPBs and no signal at septa (SYZ41). In the absence of SPA18, no signal was detected at SPBs or septa (SYZ52) **(Figure 25, B)**. We assume that the MASC domain is required for ApsB targeting to SPBs, as well as to septa.

In order to delete the MASC domain of ApsB, the left part (amplified with apsB_AscI_fwd and ΔMASC_linker_rev) and the right part (amplified with apsB_SMB_fwd and apsB-4.7_PacI_rev) were fused together by fusion PCR, cloning into pMCB17apx-*pyroA* vector and giving plasmid pYZ67. pYZ67 was also co-transformed with pAB4-1 and pCK17 respectively into SYZ3 and SYZ45, giving strains SYZ57 and SYZ58. We also only saw very weak signal at SPBs not at septa **(Figure 25, B)**. This confirms us that only the SMB domain is not enough for ApsB localizing to septa. The MASC domain is also required.

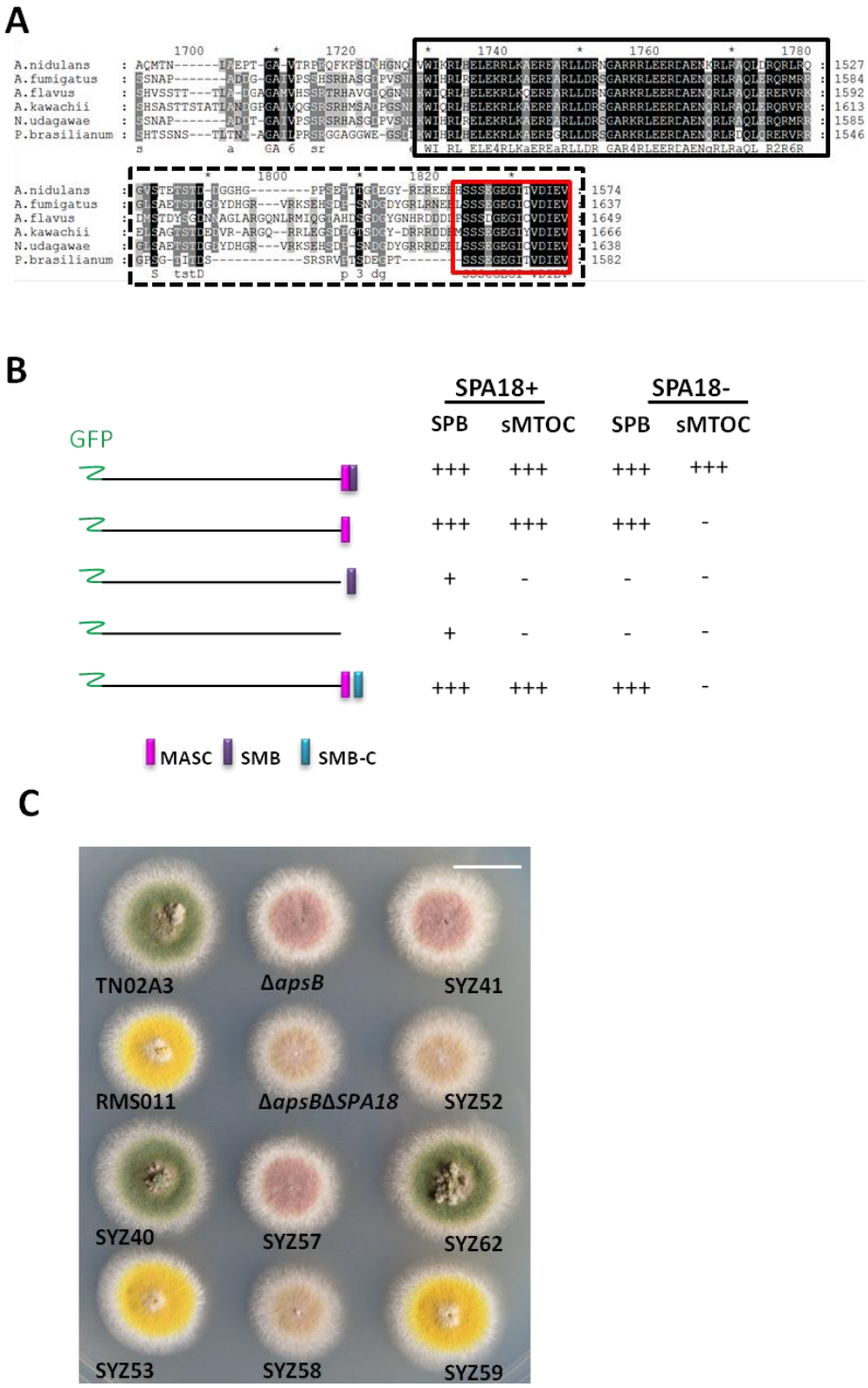

Figure 25. Characterization of the MASC domain and the SMB domain in ApsB. (A) C-terminal sequence alignment of ApsB homologs in different organisms. The MASC, SMB and SMB-C domains are indicated with black solid-line box, black dashed-line box and red box, respectively. **(B)** The localization of ApsB in the absence of MASC, SMB, or the sequence between MASC and SMB-C. Strains SYZ2, SYZ46, SYZ40, SYZ53, SYZ57, SYZ58, SYZ41, SYZ52, SYZ62 and SYZ59 were incubated in MM (2% glycerol) with appropriate selection markers at 28°C overnight and observed with fluorescent microscope. ApsB signal intensity: +++, stong; +, weak; -, no signal. **(C)** Comparison of the sporulation of the strains in **(B)**. Strains were grown on an MM (2% glycerol) agar plate with appropriate markers at 37°C for 3 days. Bar, 1 cm.

In addition, during the alignment of ApsB orthologues in different organisms, we found the last C-terminal 14 amino acids of the SMB domain are highly conserved **(Figure 25, A)**. Thus, we assumed that these 14 amino acids (termed SMB-C) were important for the function of SMB domain, while the sequence between MASC and SMB-C domain was not conserved and might be dispensable. To verify our assumption, we fused the SMB-C domain directly to MASC domain by oligonucleotides synthesis. The yielded plasmid pYZ68 was co-transformed respectively with pAB4-1 and pCK17 into SYZ3 and SYZ45, resulting in strains SYZ62 and SYZ59. However, in strain SYZ59, we still didn't see ApsB localizing to septa in the absence of SPA18 **(Figure 25, B)**, while the localization of ApsB was not affected in SYZ62 as in the absence of the whole SMB domain in SYZ40, indicating that the sequence between MASC and SMB-C is also required for ApsB targeting to septa.

Besides, it appears that the proper localization at SPBs (SYZ40, SYZ53, SYZ62 and SYZ59) was important for sporulation. The sporulation was severely affected when ApsB localization was weak (SYZ41 and SYZ57) or invisible (SYZ52 and SYZ58), like in Δ*apsB* (**Figure 25, C)**. The functions of the two domains are further discussed in **V 3**.

6 Localization of ApsB and SPA18 to septa requires SPA10

SPA10 is a septal pore-associated protein as well as an intrinsically disordered protein (IDP), which was also first identified in *N. crassa* together with SPA18 and found to be required to suppress septation (Lai *et al.*, 2012). The homolog in *A. nidulans* SPA10 (AN1948) was found by BLASTP analysis in (Shen *et al.*, 2014). SPA10-GFP still associated with mature septa after septation was completed, localizing as a central disk structure in the vicinity of the septal pore (Shen *et al.*, 2014), which is similar to ApsB and SPA18 as we saw before. SPA10 deletion strain SO1330 was provided by Stephen Osmani, and the colony appears the same as the wild type SO451, indicating no significant growth defect caused by SPA10 disruption. To answer the question how ApsB and SPA18 are recruited to the septa, SPA10 was considered as a candidate due to its similar localization pattern as ApsB and SPA18. To verify our hypothesis, ApsB and SPA18 were tagged with GFP at N-terminus by transforming plasmids pYZ26 and pYZ66 into SO1330 separately, yielding SYZ69 and SYZ74. As we expected, compared with the localization in wild type, both ApsB and SPA18 only localized to SPBs but not to septa any more **(Figure 26)**, suggesting that SPA10 is required for the localization of them. But the effect of SPA10 on ApsB and SPA18 is direct or indirect is unknown. We also analyzed whether ApsB still localized to the septa in the absence of septal pore-associated proteins SPA1 (AN4647), SPA3 (AN4698), SPA11 (AN1250), SPA13 (AN4484) and SPA14 (AN10598), as well as a septation kinase KfsA (AN0822), which also localizes at septa and contains long, intrinsically disordered domains and fulfils sequence characteristics of a SPA protein. These knockout strains were also provided by Stephen

Osmani. However, no significant difference for ApsB localization at septa was found in the absence of these SPA proteins or KfsA.

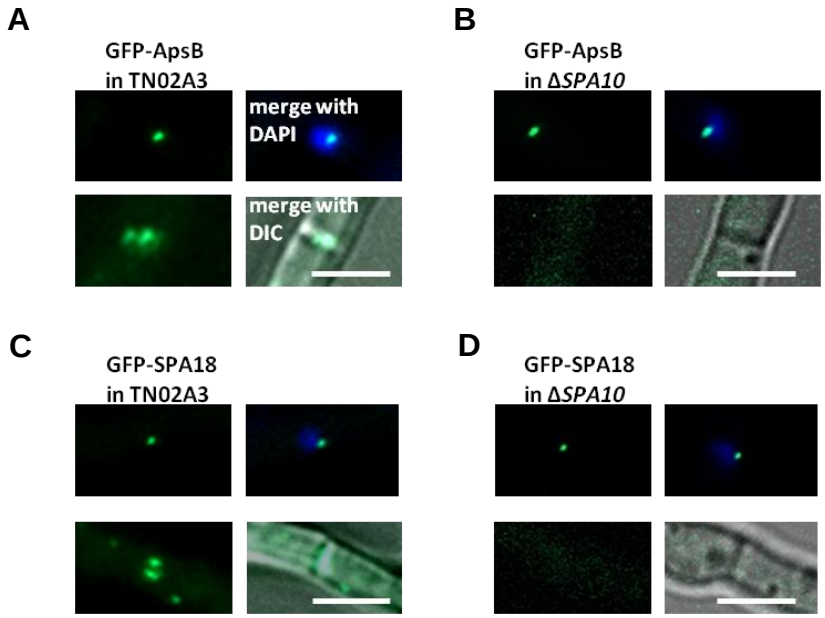

Figure 26. Localization of ApsB and SPA18 to septa requires SPA10. ApsB **(A)** and SPA18 **(C)** localized to SPBs and sMTOCs in wild type TN02A3, however, not to septa in Δ*SPA10* **(B & D)**. Strains in A, B, C and D are SYZ2, SYZ69, SYZ75, SYZ74, respectively. They were all incubated in MM (2% glycerol) with appropriate selection markers at 28°C overnight and observed. Bar, 5 µm.

7 Preliminarily differentiation of SPB and sMTOC

Based on the well characterized MTOCs in budding yeast *S. cerevisiae* and fission yeast *S. pombe*, we attempted to identify new SPB components in *A. nidulans* by homologous alignment. Within the 17 known SPB proteins in *S. cerevisiae*, 10 were found with orthologues in *A. nidulans*. They are γ-tubulin (ScTub4), GCPB (ScSpc97), GCPC (ScSpc98), ApsB (ScSpc72), SepK (ScNud1), CaM (ScCmd1), PcpA (ScSpc110), An-Ndc1 (ScNdc1), An-Cdc31 (ScCdc31) and the new identified SfiA (AN0704, ScSfi1). In case of these proteins, γ-tubulin, GCPB, GCPC and ApsB have already been mentioned before. SepK, PcpA, An-Cdc31, SfiA and a novel component of γ-TuRC MztA which was identified as an orthologue to *S. pombe* Mzt1, will be investigated below. CaM and An-Ndc1 will be described in **V 5**.

7.1 SepK is the ApsB receptor at SPBs

SepK (AN2459) is the orthologue of *S. cerevisiae* Nud1 and *S. pombe* Cdc11 in *A. nidulans*. All of these three proteins shared a highly conserved leucine-rich repeat (LRR) region at the C-terminus (http://smart.embl-heidelberg.de/) **(Figure 27, A)**, which is important for protein

interactions thus involved in signal transduction pathways (Kobe & Deisenhofer, 1995). Both SepK and Cdc11 were reported to be involved in septation initiation network (SIN) in *A. nidulans* and *S. pombe* respectively (Kim *et al.*, 2009; Tomlin *et al*., 2002). Nud1 was also required for mitotic exit network (MEN) in *S. cerevisiae*. In addition to the signal transduction, Nud1 is also a core component of SPB, binding to Cnm67 as well as recruiting C-Spc72 (ApsB) via its C-terminus (Gruneberg *et al.*, 2000). Here comes our hypothesis in *A. nidulans* that ApsB may also be recruited to the outer plaque of the SPBs by SepK, since it shares the conserved LRR region at the C-terminus with Nud1, which is responsible for Spc72 binding.

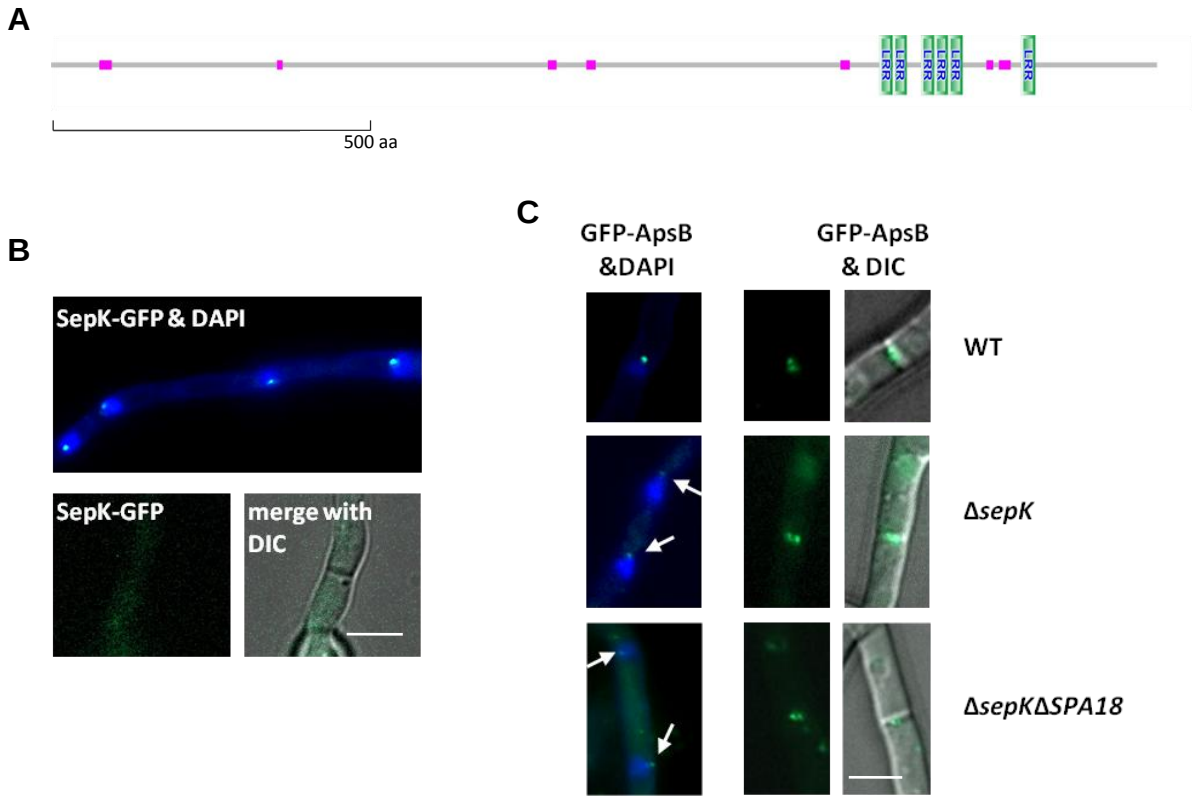

Figure 27. SepK is the ApsB receptor at SPBs. (A) SepK has a predicted leucine-rich repeat (LRR) region at the C-terminus, which was identified by domain analysis with SMART (http://smart.embl-heidelberg.de/). **(B)** SepK localizes at SPBs but not at septa. LO1591 was incubated in MM with riboflavin and pyridoxin at 28°C overnight and observed. **(C)** Localization of ApsB to SPBs and sMTOCs in WT, Δ*sepK* and Δ*sepK*Δ*SPA18*. Arrowheads indicate the weak GFP-ApsB signals at SPBs in Δ*sepK* and Δ*sepK*Δ*SPA18*. Strains SYZ2, SYZ60 and SYZ70 were incubated in MM (2% glycerol) at 28°C overnight and observed. Bar, 5 µm.

Strain LO1591 in which C-terminal SepK was tagged with GFP and *sepK* disruption strain LO1906 were kindly provided by Berl Oakley (Ohio University, US). We also detected that SepK localized only to SPBs but not at septa **(Figure 27, B)**. ApsB was tagged with GFP at N-terminus in Δ*sepK* by transforming a GFP-ApsB plasmid pYZ26 into LO1906. Compared to the wild type, the resulting SYZ60 strain exhibited the same localization pattern at septa but

much weaker signal intensity at SPBs **(Figure 27, C)**. This indicates that SepK is required but not the only receptor for targeting ApsB to SPB. Considering that SPA18 is also involved in ApsB localization, we created *sepK* and *SPA18* double mutant SYZ70 by crossing SYZ32 with LO1906, followed by transforming pYZ26 into SYZ70 to tag ApsB with GFP, yielding SYZ71. Surprisingly, the weak ApsB signal was still visualized at SPBs. We speculate that in addition to SepK, there are supposed to be other anchors for ApsB targeting to the SPB, like Kar1 ortholog, which will be discussed in **V 1.1**.

7.2 PcpA is an SPB-specific protein

Recently, PcpA (AN3062) was identified as an essential SPB component, which is crucial for microtubule organization as well as nuclear migration by binding to Calmodulin at SPBs (Chen *et al*., 2012). However, the characterization was quite limited. PcpA is highly conserved in eukaryotes such as *S. cerevisiae* (Spc110), *S. pombe* (Pcp1) and human (Pericentrin) (Knop & Schiebel, 1997; Flory *et al*., 2000; Flory *et al.*, 2002). By domain analysis (http://smart.embl-heidelberg.de/) and homologous alignment, we found that PcpA, like its orthologues, contains the three major domains CM1, SPM and PACT **(Figure 28, A)**. CM1 and SPM are required for recruitment of γ-TuRCs to SPBs, and PACT is responsible for the cellular localization of PcpA. PACT domain was also reported by (Chen *et al*., 2012).

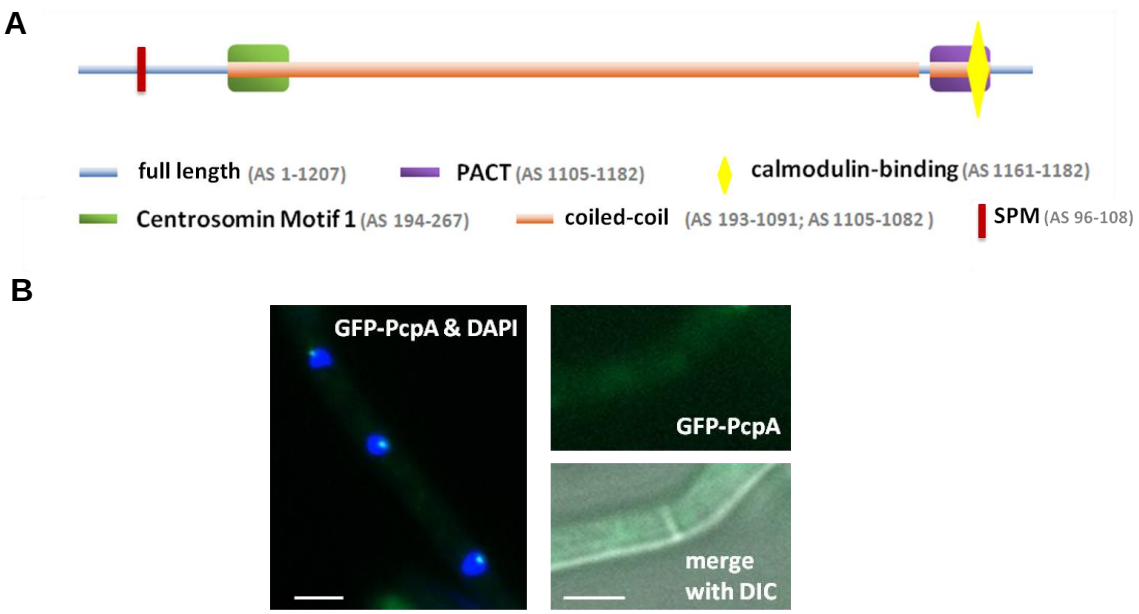

Figure 28. PcpA is an SPB-specific protein. (A) Domains of PcpA. The PACT, Calmodulin-binding, Centrosomin Motif 1 and coiled-coil domains were predicted by domain analysis (http://smart.embl-heidelberg.de/). The SPM domain was found by homologous alignment with GeneDoc. **(B)** Localization of PcpA. CPA02 was incubated in MM (2% glycerol) with riboflavin and pyridoxin at 28°C overnight and observed. Bar, 5 µm.

To our knowledge, PcpA is supposed to be localizing at the inner plaque of SPB, and

specifically required for mitotic nuclear microtubules formation. But we have no idea whether it is also a sMTOC associated protein. Therefore, we asked Ling Lu (Nanjing Normal University, China) for the GFP-PcpA strain CPA02 and observed the localization of PcpA in live cells. As we expected, we didn't see any GFP-PcpA signal at septa **(Figure 28, B)**, suggesting that PcpA is an SPB (inner plaque) specific protein.

7.3 A novel γ-TuRC component MztA

By BLASTP analysis with *S. pombe* mzt1, we identified a new γ-TuRC component, MztA (AN1361). MztA is a very tiny protein with only 63 aa and 6.7 kDa MW, residing on chromosome VIII. Bachelor student Marjorie Schmid tagged GFP at the C-terminal MztA (strain SMS4) by fusing MztA ORF plus 1 kb left border, $(GA)_5$-*GFP-AfpyrG* cassette and 1 kb right border of ORF together, followed by transformation of the fragment into TN02A3. We observed MztA-GFP localized at both SPBs and sMTOCs, with a similar localization pattern as GCPC **(Figure 20 & Figure 29)**. This is not difficult to explain since Mzt1 was reported to directly bind to Alp6 (GCPC) in *S. pombe* (Dhani *et al*., 2013). Interestingly, when we attempted to tag GFP at the N-terminus of MztA, no signal was detected. This is either because the N-terminus of MztA is required for its cellular localization or the function of MztA was influenced by the big GFP structre without a linker in between due to the tiny structure of MztA. Marjorie Schmid also created an MztA deletion strain SMS1. Since Mzt1 is essential for cell viability in both *S. pombe* and human (Dhani *et al.*, 2013; Masuda *et al*., 2013), it is surprising for us that Δ*mztA* (SMS1) is still viable, in spite of a severe defect on sporulation. This might be because MztA plays different roles in *A. nidulans* rather than γ-TuRC recruitment in *S. pombe* or human (Lin *et al*., 2015). Another reason could be that other proteins can compensate for the lack of MztA.

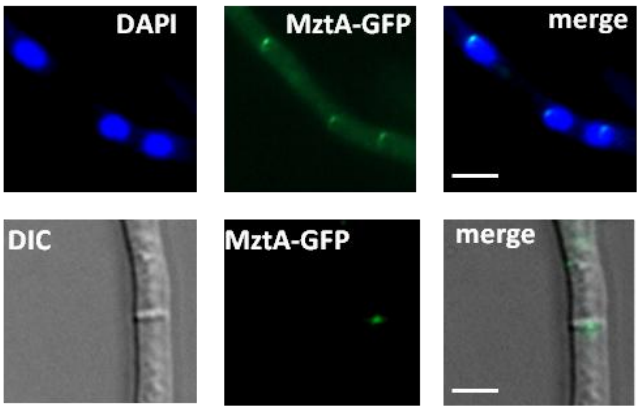

Figure 29. Localization of MztA. Strain SMS4 was incubated in MM (2% glucose) with pyridoxin at 28°C overnight and observed. Bar, 5 μm.

7.4 SPB duplication associated proteins SfiA and centrin/Cdc31

By BLASTP analysis with *S. cerevisiae* Sfi1, another SPB associated protein SfiA (AN0704) was also identified in *A. nidulans*. In *S. cerevisiae*, Sfi1 and Cdc31 are two essential SPB

components locating at the half-bridge site. These two proteins bind together with another membrane-anchored protein Kar1 to implement the duplication process of the SPBs. Marjorie Schmid created a GFP-SfiA strain SMS3 and found it localized at SPBs but not to septa. And when she transformed the SfiA deletion cassette in TN02A3, the growing transformants were always heterokaryons, indicating SfiA should be an essential gene for cell viability. Cdc31 has already been characterized in (Osmani *et al*., 2006) as an essential gene for cell cycle as well. They tagged GFP at the C-terminus of Cdc31 but this is lethal. Therefore, Marjorie Schmid attempted to tag N-terminal Cdc31 with GFP (SMS6), and fortunately visualized the localization of GFP-Cdc31 at SPBs and not to septa as well. Thus, we assume that SfiA and Cdc31 are SPB-specific duplication proteins, and not related to the organization of sMTOCs. All the results from Marjorie Schmid could be found in her Bachelor thesis (KIT library, 2015).

8 The role of peroxisomes in microtubule organization

PexC is an indispensable protein for peroxisome biosynthesis (Heiland & Erdmann, 2005). Andreas Herr deleted the full-length *pexC* ORF in TN02A3, yielding strain SAH3. The conidiospore production in SAH3 was severely affected and only produced 4.5% spores compared to the wild type **(Figure 30, A & B)**. The spore formation was again recovered when we transformed *alcA-pexC* (pYZ13) into SAH3 and obtained the re-complementation strain SYZ5 **(Figure 30, A & B)**. A very interesting fact is that when we used an *alcA-GFP-pexC* cassette (pYZ1) for re-complementation, the sporulation was not recovered, indicating the disrupted function of PexC by GFP. Peroxisomes are required for biotin biosynthesis in *A. nidulans* (Tanabe *et al.*, 2011). Thus, SAH3 is not able to grow on an MM+U/U+avidin (1 µg/ml) agar plate, resembling the biotin auxotroph strain FGSC26. Since avidin can interact with the biotin in agar, this result suggested that the biotin production was blocked and thus peroxisomes are absent in SAH3 **(Figure 30, C)**. Another evidence of the absence of peroxisomes in SAH3 is by MAS (encoded by *acuE*), an enzyme involved in malate synthesis, which contains a PTS1 for being imported into peroxisomes (Szewczyk *et al*., 2001) and has been used as a marker for peroxisomes. The peroxisomes of wild type (TALX207-10) were visualized big dot-like in the cytoplasm of the hyphae **(Figure 30, D, upper row)**. By contrast, when *GFP-acuE* (pYZ9) was transformed into SAH3, the resulting SYZ4 strain didn't exhibit any significant fluorescence signal **(Figure 30, D, lower row)**, indicating the lack of peroxisomes in the absence of PexC.

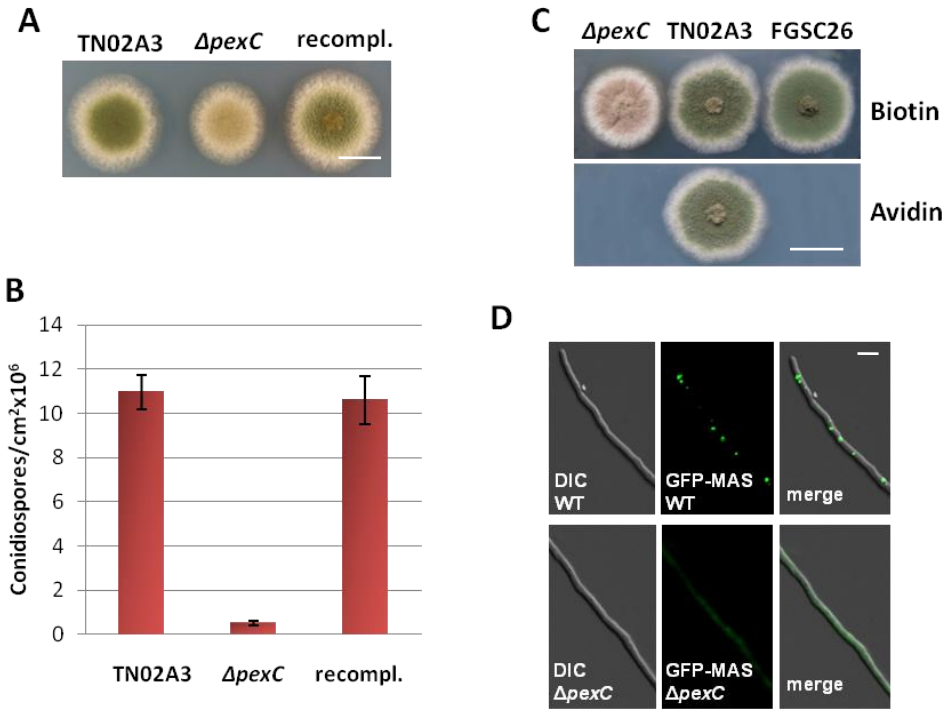

Figure 30. The phenotypes of Δ*pexC* (SYZ3) strain. (A) Comparison of the sporulation in WT (TN02A3), Δ*pexC* (SAH3) and re-complementation strain (SYZ5). Strains were grown on an MM (2% glycerol) agar plate with uridin, uracil and pyridoxin at 37°C for 3 days. Bar, 1 cm. **(B)** Quantification of the spores of the strains in **(A)**. Equivalent number of spores were spread on MM (2% glycerol) agar plates with appropriate selection markers. After 3 days at 37°C, the number of spores was counted from 5 cut pieces with the back of a 1 ml pipette tip. Spores were washed off and counted in a Neubauer chamber. **(C)** Avidin can inhibit the growth of Δ*pexC*, as well as the biotin auxotroph strain FGSC26. Strains were grown on an MM agar plate with uridin, uracil and pyridoxin at 37°C for 3 days. Avidin, 1 µg/ml; Bar, 1 cm. **(D)** The lack of peroxisomes in the absence of PexC. Strains TALX207-10 (upper row) and SYZ4 (lower row) were grown respectively in MM and MM (2% glycerol) with appropriate markers at 28°C overnight and observed. Bar, 5 µm.

Due to the conidiospore production defect in Δ*pexC* (SAH3), PexC was speculated to play a role in microtubule associated cell growth. The hyphal nuclear migration was investigated in TN02A3, Δ*pexC* (SAH3) and Δ*apsB* (SYZ3). Most distances between neighbored nuclei are between 10 and 16 µm in TN02A3, While in Δ*apsB*, most nuclei are too close or too far away **(Figure 23, A & Figure 31, A)**, indicating a severe nuclear migration defect in it. By contrast, in Δ*pexC*, only partially nuclear migration defect was found in comparison to TN02A3 and Δ*apsB* **(Figure 31, A & B)**. As for conidiophores, 98% of the wild type could succeed with proper migration of nuclei into the conidiophore metulae, while 52% failed in Δ*pexC* **(Figure 31, C)**.

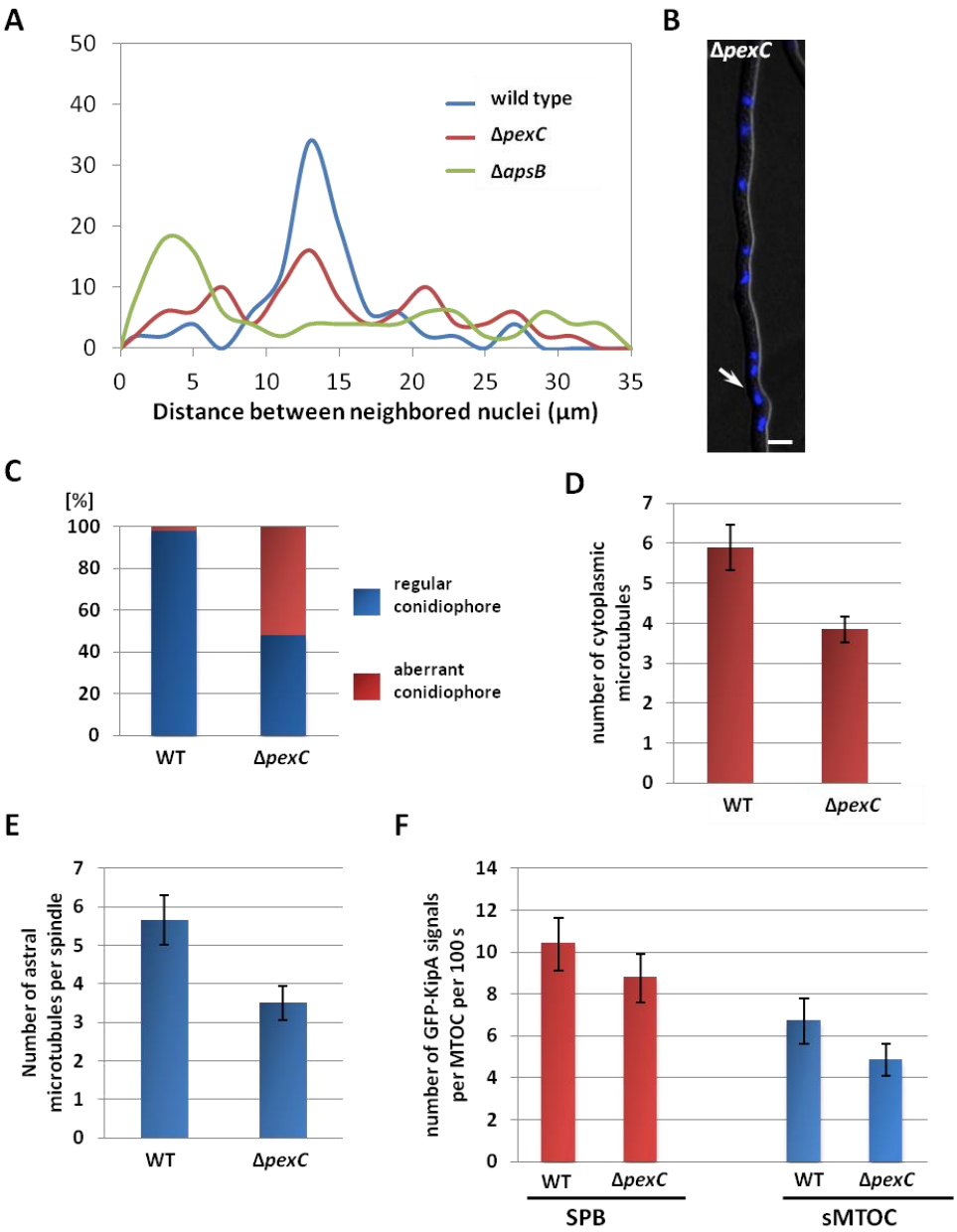

Figure 31. Microtubule organization in WT and Δ*pexC*. (A) Distribution profile of distances between neighbored nuclei in WT (TN02A3), Δ*apsB* (SYZ3) and Δ*pexC* (SAH3). Strains were grown in MM with appropriate markers at 28°C overnight and observed. 200 distances were counted for each strain. **(B)** Nuclear migration in vegetative hypha of Δ*pexC* (SAH3). The arrowhead indicates the defective migration. Bar, 5 µm. **(C)** Quantitative analysis of nuclear migration in conidiophores. The same strains as in (A) were on a thin layer of solid MM with 1.5% agarose and the appropriate selection markers on the glass slide at 37°C for 2-3 days. 50 conidiophores were observed for each strain. **(D)** Comparison of the number of cytoplasmic MTs in WT and Δ*pexC.* 100 hyphae were counted for each strain. Strains were grown in MM with appropriate markers at 28°C overnight and observed. **(E)** Number of astral MTs of the spindles during mitosis in WT and Δ*pexC*. 50 spindles were counted for each strain. For (D) and (E), strains SJW02 and SYZ4 were grown in MM (2% glycerol) with appropriate markers at 28°C overnight and observed. **(F)** Quantitative analysis of GFP-KipA counts at different MTOCs. Strains SSK92 and SYZ8 were grown in MM (2% glycerol) with appropriate markers at 28°C overnight. 50 SPBs and 50 sMTOCs were counted for each strain.

To investigate whether peroxisomes play a role in microtubule organization, we used KipA to determine the activity of SPBs and sMTOCs for Δ*pexC*. SSK92 was crossed to SAH3, generating strain SYZ8 with GFP-KipA and no peroxisomes. By time-lapse analysis, in 100 s, we observed 15.2% reduction of newly emanating GFP-KipA signals from SPBs and 28.4% from sMTOCs in SYZ8 compared with wild type **(Figure 31, F)**. TubA was tagged with GFP in Δ*pexC* by crossing SAH3 with SJW02, yielding strain SYZ10. During interphase, cytoplamic MTs decreased 34.7% in the absence of peroxisomes **(Figure 31, D)**. And in mitosis, astral MTs were observed to be reduced by 38.6% in SYZ10 compared with SJW02 **(Figure 31, E)**, which might explain the effect on sporulation. All of these evidences provided us a potential role of peroxisomes in microtubule organization. However, since proxisomes are involved in multiple metabolic processes, we don't know whether these influences are indirect.

9 S-tag affinity purification to identify interaction partners of ApsB

S-tag affinity purification was established based on the two parts of RNase which are cleaved by subtilisin, S-peptide (residues 1-20) and S-protein (residues 21-124). S-peptide (even reduced to 15 aa) can bind to S-protein very tightly. Due to the small size of S-peptide and high affinity, this approach has been widely used for protein affinity putification (Kim & Raines, 1993; Liu *et al.*, 2010). To identify new ApsB interaction partners in *A. nidulans*, S-peptide was fused at the N-terminus of ApsB (SYZ17). After purification, the protein samples were run on a SDS-PAGE gel and followed by coomassie staining and silver staining **(Figure 32, A & B)**. Western Blot was performed with S-Tag Monoclonal Antibody (Novagen, Germany) to confirm the S-tag-ApsB band **(Figure 32, C)**. Afterwards, the remaining samples were run through the stacking gel and just into the separating gel. The cut gel piece was sent for MS analysis (TopLab, Munich). As a result, we identified over 200 proteins including ApsB. However, the known ApsB binding partner SPA18 or γ-TuRC components had not been purified, although the abundant α/β tubulin, septins or hexA were found in the sample.

10 Laser capture microdissection and mass spectrometry to indentify septum-associated proteins

Besides homologous alignment to obtain new components of different MTOCs, we also established a new strategy which combined the laser capture microdissection (LCM) with mass spectrometry (MS) to identify new septum-associated-proteins. After culturing FGSCA4 overnight and fixed in 100% ethanol for 12 h on a special membrane slides, LCM was performed and 3000 septa were collected on the lid of a special tube. Proteins were extracted from the collected septa followed by LC-ESI-MS/MS analysis. Afterwards, the MS data were

used for a database search with the software Mascot (Matrix Science) using the *A. nidulans* protein sequences. The mass-spectrometric analysis was done commercially by TopLab GmbH (Munich). As a result, 7 proteins were identified, one of which was ANID_05521. 14 peptides from the N-terminal part of this protein were detected, giving a sequence coverage of 26% and a protein score of 643. Additional six proteins were identified as single peptide and with lower scores. Because of the low coverage we did not analyze them further **(see Table 3)**.

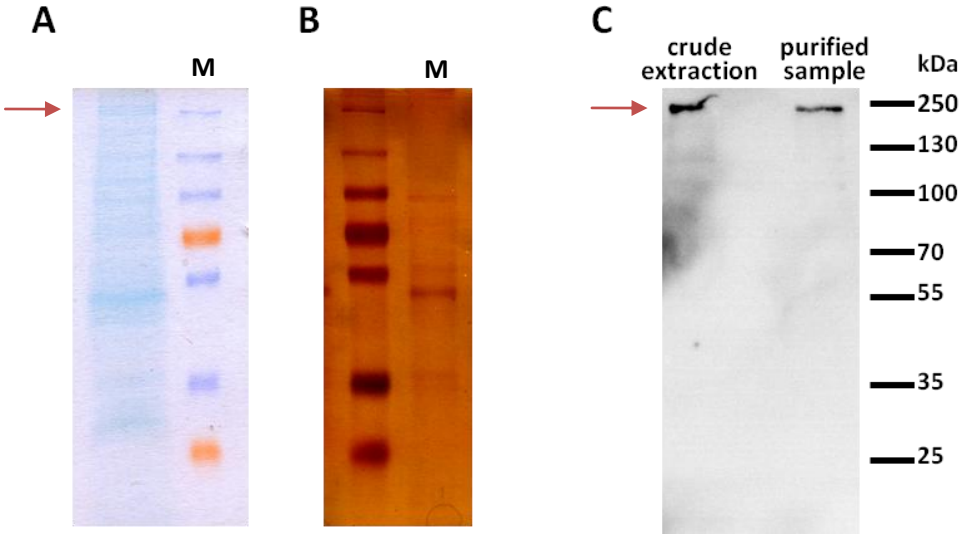

Figure 33. S-tag affinity purification with ApsB. (A) Coomassie staining with the purified sample. **(B)** Silver staining with the purified sample. **(C)** Western Blot with the crude extraction and purified sample. The arrowheads indicate the S-tag-ApsB. M, PageRuler™ Plus Prestained Protein Ladder, 10 to 250 kDa (ThermoFisher Scientific).

AlpA is a highly conserved protein in eukaryotes, whose orthologues include *S. cerevisiae* Stu2, *S. pombe* Dis1 and Alp14, *X. laevis* XMAP215 and human TOG etc.. They are known to be involved in various microtubule and spindle functions, including microtubule polymerization, spindle formation, kinetochore function and cell morphogenesis (Brouhard *et al.*, 2008; Garcia *et al.*, 2001; Ohkura *et al.*, 2001; Takeshita *et al.*, 2013). In *A. nidulans*, AlpA localized at the plus-end of the MT and along it as a microtubule polymerase, and also might contain other roles for microtubule elongation (Brouhard *et al.*, 2008; Enke *et al.*, 2007). By interaction with the cell end marker TeaA at the hyphal tip cortex, AlpA also play roles in microtubule guidance and polarity maintenance (Takeshita *et al.*, 2013). During anaphase, AlpA migrates to the kinetochores and moves to the poles together with them. The role for AlpA could be promoting anaphase depolymerization of the spindle microtubules (Herrero *et al.*, 2010). We re-investigated the localization of AlpA and indeed found AlpA also localized at the plus-end of microtubules emerging from septa (SCE05) **(Figure 33)**. We proposed that it also has a microtubule polymerization function at sMTOCs. But whether it plays other rules in sMTOC still needs to be determined.

Table 3. Proteins indentified from nano-LC-ESI-MS/MS.

Protein	Description	Score	Queries Matched
ANID_05521	AlpA, MT polymerase, spindle function	643	26
ANID_06750	Domain(s) with predicted oxidoreductase activity and role in metabolic process	36	1
ANID_02138	DEAD/DEAH box helicase	32	2
ANID_00944	ATP-dependent RNA helicase Rok1	31	1
ANID_03024	Nuclear protein, localizing to the whole nucleus	26	1
ANID_04189	MkkA, essential mitogen-activated protein kinase kinase (MAP2K), mutants arrest as branched germlings; Ortholog in *S. pombe* is a cellular component of septum, as well as a component of bud neck and bud tip in *S. cerevisiae*.	24	1
ANID_11793	Ortholog(s) have roles in cellular response to biotic stimulus and filamentous growth of a population of unicellular organisms in response to biotic stimulus.	22	1

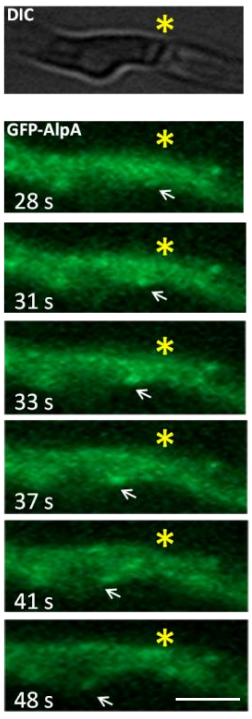

Figure 33. Localization of AlpA to the plus-end of MTs emerging from sMTOC. Strain SCE05 was grown in MM (2% glycerol) with arginin and pyridoxin at 28°C overnight and observed with time-lapse. The arrowheads indicate the MT plus-end AlpA. The asterisks indicate the septum. Bar, 5 µm.

V Discussion

1 How are ApsB and SPA18 targeted to SPBs and sMTOCs?

1.1 SepK is not the sole receptor of ApsB to SPBs

In *S. cerevisiae*, Spc72 (ApsB orthologue) is recruited to the outer plaque of the SPBs by Nud1, which can also bind to Cnm67 (Adams and Kilmartin, 1999; Brachat *et al.*, 1998; Elliott *et al*., 1999), a linker between center plaque and outer plaque. The Cnm67 orthologue in *A. nidulans* was not found by BLASTP. Thus, it's an opening question which and how many proteins lie in between outer plaque and center plaque in *A. nidulans*. Depletion of Cnm67 is not lethal and doesn't block the nucleation of cytoplamic microtubules completely (Gruneberg *et al*, 2000), although in a lack of outer plaque of the SPB. In *A. nidulans*, cytoplasmic microtubules are still nucleated and maintained in the absence of ApsB, the γ-TuRC receptor at the outer plaque. All of these findings indicate the existence of other ways for cytoplasmic MTs nucleation besides ApsB/Spc72 mediated outer plaque SPB. In our work, during interphase, we found SepK (ScNud1) could recruit ApsB to the SPBs, but it is not the only anchor, since weak signal of ApsB was still visualized in the complete absence of SepK. This also suggested the existence of other microtubule nucleation sites in addition to the outer plaque of SPB. Another evidence for this hypothesis is the fact that in *S. cerevisiae* Kar1 can target Spc72 to the half-bridge to nucleate cytoplasmic microtubules in a γ-TuSC dependent manner during G1 and karyogamy. Although we didn't find the Kar1 orthologue in *A. nidulans* by BLASTP analysis, there is supposed to be a Kar1 orthologue (or more), which can bind to SfiA and Cdc31 to facilitate SPB duplication and may also recruit ApsB to nucleate cytoplasmic MTs at half-bridge.

In addition to being a receptor for ApsB, SepK was found to localize to SPBs in a septation initiation network (SIN) protein SNAD dependent manner (Kim *et al*., 2009). Whether SNAD is the functional homolog of Cnm67 or a structural component of SPB is still unknown. Moreover, SepK is required for localizing SIN proteins SIDB and MOBA to the SPB and for proper timely septation. SPB localization of SIN components is not essential for septation, but critical for septation to take place in a timely manner. Similarly, in *S. pombe*, Cdc11 (SepK orthologue) locates constitutively at SPBs and its function appears to be required for the localization of all the other SIN components to SPBs with the exception of Sid4p. Cdc11 localizes to SPBs via C-terminus and in a Sid4p-dependent manner. Both Cdc11p and Sid4p are indispensable for septa formation, suggesting the localization of SIN molecules to the SPB might be required for septation

(Tomlin *et al*., 2002). In like manner, in *S. cerevisiae*, Nud1 binds to the spindle checkpoint to control proteins Bfa1 and Bub2 to the SPB, and is part of the mitotic exit network (MEN) in which it functions upstream of CDC15 and downstream of LTE1 (Gruneberg *et al*, 2000). In addition to MEN signaling, we have already known that Nud1 is an SPB component, which can also prove our hypothesis that SPB components are involved in cytokinesis pathway.

1.2 SPA10 recruits both ApsB and SPA18 to septa

SPA10 is a septal pore-associated (SPA) protein first identified in *N. crassa* and reported to be required for suppressing septation. In *A. nidulans*, during septum formation, SPA10-GFP located to a closing ring structure reminiscent of the contractile actomyosin ring (CAR) to drive the cytokinesis. And SPA10-GFP still associated with mature septa, which is different from the other CAR-associated proteins, such as actin and myosin II (Seiler & Justa-Schuch, 2010; Lee *et al.*, 2012). SPA10-GFP was also found to localize as a central disk structure around septal pore (Shen *et al*., 2014), resembling ApsB and SPA18. The recruitment function of SPA10 for ApsB and SPA18 revealed to us a new role for SPA proteins, in addition to Woronin body activation, septation regulation and septal pore organization (Lai *et al*., 2012; Shen *et al*., 2014). The flexible structure of SPA10 due to its intrinsically disordered sequence may also facilitate multiple roles of SPA10 for different processes. However, it is still unclear how ApsB or SPA10 are targeted to the septa via SPA10. Do SPA10 interact with them directly or indirectly via other proteins? Are ApsB and SPA18 interdependent in this process? Lots of questions still need to be answered.

1.3 Interdependence between ApsB and SPA18

In *S. pombe*, Mto2 localized to multiple different MTOCs in an Mto1-dependent manner (Samejima *et al*., 2005), indicating that Mto1 is the anchor of Mto2. In *A. nidulans*, a tremendous distinct from *S. pombe* is that SPA18 localization was not affected in the absence of ApsB, indicating ApsB is not the (or major) recruiting factor for SPA18. How SPA18 targets to different MTOCs is still unclear. On the other hand, ApsB localizing to SPBs and sMTOCs is partially dependent on SPA18, especially when the main receptor is absent or the binding domain for the receptor in ApsB is depleted. This is also in agreement with the finding in *S. pombe* that Mto1 localization only partially depends on Mto2, especially for non-SPB MTOCs (Samejima *et al*., 2005; Venkatram *et al*., 2005). The interdependence between ApsB and SPA18 might be helpful to answer the question how ApsB and SPA18 target to different MTOCs, as well as the mechanism of γ-TuRC recruitment.

2 Recruitment of γ-TuRCs to different MTOCs

2.1 γ-Tubulin complexs are targeted to distinct MT nucleation sites by different anchors

In eukaryotes, the γ-TuRC/γ-TuSC receptors mainly contain four types. degSPM-degCM1-PACT family (here deg stands for degeneration), CM1-CM2 family, SPM-CM1-PACT family and CM1-MASC family (Lin *et al*., 2015). degSPM-degCM1-PACT proteins (human Pericentrin and AKAP9) and CM1-CM2 proteins (CDK5RAP2 and myomegalin) were only found in higher eukaryotes like human, while SPM-CM1-PACT family and CM1-MASC family proteins only exist in fungi. The SPM-CM1-PACT proteins including *A. nidulans* PcpA, *S. cerevisiae* Spc110 and *S. pombe* Pcp1 are required for γ-TuRC localizing to the inner plaque of the SPBs for nuclear MTs formation during mitosis. SPM and CM1 domains are responsible for recruiting γ-TuRC/γ-TuSC, while PACT domain is for cellular localization of the proteins. *A. nidulans* ApsB, *S. cerevisiae* Spc72 and *S. pombe* Mto1 are belonged to the CM1-MASC family, in which CM1 is the γ-TuRC/γ-TuSC recruiting domain and MASC is for self-localization of the proteins. However, CM1 was reported to be not sufficient to recruit γ-TuRC in Mto1, another Mto2 binding domain was also indispensable (Samejima *et al*., 2008), suggesting that CM1-MASC family proteins also need their binding partner (Mto1-Mto2, ApsB-SPA18) for proper recruitment. Interestingly, Spc72 doesn't have an interaction partner in *S. cerevisiae*. This can be explained by the difference between γ-TuSC and γ-TuRC, which indicates γ-TuRC needs a more complicated recruiting mechanism than γ-TuSC. Another explanation could be Spc72 contains a domain which has the identical function as Mto2/SPA18 at the N-terminus, since the N-terminal Spc72 is responsible for binding to Spc97 and Spc98 and targeting γ-TuSCs (Chen *et al.*, 1998). γ-TuRCs/γ-TuSCs are recruited by distinct receptors for nucleation of different microtubules during cell cycle, under the regulation of various factors.

In *A. nidulans*, PcpA is essential for cell viability, indicating the PcpA-γ-TuRC center is indispensable for nuclear microtubule nucleation. However, the depletion of the other γ-TuRC receptor ApsB is not lethal. The cytoplamic microtubules are also able to be nucleated in the absence of ApsB, indicating a substitutive way for cytoplamic microtubule organization. One possibility is that PcpA-γ-TuRC centers can nucleate cytoplasmic MTs when ApsB/SPA18-γ-TuRC centers are absent. As in *S. pombe*, when Mto1 was absent, cytoplamic microtubules were still visible during interphase (Samejima *et al*., 2005), suggesting Pcp1-γ-TuRC centers might also be responsible for cytoplasmic microtubules nucleation. However, this is never proved directly. It is also unclear whether PcpA-γ-TuRCs are involved in cytoplasmic microtubule nucleation when

ApsB/SPA18-γ-TuRCs are present in the cells. Another interesting fact is that in *A. nidulans* ApsB is crucial for astral microtubule nucleation in mitosis, whereas the binding partner SPA18 is not required for astral MT formation, as well as in *S. pombe* (Samejima *et al*., 2005). Thus, we assume that the cytoplasmic MTs and astral MTs were nucleated from different organized γ-TuRC centers. Besides, it is reported in *S. cerevisiae*, Spc72 directly interact with Stu2 to anchor astral MTs at the cytoplasmic side of the SPB and to regulate astral MT dynamics (Usui *et al*., 2003). Therefore, we speculate AlpA may also bind to ApsB to facilitate the astral MT organization in *A. nidulans*. SPA18 is absent or dispensable in this process, and other interaction partners or regulators for ApsB may also be involved besides AlpA. The fact that the number of cytoplasmic microtubules are decreased in the absence of ApsB or SPA18 confirmed our hypothesis that both ApsB and SPA18 is important for cytoplamic microtubules organization, in agreement with the finding in *S. pombe*.

2.2 ApsB/SPA18 complex as a γ-TuRC anchor

In *A. nidulans*, ApsB and SPA18 form a higher-order multimerization complex for recruiting γ-TuRCs (Lynch *et al*., 2014). According to data from *S. pombe*, the stoichiometry of ApsB:SPA18:γ-Tubulin:GCPB:GCPC is approximately 2:2:2:1:1 (Lynch *et al*., 2014), suggesting that each γ-TuSC in an actively nucleating complex may be associated with two copies each of ApsB and SPA18. As we know the CM1 domain in ApsB is responsible for targeting γ-TuRCs, the function of SPA18 in the complex becomes a mistery, bringing us two hypotheses. First, it was suggested that in *S. pombe* Mto2 was required for assembly of the complex, while Mto1 only played a minor role during this process (Lynch *et al*., 2014), although the self-binding of Mto1 orthologues were found in *A. nidulans* (Veith *et al*., 2005) and *S. cerevisiae* (Chen *et al*., 1998). The other hypothesis is based on the finding that Mto2 was found in the co-purified γ-TuRCs, although very small amount when Mto1 was absent, as well as Mto1 in co-purifiedγ-TuRCs in the absence of Mto2 (Samejima *et al*., 2008). Here comes our assumption that SPA18 might also slightly bind to γ-TuRCs when ApsB is absent, which indicates the role of SPA18 is directly binding to γ-TuRCs, together with ApsB. As we have already known that in SPM-CM1-PACT family proteins like PcpA, only CM1 domain is not sufficient for recruiting γ-TuRCs. Therefore, it is not surprising that SPA18 is also indispensable for recruitment of γ-TuRCs to compensate for the lack of an important domain like SPM.

2.3 The role of MztA in microtubule organization

As a highly conserved γ-TuRC component in eukaryotes (except for *S. cerevisiae*), the othologues of MztA are essential for cell viability in *S. pombe* (Masuda *et al*., 2013) and human (Hutchins *et al*., 2010). In *S. pombe*, Mzt1 was also identified to directly interact

with Alp6 (GCPC) and with the approximately equal stoichiometry with Alp4 (GCPB) thus Alp6 (GCPC) (Dhani *et al*., 2013; Masuda *et al*., 2013)**. In** *A. nidulans*, we observed that MztA had the similar localization patter as GCPC. All of these findings provide us an evidence that Mzt1 might be a component of γ-TuRCs and crucial for γ-TuRC assembly. However, New findings in *S. pombe* and human suggested Mzt1/Mozart1 was required for γ-TuRC recruitment rather than assembly (Hutchins *et al*., 2010; Masuda *et al*., 2013). But it is still unclear how this process is organized and whether MztA in *A. nidulans* plays the same role as in *S. pombe* and human, considering MztA is not essential in *A. nidulans* despite of being crucial for sporulation. There might be one (or more) other proteins which can compensate for the lack of MztA in *A. nidulans*. The deuterostome specific MOZART 2A/2B were also not found in *A. nidulans*, which were reported to be not essencial but required for γTuRC recruitment to interphase centrosomes, not for γTuRC assembly as well (Teixidó-Travesa *et al*., 2010). Since MztA is a GCPC-binding partner, it is surprising that no homolog of MztA was found in *S. cerevisiae*. What's more, MztA was found in some other Saccharomycotina species which shares the same basic microtubule nucleation systems as *S. cerevisiae*, indicating that MztA was lost from the *S. cerevisiae* genome during evolution. It is proposed that Spc98, Spc110 or Spc72 might also have structural evolution to be compensable for the lack of MOZART in *S. cerevisiae* (Lin *et al*., 2015).

3 Multiple domains in ApsB

ApsB is a 1574 aa huge protein, with predicted (http://smart.embl-heidelberg.de/) four coiled-coil regions (562-722 aa; 769-807 aa; 848-1036 aa and 1080-1177 aa), facilitating its interaction with several other proteins **(Figure 34)**. In this work, two conserved domains CM1 and MASC, as well as a C-terminal SMB motif were identified. CM1 domain is highly conserved in eukaryotes for γ-TuRC/γ-TuSC recruitment (Samejima *et al*., 2008; Zhang *et al*., 2007; Lin *et al*., 2014). MASC, SMB and other binding domains will be discussed here.

3.1 Septal targeting domains

SMB domain is considered to be crucial for ApsB targeting to septa, but not sufficient. We know that ApsB can still localize to septa in the absence of SMB domain, but not any more in a lack of both SMB and SPA18, or when MASC domain is deleted but SPA18 is still present. Here comes a hypothesis that SPA18 might be binding to ApsB via MASC domain. But this was rejected by the fact that ApsB could still localize to the SPBs weakly in the absence of MASC and SMB domain, but could not be visualized when MASC, SPB and SPA18 were all lost. Another evidence is the Mto1/Mto2 binding site identified in

fission yeast *S. pombe* (Samejima *et al*., 2005), which is in the middle of Mto1 (461-549 aa). It is also reported that the minimal version of Mto1/Mto2 complex Mto1/2[bonsai] which only contains the 131-549 aa of Mto1 can still implement the binding of Mto1 and Mto2 (Samejima *et al*., 2015). Thus, we don't think SPA18 may bind with ApsB via its MASC domain. Besides SMB domain, MASC is also required for septal targeting. There might be a possibility that both MASC and SMB domains are required for SPA10 recruitment. Interestingly, it seems like that binding of SPA10 with the ApsB MASC domain is essential but not sufficient for septal targeting. When one of SPA18 and SMB is absent, ApsB septal localization will not be affected. But when both are deleted, ApsB is not able to target to septa any more. Only SMB or even together with SPA18 can not facilitate the ApsB septal localization. Besides, we found that the last 14 aa (termed SMB-C) is very conserved between different filamentus fungi, hence we deleted the non-conserved sequence between MASC and SMB-C to see if the septal localization was influenced. To our surprise, only the MASC and SMB-C domains are not sufficient for binding to the septal receptor, indicating an indispensable function for the non-conserved region. Does SMB-C contain important motifs or just act as a bridge in between? The indeed function of it is still unclear.

3.2 SPB-targeting domains

In addition to being as a septal receptor binding motif, the MASC domain is also crucial for targeting ApsB to the SPB through a potential receptor SepK. Under the MASC-depletion condition, extremely weak localization of ApsB could be visualized, as in *sepK* mutant, resulting in scarce sporulation, which is supposed to be due to astral microtubule defect. No signal could be detected in a SPA18 and MASC absent manner, indicating the faint signal under MASC-deletion condition was contributed by ApsB-SPA18 interaction. For us, it is very strange that ApsB was not able to be targeted to SPBs in the absence of MASC domain and SPA18, while in a lack of SepK and SPA18, a faint signal could still be detected at SPBs. Therefore, a kar1 functional orthologue is also speculated here **(see V 1.1)**, which can bind to ApsB at the C-terminus via an overlapping binding region **(see Figure 34)** with MASC (and SMB) domain. This mechanism has already been found in *S. cerevisiae* (Gruneberg *et al*., 2000).

3.3 Other proposed domains in ApsB

In *S. cerevisiae*, Spc72 directly interacts with Stu2 (AlpA) via a binding region (99-267 aa) (Usui *et al*., 2003). There is also a possibility that ApsB binds to AlpA in *A. nidulans*. Further analysis still needs to be done to verify this hypothesis. Another interesting region is the N-terminal ApsB. In *S. pombe*, the N-terminal 130 aa from starting codon are required for localizing to nuclear envelope, forming one type of the iMTOCs (Samejima *et*

al., 2015). In *A. nidulans*, we also found that the first 523 aa are functionally important, since the re-complementation without this region was not able to recover the sporulation in deletion strain. However, since nuclear envelope derived microtubules were not found in *A. nidulans*, we can't relate this N-terminal region to any functions yet. However, interestingly, a phosphosite at 321S was found in ApsB by MS (Xiaolei Gao), which might be associated to the regulation of ApsB during cell cycle.

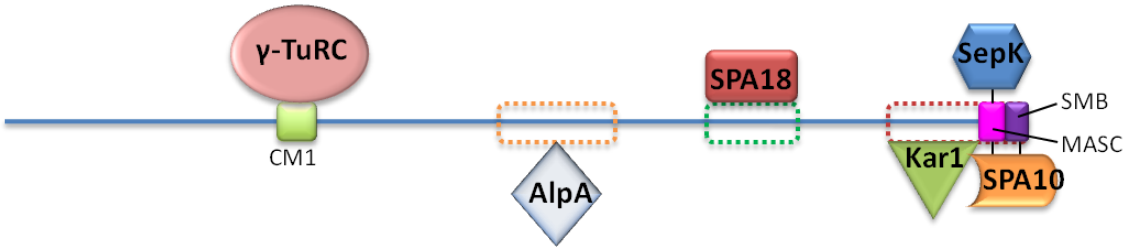

Figure 34. Domains of ApsB. The dotted-line boxes indicate the potential binding domains, which have not been confirmed yet. Full length, 1573 aa.

4 The role of sMTOCs in filamentous fungi

A. nidulans sMTOC is an analogous structure to *S. pombe* eMTOC, which is activated by SIN pathway in an F-actin and myosin-dependent manner (Heitz *et al*., 2001). eMTOC was also suggested to be a ring-like structure (Hagan & Petersen, 2000), which resembles sMTOC as we saw in *A. nidulans*. A tremendous distinct between eMTOC and sMTOC is that eMTOC is formed transiently in anaphase and then disassembled during the septation after releasing the cytoplamic microtubules (Heitz *et al*., 2001), while sMTOC exists permanently during the cell cycle. However, the indeed function of sMTOC in *A. nidulans* is still unclear. What is clear is that sMTOC is not required for conidiospore formation, since in a SPA18-absent manner, the resulting lack of sMTOC didn't cause any significant sporulation defect. Septum formation was also not significantly affected in the absence of sMTOC, when *apsB* or *SPA18* was deleted. The role of sMTOC still needs to be further determined.

5 The proposed model of SPB and sMTOC in *A. nidulans*

Besides the canonical microtubule organization center centrosome/SPB in eukaryotes, there are many specific MTOCs in different organisms, such as Golgi MTOC, NE MTOC, MT branching MTOC, as well as eMTOC and iMTOC in *S. pombe*. *A. nidulans* also has a

specific sMTOC, whose analogue was only found in *S. pombe* but not in *S. cerevisiae*. Besides, the γ-Tubulin complex of *A. nidulans* has 4 more components (GCPD, GCPE, GCPF and MztA) than *S. cerevisiae*, although all of them are not essential. And ApsB needs a binding partner SPA18 for the recruitment of γ-TuRCs, which is also not found in *S. cerevisiae*. In spite of varieties of differences in these two species, it is still an easy and efficient way to identify new candidates by homologous alignment, since the *S. cerevisiae* SPB was well characterized and close to *A. nidulans* in evolution. As a result, 10 genes were found in the *A. nidulans* genome. Besides our known γ-tubulin, GCPB, GCPC, ApsB, PcpA, SepK, Cdc31 and SfiA, Calmodulin and An-Ndc1 (ScNdc1) were also found by BLASTP.

Calmodulin (CaM) is an intracellular receptor for Ca^{2+} in eukaryotes. The Ca^{2+}/ CaM binding is reversibly and involved in regulating numerous processes such as secretion, cell motility, cell cycle, ion homeostasis, gene transcription and neurotransmission (Catalano & O'Day, 2008; Lu & Means, 1993; Rasmussen *et al*., 1992; Ravindran *et al*., 2008; Tadross *et al*., 2008). Recent study in *A. nidulans* reported that highly concentrated CaM located at the position of extreme apex and seemed to determine the hyphal orientation. CaM also localized at septa during cytokinesis transiently, which is essential for septum formation since depletion of CaM resulted in a completely blocked septation (Chen *et al*., 2012). By personal contact with the author, we know that CaM also co-localizes with PcpA at the SPBs permanently. Therefore, we propose that CaM also regulates the anchoring of PcpA to the central plaque of SPB, via binding at the C-terminus of PcpA.

An-Ndc1 is a conserved transmembrane protein in eukaryotes which localizes at both nuclear pore complexes (NCP) and SPBs for targeting them to the nuclear envelope. Ndc1 is essential and required for SPB insertion, duplication and spindle formation in *S. cerevisiae*, *S. pombe* and higher eukaryotes (Chial *et al*., 1998; Lau *et al*., 2004; Osmani *et al*., 2006; West *et al*., 1998). However, in *A. nidulans* (Osmani *et al*., 2006) and *C. elegans* (Stavru *et al*., 2006), depletion of Ndc1 did not cause a significantly defective phenotype. Therefore, we suggest that other proteins or pathways might be involved to compensate for the lack of Ndc1 in *A. nidulans*. The other SPB anchor proteins Mps2 and Bbp1 were not found in *A. nidulans*.

Based on the components identified, we proposed a model for *A. nidulans* SPB **(Figure 35, A)**. SepK, ApsB, SPA18 and γ-TuRCs build the outer plaque of SPB towards the cytoplasmic face, while the inner plaque is composed of PcpA and γ-TuRCs for nuclear microtubule nucleation. However, the components of the central plaque were not identified by homologous alignment, except for the PcpA binding partner Calmodulin. The

inner layer 1 and inner layer 2 which exist in *S. cerevisiae* were not presented in this sketch map. Other NE anchors for SPB still need to be indentified in addition to Ndc1, as well as other half-bridge associated proteins like a Kar1 functional homolog in *A. nidulans*.

By contrast, the constitution of sMTOC may not be as complicated as SPB. Due to the lack of PcpA, SfiA and Cdc31, we assume that only the outer plaque of SPB stands at the sMTOC. This is not surprising since sMTOC only nucleates cytoplasmic microtubules. Notably, the receptors for ApsB/SPA18-γ-TuRCs are different at SPBs and sMTOCs. All the processes are regulated precisely by binding to different domains of ApsB (or SPA18). It is also speculated that sMTOC is a disk (ring)-like structure around the septal pore **(Figure 35, B)**. Nevertheless, the organization of sMTOC as well as its interdependence with other septal-pore associated proteins is still not so clear. It is reported that septal pores are open in interphase and closed during mitosis in *A. nidulans* (Shen *et al*., 2014). And we found sMTOC also abolished cytoplasmic microtubule nucleation during mitosis, indicating there might be a relation between septal-pore closing and the transient sMTOC dormancy.

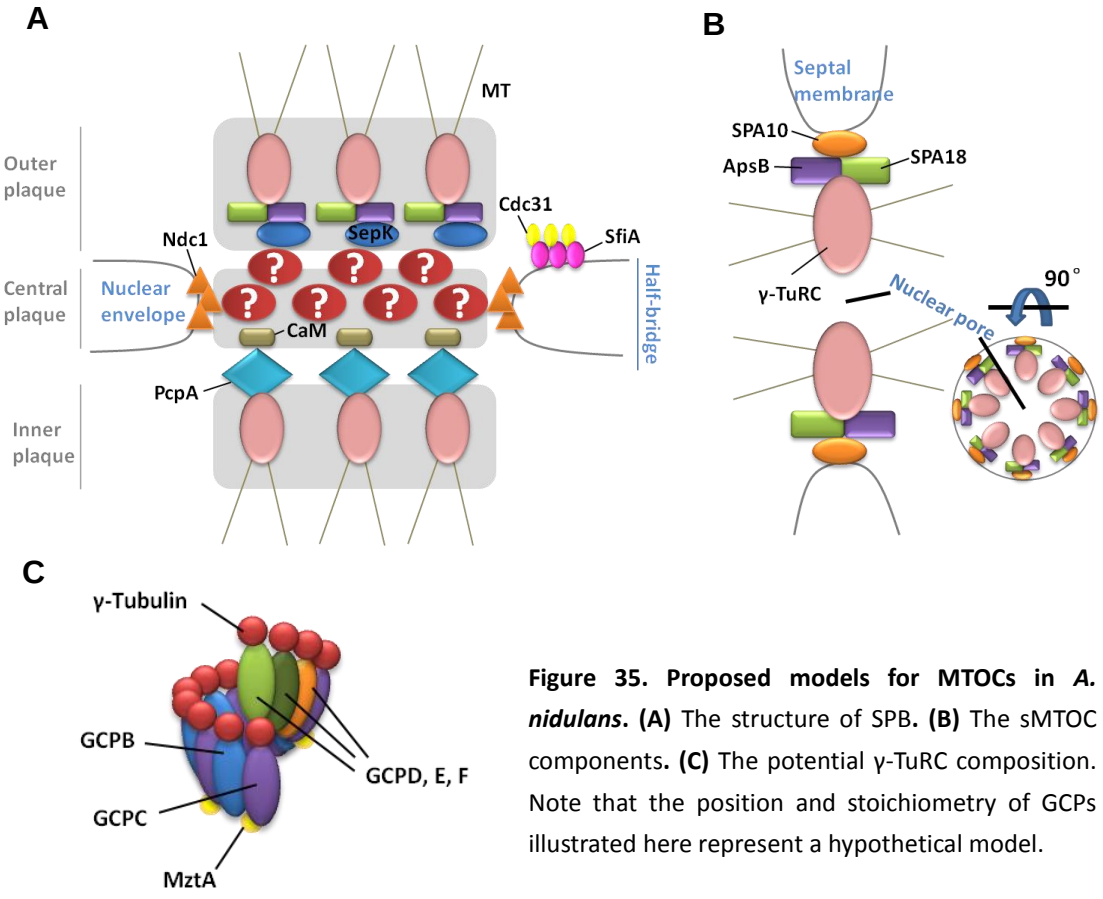

Figure 35. Proposed models for MTOCs in *A. nidulans*. (A) The structure of SPB**. (B)** The sMTOC components**. (C)** The potential γ-TuRC composition. Note that the position and stoichiometry of GCPs illustrated here represent a hypothetical model.

6 The role of peroxisomes in microtubule organization

Based on the fact that ApsB$^{3.2}$ has a predicted PTS2 domain at the N-terminus, ApsB$^{3.2}$ was suggested to be a peroxisomal protein (Zekert *et al*., 2010). However, we didn't see the co-localization of GFP-ApsB$^{4.7}$ and mRFP-MAS (peroxisomes) in our analysis. Besides, no PTS2 domain could be detected any more in ApsB$^{4.7}$ after adding the missing 523 aa to ApsB$^{3.2}$ at the N-terminus. Although ApsB was able to directly interact with the Woronin body (peroxisome derived) protein HexA, it is still not convincing that peroxisomes can play a role on the behavior of ApsB in *A. nidulans*. Therefore, the role of peroxisomes in microtubule organization is still a mystery. On the other hand, peroxisomes are involved in numerous physiological processes such like peroxide metabolism, ß-oxidation of long-chain fatty acids and biosynthesis of ether phospholipids, siderophore, penicillin and biotin depending on the species (Kovacs *et al*., 2003; Wanders, 2004; Tanabe *et al*., 2011). Consequently, despite many evidences indicate microtubule associated defects in the absence of peroxisomes, they might be caused by a very sick cellular environment which caused by the aberrance of many physiological processes. Anyway, how peroxisomes are involved in cell cytoskeleton still needs to be further investigated.

7 Different strategies to identify new components of MTOCs

7.1 LMD and MS to indentify septum-associated proteins

The analysis of subtle genetic differences at the cellular or sub-cellular level is one of the current challenges. Whereas previously many approaches used entire tissues to identify differentially expressed genes, laser capture microdissection (LCM) allows isolation of single cells out of a tissue and subsequently to analyze those. The method was developed in 1996 (Emmert-Buck *et al*., 1996), then widely used for DNA, RNA and protein analysis in animal or plant tissues, fungi, chromosome preparations etc. (MacDonald *et al.*, 2012; Liu *et al*., 2010; Teichert I *et al.*, 2012; Kubickova *et al.*, 2002). In fungi, subcellular structures such as the hyphal tip or septa are excellent candidates to be analyzed by LCM. However, in many fungi, hyphae are rather small with hyphal diameters of 2-3 µm. Therefore, the collected material contains only very small amounts of the molecules to be analyzed subsequently. This may be less important if DNA or RNA will be analyzed, because the molecules can be easily amplified by PCR-based methods, but this amplification step is missing if proteins were analyzed. Here we developed a protocol to isolate septa from *A. nidulans* and to identify septum-associated proteins. Septa were isolated before by LCM from *Rhizoctonia solani*, but the analysis was

restricted to an electron microscopic analysis (van Driel *et al.*, 2007).

However, besides AlpA, we didn't find other septum-associated proteins probably due to the low amount of proteins in the preparation. This raises the question whether AlpA is really an abundant protein at septa, because the protein is also found at the microtubule plus ends in the cytoplasm. However, we did not find other highly abundant cytoplasmic proteins such as tubulin or ribosomal proteins. This shows that the method in principal is suitable for the isolation of septum-associated proteins. However, in order to facilitate the collection of septa, the process should be automatized. This could be achieved by fluorescently labeling the structures of interest. In the case of septa, sMTOC-associated proteins such as ApsB, SPA18, GCPC or MztA could be used. However, currently the system does not allow sampling of individual septa in *A. nidulans* because of the small size. In comparison, collection should be no problem in hyphae of *Sordaria macrospora* or *N. crassa*, which has thick hyphae.

7.2 Affinity purification to identify novel MTOC components

Affinity purification is a basic approach for finding interaction partners. We used ApsB as bait protein for S-tag affinity purification, but did not identify any interaction partners of ApsB. Another Ph.D. student Xiaolei Gao also performed GFP-trap (established by Gerhard Braus lab, Göttingen) with ApsB, but she also didn't find any interest proteins. There might be several reasons, one of which might be the influence by the N-terminal tagging. However, ApsB still localized to MTOCs and didn't cause any significant phenotype defect with GFP at the N-terminus. Another explanation would be the N-terminus of ApsB is required for binding to or surrounded by the other proteins, which can not be pulled down by the corresponding affinity beads. However, the C-terminal tagged ApsB was not able to localizing to sMTOCs (Veith *et al*., 2005) due to the SMB (and MASC) domain at the C-terminus. It appears that affinity purification is not an efficient approach using ApsB as a bait protein.

7.3 Other strategies

Since the proteins indentified by homology alignment are limited, as well as the inapplicability of the affinity purification and LCM, we are trying to establish other strategies to characterize the MTOCs in *A. nidulans*. One of these is the BioID method (Xiaolei Gao). This approach is based on a mutant of a 35-kDa DNA-binding biotin protein ligase BirA (BirA*) in *Escherichia coli*, which can biotinylate the near-neighbors of the bait protein. Subsequently, biotinylated proteins can be affinity captured and identified by mass spectrometry (Morriswood *et al*., 2013). Yeast two hybrid screening with ApsB is also in progress at the moment.

VI Materials and Methods

1 General chemicals and equipments used in this work

Chemicals were purchased from Roche (Mannheim), Merck (Darmstadt), Sigma (Taufkirchen), Roth (Karlsruhe), BIOMOL (Hamburg), AppliChem (Darmstadt), Difco (Augsburg), Gibco (Karlsruhe) and Stratagene (Amsterdam, Netherlands), otherwise the origin will be written in the text.

The common equipments used in this study are lised in **Table 4**. The special equipments used in certain experiments will also be written in the text.

Table 4. Common equipments used in this study.

Equipment	Type	Manufacturer
Autoclave	Systec 3850 ELV	Systec GmbH, Wettenberg
	Systec VE-75	Systec GmbH, Wettenberg
Centrifuge with rotors	Beckman J2-21 centrifuge	Beckman Coulter, Krefeld
	Eppendorf centrifuge 5403	Eppendorf, Hamburg
	Eppendorf centrifuge 5415 R	Eppendorf, Hamburg
	Eppendorf centrifuge 5424	Eppendorf, Hamburg
	Heraeus Biofuge 13	Kendro, Langenselbold
	Kontron ultracentrifuge TGA-65	Kontron, Zürich,Switzerland
	Sorvall RC 6+ centrifuge	Thermo Scientific, Germany
	Universal 320 R	Hettich Zentrifuge, Germany
Digital camera	Canon PowerShot G15	Canon, Japan
Heat block	Thermo mixer 5436	Eppendorf, Germany
Hybridization oven	UVP hb-1000 Hybridizer	UVP, USA
Power supply apparatus	Power Pac 3000	Bio-Rad, Munich
Shaker/ incubator	Heraeus-Brutschrank Baureihe 6000	Kendro, Langenselbold
	HT Infors	Infors AG, Switzerland

	Kleinschüttler KM-2	Edmund Bühler GmbH, Tübingen
UV-cross Linker	UV Stratalinker 2400	Stratagene, Heidelberg
pH meter	Hanna HI 208	Hanna, Romania
Magnetic stirrer	Heidolph MR3000	Heidolph, Germany
Sonication	Bandelin sonopuls	Bandelin, Germany
Weighing instrument	Kern 440-47N Sartorius R200D	Kern, Germany Sartorius, Göttingen
Speed Vac	Savant sc110	Savant, USA
Freeze drier	Christ Alpha 1-2	Christ, Germany
Homogenizer	Retsch MM200	Retsch, Germany

2 Microbiological and genetic methods

2.1 Cultivation and storage of *E. coli* and *A. nidulans* strains

Media for *E. coli* were prepared as described (Sambrook & Russel, 1989) (**Table 5),** appropriately supplemented with antibiotics in certain experiments **(Table 6)**. Ingredients were added to ddH_2O and autoclaved at 121°C for 20 min. For solid media, 15 g agar per liter was added. Heat-sensitive solutions such as antibiotics, amino acids and vitamins were filter-sterilized with 0.22 µm pore filter membrane (Schleicher und Schüll, Dassel), and added to the media after autoclaving and cooled until 50-60°C.

Table 5. Media for *E. coli*.

Medium	Ingredients (1 liter)
Luria-Bertani (LB)	10 g Trypton; 10 g Yeast extract; 5 g NaCl; pH 7.5
SOC	20 g Trypton; 5 g Yeast extract; 0.58 g NaCl; 0.185 g KCl; 2.03 g $MgCl_2$ x $7H_2O$; 2.46 g $MgSO_4$ x $7H_2O$; 3.6 g glucose

Table 6. Antibiotics for *E. coli* media.

Substance	Stock solutions/Storage	Final concentration
Ampicillin (Amp)	50 mg/ml in ethanol / -20°C	100 µg/ml
Kanamycin (Kan)	10 mg/ml in water / -20°C	50 µg/ml

Minimal medium (MM), YAG medium for *A. nidulans* growth were prepared according to the protocols **(Table 7)** (Pontecorvo *et al.*, 1953); MMurea protocol was provided by Stephen Osmani (Ohio University, US). For solid media, 15 g agar per liter was added. The supplemented vitamins, amino acids and nucleotides for auxotrophic *A. nidulans* strains were listed in **(Table 8)**. The *A. nidulans* selection markers were listed in **Table 9.** *A. nidulans* strains used in this work were listed in **Table 10**.

Table 7. Media and stock solutions for *A. nidulans*.

Medium or Stock	Ingredients (1 liter)
MM	50 ml 20x Salt stock solution; 1 ml 1000x Trace elements stock solution; 20 g glucose/20 g glycerol, 2 g glucose/20 g Threonin, 2 g glucose; pH 6.5
YAG	50 ml 20x Salt stock solution; 5 g Yeast extract; 1 ml 1000x Trace elements stock solution; 1 ml Vitamin stock solution; 10 g glucose; 0.49 g $MgSO_4$ x $7H_2O$ for fluid medium (2.47 g for liquid medium); pH 6.5
20x Salt stock solution	120 g $NaNO_3$; 10.4 g KCl; 10.4 g $MgSO_4$ x $7H_2O$; 30.4 g KH_2PO_4
1000x Trace elements stock solution	22 g $ZnSO_4$ x $7H_2O$; 11 g H_3BO_3; 5 g $MnCl_2$ x $4H_2O$; 5 g $FeSO_4$ x $7H_2O$; 1.6 g $CoCl_2$ x $5H_2O$; 1.6 g $CuSO_4$ x $5H_2O$; 1.1 g $(NH_4)_6Mo_7O_{24}$ x $4H_2O$; 50 g Na_4 EDTA; adjust pH to 6.5-6.8 using KOH
1000x Vitamin stock solution	0 .1 g D-Biotin; 0.1 g Pyrodoxin-HCl; 0.1 g Thiamin-HCl; 0.1 g Riboflavin; 0.1 g p-Aminobenzoic acid; 0.1 g Nicotinic acid
MMurea	20 ml 50x Urea; 10 g glucose; 1 ml Trace elements stock solution; add 12 ml 1 M phosphate pH 6.8 and 4 ml $Na_2S_2O_3$ stock solution (1 g in 5 ml H_2O, filter sterilization) after autoclaving

50x Urea	Urea 30 g; KCl 26 g; $MgSO_4$ x $7H_2O$ 25 g

Table 8. Vitamins, amino acids, nucleotides and other substances for medium.

Substance	Stock Concentration	Volume or weight per liter
Pyridoxin-HCl	0.1 %	1 ml
Arginin	500 mM	10 ml
Uracil	-	1 g
Uridin	-	1.2 g
Biotin	0.05 %	1 ml
p-Aminobenzoic acid (PABA)	0.1 %	1 ml
Riboflavin	0.25 %	1 ml

Table 9. *A. nidulans* selection markers.

Marker	Function	Chromosome	Reference
argB2	Arginine auxotrophy (ornithine carbamoyltransferase)	III	(Upshall *et al.*, 1986)
bar	Glufosinate resistance	-	(Nayak *et al.*, 2006)
biA1	Biotin auxotrophy	I	FGSC
pabaA1	Para aminobenzoic acid auxotrophy	I	FGSC
pyroA4	Pyridoxin auxotrophy	IV	FGSC
pyrG89	Uracil auxotrophy (orotidine-5'-phosphate decarboxylase)	I	(Balance *et al.*, 1983)
riboB2	Riboflavin auxotrophy	VIII	(Kim *et al.*, 2009)
trpC801	Tryptophan auxotrophy	VIII	(Yelton *et al.*, 1984)

	(phosphoribosylanthranilat isomerase)		
veA1	Conidia production in the dark	VIII	FGSC
wA3	White spores (polyketide synthase)	II	(Mayorga & Timberlake, 1990)
yA2	Yellow spores (laccase)	I	(Aramayo *et al.*, 1989)

Table 10. List of *A. nidulans* strains in this work.

Strain	Genotype	Source
CPA02	*pyrG89*; *pyroA4*, *nkuA*::*argB2*; *alcA(p)*::*GFP*::*AnpcpA*::*pyr4*; *riboB2*	(Chen *et al.*, 2012)
FGSC26	*biA1*; *veA1*	FGSC
FGSCA4	*A. nidulans* wild type	FGSC
LO1591	*pyrG89*; *pyroA4*, *nkuA*::*argB*; *sepK*::GFP::*AfpyrG*; *riboB2*	Berl Oakley, Ohio University, US
LO1906	*pyrG89*; *pyroA4*, *nkuA*::*argB*; Δ*sepK*::*AfpyrG*; *riboB2*; *HH1-mRFP*::*AfriboB*	Berl Oakley, Ohio University, US
RMS011	*pabaA1*, *yA2*; *argB*::*trpC*Δ*B*	(Stringer *et al*., 1991)
SAH3	*pyrG89*; *argB2*; *pyroA4*, Δ*nkuA*::*argB*; Δ*pexC*::*pyroA*	Andreas Herr
SCE05	Δ*argB*::*trpC*Δ*B*; *pyroA4*; *alcA*(*p*)::*GFP*::*alpA*	(Enke *et al*., 2007)
SJW02	*wA3*; *pyroA4*; Δ*argB*::*trpC*Δ*B*; *alcA(p)*::*GFP*::*tubA*::*pyr4*	J. Warmboldt, Marburg
SMS1	*pyrG89*; *argB2*; *pyroA4*, Δ*nkuA*::*argB*; Δ*mztA*::*pyroA*	Marjorie Schmid
SMS3	*pyrG89*; *argB2*; *pyroA4*, Δ*nkuA*::*argB*; *alcA(p)*::*GFP*::*sfiA*::*pyr4*	Marjorie Schmid
SMS4	*pyrG89*; *argB2*; *pyroA4*, Δ*nkuA*::*argB*; *mztA*::*GFP*::*AfpyrG*	Marjorie Schmid

SMS6	*pyrG89*; *argB2*; *pyroA4*, Δ*nkuA*::*argB*; *alcA(p)*::*GFP*::*Ancdc31*::*pyr4*	Marjorie Schmid
SNZ-SH80	*alpB(p)*::*alpB*::*GFP*; *pyroA4*, Δ*nkuA*::*argB*	(Zekert *et al*., 2010)
SO451	*fwA1*; *pyrG89*; *chaA1*, *sE15*, *wA3*; *argB2*; Δ*nkuA*::*argB*, *pyroA4*; *nirA14*	Stephen Osmani, Ohio University, US
SO1312	*fwA1*; *pyrG89*; *chaA1*, *sE15*, *wA3*; *argB2*, *AnSPA18*::*GFP/S-tag*::*AfpyrG*; Δ*nkuA*::*argB*, *pyroA4*; *nirA14*	Stephen Osmani, Ohio University, US
SO1330	*fwA1*; *pyrG89*; *chaA1*, *sE15*, *wA3*; *argB2*; Δ*nkuA*::*argB*, *pyroA4*; Δ*AnSPA10*::*AfpyrG*; *nirA14*	Stephen Osmani, Ohio University, US
SO1334	*fwA1*; *pyrG89*; *chaA1*, *sE15*, *wA3*; *argB2*, Δ*AnSPA18*::*AfpyrG*; Δ*nkuA*::*argB*, *pyroA4*; *nirA14*	Stephen Osmani, Ohio University, US
SRS31	*pyrG89*; Δ*argB*::*trpC*Δ*B*; *pyroA4*; Δ*apsB*::*argB*	(Suelmann *et al*., 1998)
SSH27	*wA3*, *alcA(p)*::*GFP*::*kipA*::*pyr4*; Δ*argB*::*trpC*Δ*B*	(Herrero *et al*., 2011)
SSK92	*pyrG89*; *wA3*, *alcA(p)*::*GFP*::*kipA*::*pyr4*; *pyroA4*	(Konzack *et al*., 2005)
SYZ2	*pyrG89*; *argB2*; *pyroA4*, Δ*nkuA*::*argB*; *alcA(p)*::*GFP*::*apsB*::*pyr4* (TN02A3 transformed with pYZ6)	This study
SYZ3	*pyrG89*; *argB2*; *pyroA4*, Δ*nkuA*::*argB*; Δ*apsB*::*pyroA* (TN02A3 transformed with pYZ11)	This study
SYZ4	*pyrG89*; *argB2*; *pyroA4*, Δ*nkuA*::*argB*; Δ*pexC*::*pyroA*; *alcA(p)*::*GFP*::*acuE*::*pyr4* (SAH3 transformed with pYZ9)	This study
SYZ5	*pyrG89*; *argB2*; *pyroA4*, Δ*nkuA*::*argB*; Δ*pexC*::*pyroA*; *alcA(p)*::*pexC*::*pyr4* (SAH3 transformed with pYZ13)	This study
SYZ6	*pyrG89*; *argB2*; *pyroA4*, Δ*nkuA*::*argB*; Δ*apsB*$^{4.7}$::*pyroA*; *alcA(p)*::*apsB*$^{3.2}$::*pyr4* (SYZ3 transformed with pYZ14)	This study

SYZ7	*pyrG89*; *argB2*; *pyroA4*, Δ*nkuA*::*argB*; Δ*apsB*$^{4.7}$::*pyroA*; *alcA(p)*::*apsB*$^{4.7}$::*pyr4* (SYZ3 transformed with pYZ15)	This study
SYZ8	*wA3*, *alcA(p)*::*GFP*::*kipA*::*pyr4*; Δ*pexC*::*pyroA* (SSK92 crossed with SAH3)	This study
SYZ9	*wA3*, *alcA(p)*::*GFP*::*kipA*::*pyr4*; Δ*apsB*$^{4.7}$::*pyroA* (SSK92 crossed with SYZ3)	This study
SYZ10	*wA3*; Δ*pexC*::*pyroA*; *alcA(p)*::*GFP*::*tubA*::*pyr4* (SJW02 crossed with SAH3)	This study
SYZ11	*wA3*; Δ*apsB*$^{4.7}$::*pyroA*; *alcA(p)*::*GFP*::*tubA*::*pyr4* (SJW02 crossed with SYZ3)	This study
SYZ17	*pyrG89*; *argB2*; *pyroA4*, Δ*nkuA*::*argB*; *alcA(p)*::*S-tag*::*apsB*::*pyr4* (TN02A3 transformed with pYZ18)	This study
SYZ31	*argB2*, Δ*AnSPA18*::*AfpyrG*; *pyroA4* (SO1334 crossed with RMS011)	This study
SYZ32	*argB2*, Δ*AnSPA18*::*AfpyrG* (SO1334 crossed with RMS011)	This study
SYZ33	*pabaA1*, *yA2*; Δ*AnSPA18*::*AfpyrG*; *pyroA4* (SO1334 crossed with RMS011)	This study
SYZ34	*wA3*; Δ*AnSPA18*::*AfpyrG*; *pyroA4*; *alcA(p)*::*GFP*::*tubA*::*pyr4* (SO1334 crossed with SJW02)	This study
SYZ35	*argB2*, Δ*AnSPA18*::*AfpyrG*; Δ*apsB*::*pyroA* (SYZ31 crossed with SYZ3)	This study
SYZ38	*fwA1*; *AnSPA18*::*GFP*::*AfpyrG*; Δ*apsB*::*pyroA* (SYZ1312 crossed with SYZ3)	This study
SYZ39	*wA3*; *GCPC*::*GFP*::*AfpyrG*; Δ*apsB*::*pyroA* (SYZ3 crossed with SNZ-SH80)	This study
SYZ40	*argB2*; *pyroA4*, Δ*nkuA*::*argB*; Δ*apsB*::*pyroA*;	This study

	alcA(p)::*GFP*::*apsB*Δ*SMB* (SYZ3 co-transformed with pYZ29 and pAB4-1)	
SYZ41	*argB2*; *pyroA4*, Δ*nkuA*::*argB*; Δ*apsB*::*pyroA*; *alcA(p)*::*GFP*::*apsB*Δ*MASC*Δ*SMB* (SYZ3 co-transformed with pYZ28 and pAB4-1)	This study
SYZ42	Δ*AnSPA18*::*AfpyrG*, *GCPC*::*GFP*::*AfpyrG*; *pyroA4* (SYZ31 crossed with SNZ-SH80)	This study
SYZ43	*wA3*, *alcA(p)*::*GFP*::*kipA*::*pyr4*; Δ*AnSPA18*::*AfpyrG* (SYZ33 crossed with SSH27)	This study
SYZ44	Δ*AnSPA18*::*AfpyrG*, *GCPC*::*GFP*::*AfpyrG*; Δ*apsB*::*pyroA* (SYZ35 crossed with SNZ-SH80)	This study
SYZ45	*pabaA1*, *yA2*; Δ*AnSPA18*::*AfpyrG*; Δ*apsB*::*pyroA* (SYZ33 crossed with SYZ3)	This study
SYZ46	Δ*AnSPA18*::*AfpyrG*; *alcA(p)*::*GFP*::*apsB*::*pyr4* (SYZ32 crossed with SYZ2)	This study
SYZ47	*AnSPA18*::*GFP/S-tag*::*AfpyrG*; *alcA(p)*::*mCherry*::*apsB*::*pyr4* (SO1312 transformed with pYZ27)	This study
SYZ49	Δ*AnSPA18*::*AfpyrG*; Δ*apsB*::*pyroA*; *alcA(p)*::*GFP*::*tubA*::*pyr4* (SYZ45 crossed with SJW02)	This study
SYZ51	*wA3*, *alcA(p)*::*GFP*::*kipA*::*pyr4*; Δ*AnSPA18*::*AfpyrG*; Δ*apsB*::*pyroA* (SYZ45 crossed with SSH27)	This study
SYZ52	*yA2*; Δ*AnSPA18*::*AfpyrG*; Δ*apsB*::*pyroA*; *alcA(p)*::*GFP*::*apsB*Δ*MASC*Δ*SMB* (SYZ45 co-transformed with pCK17 and pYZ28)	This study
SYZ53	*yA2*; Δ*AnSPA18*::*AfpyrG*; Δ*apsB*::*pyroA*; *alcA(p)*::*GFP*::*apsB*Δ*SMB* (SYZ45 co-transformed with pCK17 and pYZ29)	This study
SYZ56	*pyrG89*; *argB2*, *GCPC*::*GFP*::*AfpyrG*; *pyroA4*, Δ*nkuA*::argB; Δ*apsB*::*pyroA*; *alcA(p)*::*mCherry*::*apsB*Δ*CM1*::*pyr4* (SYZ3	This study

	co-transformed with pYZ65 and *GCPC*::*GFP*::*AfpyrG*::*RB-GCPC* fusion PCR)	
SYZ57	*argB2*; *pyroA4*, Δ*nkuA*::*argB*; Δ*apsB*::*pyroA*; *alcA(p)*::*GFP*::*apsB*Δ*MASC* (SYZ3 co-transformed with pYZ67 and pAB4-1)	This study
SYZ58	*yA2*; Δ*AnSPA18*::*AfpyrG*; Δ*apsB*::*pyroA*; *alcA(p)*::*GFP*::*apsB*Δ*MASC* (SYZ45 co-transformed with pCK17 and pYZ67)	This study
SYZ59	*yA2*; Δ*AnSPA18*::*AfpyrG*; Δ*apsB*::*pyroA*; *alcA(p)*::*GFP*::*apsB*Δ*SMB*::*SMB-C* (SYZ45 co-transformed with pCK17 and pYZ68)	This study
SYZ60	*pyrG89*; *pyroA4*, *nkuA*::*argB*; Δ*sepK*::*AfpyrG*; *riboB2*; *HH1*-mRFP::*AfriboB*; *alcA(p)*::*GFP*::*apsB*::*pyroA* (LO1906 tranformed with pYZ26)	This study
SYZ61	*pyrG89*; *argB2*; *pyroA4*, Δ*nkuA*::*argB*; *alcA(p)*::YFP^N::*SPA18*::*pyroA*; *alcA(p)*::YFP^C::*apsB*::*pyr4* (TN02A3 co-transformed with pYZ56 and pYZ47)	This study
SYZ62	*argB2*; *pyroA4*, Δ*nkuA*::*argB*; Δ*apsB*::*pyroA*; *alcA(p)*::*GFP*::*apsB*Δ*SMB*::*SMB-C* (SYZ3 co-transformed with pYZ68 and pAB4-1)	This study
SYZ69	*fwA1*; *pyrG89*; *chaA1*, *sE15*, *wA3*; *argB2*; Δ*nkuA*::*argB*, *pyroA4*; Δ*AnSPA10*::*AfpyrG*; *nirA14*; *alcA(p)*::*GFP*::*apsB*::*pyroA* (SO1330 transformed with pYZ26)	This study
SYZ70	Δ*AnSPA18*::*AfpyrG*; *pyroA4*; Δ*sepK*::*AfpyrG* (SYZ32 crossed with LO1906)	This study
SYZ71	Δ*AnSPA18*::*AfpyrG*; *pyroA4*; Δ*sepK*::*AfpyrG*; *alcA(p)*::*GFP*::*apsB*::*pyroA* (SYZ70 transformed with pYZ26)	This study
SYZ74	*fwA1*; *pyrG89*; *chaA1*, *sE15*, *wA3*; *argB2*, *AnSPA18*::*GFP*::*pyroA*; Δ*nkuA*::*argB*, *pyroA4*; Δ*AnSPA10*::*AfpyrG*; *nirA14* (LO1906 transformed	This study

	with pYZ66)	
SYZ75	*pyrG89*; *argB2*, *alcA(p)*::*GFP*::*SPA18*::*pyroA*; *pyroA4*, ∆*nkuA*::*argB* (TN02A3 transformed with pYZ66)	This study
TALX207-10	*yA1*; *pyroA4*; *areA102*; *gpd(p)*::*GFP*::*acuE*	(Hynes *et al.*, 2008)
TN02A3	*pyrG89*; *argB2*; *pyroA4*, ∆*nkuA*::*argB*; *veA1*	(Nayak *et al.*, 2006)

2.2 Transformation methods

2.2.1 Transformation of DNA into *E. coli*

Plasmid DNA was transformed into *E. coli* Top10 (Invitrogen) through its Calcium Chloride competent cells (Mandel & Higa, 1970). To prepare the competent cells, a single colony was picked with toothpick and inoculated in 10 ml LB medium overnight at 37°C. Then 1 ml culture was inoculated to 100 ml LB medium and shaken until it came to an OD_{600} of ~0.375, which would take 3-4 h. The culture was put on ice for 5-10 min and transferred into four 50 ml falcons followed by centrifugation at 1600 *g* 4°C for 7 min. Afterwards, the supernatant was decanted and the pellets were re-suspended in 10 ml 0.1 M $CaCl_2$, followed by centrifugation at 1100 *g* 4°C for 5 min. The supernatant was again removed before adding another 10 ml 0.1 M $CaCl_2$. After putting on ice for 30 min and centrifugation the competent cells were at the bottom of the falcons. Finally, the competent cells were re-suspended with 2 ml 0.1 M $CaCl_2$ for each falcon and made aliquorts with 100 µl in each EP. The competent cells could be stored at -80°C for several months.

To transform DNA into *E. coli*, 1 µl of circular plasmid or 10 µl ligation reaction was added to 100 µl competent cells and mixed with pipette. After incubation on ice for 10-15 min, the mixture was given a heat shock in 42°C water bath for 2.5 min. The EP was then put on ice for at least for 1 min followed by adding 900 µl SOC medium and shaken at 37°C for 1 h. Afterwards, the culture was centrifuged at 13000 rpm for 1 min and removed 700 µl supernatant, the rest 300 µl were re-suspended and spread on LB agar plate with Ampicillin or Kanamycin. After incubation upside down of the plate for 12-14 h at 37°C, the visible colonies could be picked and inoculated into LB liquid medium with antibiotics. Further colony PCR or miniprep combined with restriction digestion could be performed to select the correct strains.

2.2.2 Transformation of DNA into *A. nidulans*

Standard procedures of *Aspergillus* protoplast transformation were used (Yelton *et al.*, 1984). Spores were harvested from freshly grown plates, inoculated in 300 ml minimal medium with

appropriate suppplements, and shaken at 30°C 180 rpm for 12-16 h until the spores had germinated. The culture was filtered through sterile Miracloth followed by washing with Wash solution. The washed mycelium was collected on ice in a sterile 100 ml Erlenmeyer flask with 5 ml of Osmotic medium. After addition of 180 mg GlucanX (Novozyme) and 10 mg BSA and 5 min incubation on ice, the digestion mixture was incubated at 30°C 120 rpm for 1.5-2 h until enough protoplasts were released. The digestion mixture were then transferred to a 50 ml falcon and added with 10 ml Trapping buffer very slowly, followed by a centrifugation at 5000 rpm for 15 min with small acceleration and deceleration rates. The obtained protoplast band between Osmotic medium and Trapping buffer layers was transferred into a new sterile tube, followed by washing with STC and centrifugation at 5000 rpm for 8 min. The protoplast pellet was gently re-suspended in 200-800 µl STC for following transformation. Maximun10 µl of DNA (4-10 µg) filled up to 50 µl with STC, 200 µl of protoplasts in STC and 50 µl PEG solution were mixed and incubated for 20 min on ice. Afterwards, 1 ml PEG was added and mixed with pipette until the mixture was homogeneous, followed by 5-20 min incubation at RT. The mixture was then transferred to a 50 ml falcon with 5 ml STC and rolled until it was homogeneous. After addition of 25-30 ml 47°C MMR-Top, the entire mixture was mixed and poured on MMR agar plates with appropriate selection markers. The plates were incubated at 37°C until colonies were visible after 3-4 days. The solutions or media used are listed in **Table 11**).

Table 11. Solutions used for *A. nidulans* transformation.

Buffer or medium	Composition
Mycelium wash solution	0.6 M $MgSO_4$
Osmotic medium	1.2 M $MgSO_4$, 10 mM Na_3PO_4 buffer, pH 5.8
Trapping buffer	0.6 M sorbitol, 0.1 M Tris-HCl, pH 7.0
STC	1.2 M sorbitol, 10 mM $CaCl_2$, 10 mM Tris-HCl, pH 7.5
PEG solution	60% PEG 4000, 10 mM $CaCl_2$, 10 mM Tris-HCl, pH 7.5
MMR	50 ml Salt stock solution; 1 ml Trace elements stock solution; 342 g saccharose; 15 g agar; pH 6.8; add 100 ml 10x glucose stock solution (200 g in 1 L H_2O) and 10 ml 100x Ammonium Tartrate stock solution (92 g in 1 L H_2O) after autoclaving
MMR-TOP	50 ml Salt stock solution; 1 ml Trace elements stock solution; 342 g saccharose; 6 g agar; pH 6.8

2.3 Crossing of strains

The strains used for crossing were inoculated side by side onto YAG agar plates plus appropriate markers for 2-3 days, until the mycelia of both strains fused at the borders. Small and thin agar square pieces were cut from these fused edges and transferred to MM agar plates with appropriate markers, where just the growth of a heterokaryon is available. Plates were sealed with adhesive tape and wrapped with Aluminium foil in order to avoid the oxygen and light, as well as elevation of the pressure of CO_2, and thus activate sexual development. After incubation for 10-14 days at 37°C or 30°C in a humid chamber, the fruiting bodies (cleistothecia) developed were isolated with a sterile inoculating needle under stereo microscope (Wild M5A, Heerbrugg, Switzerland) rolled until completely cleaned from Hülle cells on the surface of an agar plate, and smashed in an Eppendorf tube with 500 µl sterile ddH_20. The aliquots of the ascospore suspension were inoculated onto 3 YAG agar plates with appropriate markers. After incubation for 2-3 days, the grown colonies were transferred onto raster MM plates with different selection markers, which could accommodate 21 colonies on each plate (Sievers *et al.*, 1997), to select the auxotrophic strains we needed.

3 Molecular biological methods

3.1 DNA manipulations

3.1.1 Polymerase Chain Reaction

Polymerase chain reaction (PCR) was performed with Taq or Phusion polymerases from New England Biolabs (NEB, Frankfurt am Main) according to manufacturer protocols. Oligonucleotides synthesis was performed by MWG Biotech (Ebersberg), and the final concentration is 0.2 µM in 25 µl or 50 µl PCR reactions, in which ~10 ng plasmid DNA or ~100 ng genomic DNA or cDNA were used as templates, in addition to 0.5 µl Taq or Phusion polymerase. dNTPs were from Roth (Karlsruhe) with a final concentration of 200 µM. The PCR reactions were carried out in SensoQuest Labcycler (Göttingen) or Biometra Thermocycler T3 (Biometra, Göttingen) PCR machines. The PCR programs are changeable due to the length of the amplified fragments. After pre-denaturation at 95°C or 98°C for 3 min, 25-35 cycles are executed with 95°C/30 s (Taq) or 98°C/10 s (Phusion) denaturation, annealing at appropriate primer-dependent temperature for 30 s and elongation at 68°C at a speed of 1kb/min (Taq) or 72°C at 1kb/30 s (Phusion). The final extension after the cycles took 5 min. For colony PCR of *E. coli*, Taq polymerase was used and the pre-denaturation time was 10 min. As for fusion PCR, 10 cycles were performed in the absence of primes followed by another 35 cycles with primers. The primers used in this work are listed in **(Table 12)**.

Table 12. Primers used in this work.

Primer	Sequence	Discription
apsB-LB-linker_rev	ACTGACCTTACGACAGCTTCGCCTTACCC	
apsB-LB-linker_rev	ACTGACCTTACGACAGCTTCGCCTTACCC	
pyroA-linker_fwd	GAAGCTGTCGTAAGGTCAGTTCGAGACCA	
pyroA-linker_rev	ATCATCGTACGAATGCACAGAACACCCTAACA	***apsB*$^{4.7}$ deletion**
apsB-RB-linker_fwd	TCTGTGCATTCGTACGATGATTGTTTGGCTG	
apsB-RB_rev	ACTTTCACCCACAGAATCCG	
apsB-LB-N-fwd	GGTCACCACCGTCTTCATC	
apsB-RB-N_re	GACGACCTCATAGGGAAGC	
apsB_AscI_fwd	A*GGCGCGCC*AATGTCGACCTCATCCCAAC	
apsB-1_PacI_rev	CC*TTAATTAA*TACTCCTTCGGCTACCTCT	**ApsB localization**
apsB-4.7_PacI_rev	CC*TTAATTAA*TCAAACTTCGATATCAACTGTGA	
SPA18_AscI_fwd	A*GGCGCGCC*AATGCTCCACGACAAAGAATCT	**SPA18 localzation**
SPA18-1_PacI_rev	CC*TTAATTAA*GTCGGACCTCGCAATGT	
SPA18-f_PacI_rev	CC*TTAATTAA*TCAGTCAATGCTGTCGTTGA	
Y2H_SPA18_NdeI_F	CGC*CATATG*CTCCACGACAAAGAATCT	
Y2H_SPA18_BamHI_R	CGC*GGATCC*TCAGTCAATGCTGTCGTTGA	**Yeast two Hybrid**
Y2H_ApsB_NdeI_F	CGC*CATATG*TCGACCTCATCCCAAC	

Y2H_ApsB_BamHI_R	AGC*GGATCC*TCAAACTTCGATATCAACTGTGATG	
∆CM1_L_linker_R	CGACTCCTTATCTGACTGCTGCATGGATCTGCCACTGCG	**Deletion the CM1 domain of ApsB**
∆CM1_R_F	CAGCAGTCAGATAAGGAGTCG	
Alp6_Nprimer_fwd	CCAGTCTCGAGACCTCAATTG	**GCPC localization**
Alp6_Nprimer_rev	TTATCACCTGCTGGTTCTGAG	
apsB_∆SMB_PacI_rev	CC*TTAATTAA*TTAACGCTGTCGGTCCAAC	
apsB_∆MASC∆SMB_PacI_rev	CC*TTAATTAA*TTATTCTTGATTGCCGTGGTTATCT	
∆MASC_linker_rev	GAGACTCCTTGGCGGAGTTCTTGATTGCCGTGGTTATCT	**Functional analysis of the MASC, SMB, and SMB-C domains**
apsB_SMB_fwd	CTCCGCCAAGGAGTCTC	
SMB-C_R	CC*TTAATTAA*TCAAACTTCGATATCAACTGTGATGCCTTCCCCCTCACTCGAGCTACGCTGTCGGTCCAAC	
acuE_AscI_fwd	A*GGCGCGCC*AATGTCTCAGGTCGACGC	**Peroxisome marker**
acuE_PacI_rev	CC*TTAATTAA*TTAGAGCTTTGAAGCAGTACC	
pexC_AscI_fwd	A*GGCGCGCC*AATGATCAGTGCTACGAGGC	***pexC* re-complementation**
pexC_PacI_rev	CC*TTAATTAA*TCACTTGCCGTCAACGA	
S-apsB_fwd	GG*GGTACC*ATGAAAGAAACCGCTGCTGCTAAATTCGAACGCCAGCACATGGACAGCATGTCGACCTCATCCCAAC	**S-tag of ApsB**

3.1.2 DNA agarose gel electrophoresis

DNA fragments were separated by running on 0.8% agarose gel at 50-100 V for 30 min - 4 h with 0.5x TAE buffer **(Table 13)** (Sambrook & Russel, 1989), The gels were prepared by heating and melting agarose in 0.5x TAE buffer and pouring it into gel chambers, which could solidify in room temperature (RT). DNA products were mixed with 6x DNA Loading buffer and loaded. 1 kb, 100 bp or 2-Log DNA ladders from NEB were used in this study. After running, the gels were stained for 15-30 min in ddH_2O with ethidium bromide (EB, 1 µg/µl), and then the DNA bands could be visualized under the 302 nm UV light. Photos were taken using a camera (INTAS, Göttingen) connected to a printer. The DNA bands of interest were cut out under UV light.

Table 13. Solutions used for DNA agarose gel electrophoresis.

Solution	Composition
50x TAE buffer	40 mM Tris-Acetate; 1 mM EDTA; pH 8.0
1x Loading buffer	15% Ficoll 400; 5 mM EDTA (pH 8.0); 1% SDS; 1.5 M Bromphenol blue

3.1.3 DNA purification, digestion and ligation

The cut gel of DNA was purified with Zymoclean Gel DNA Recovery Kit (Zymo Research, US) according to the protocols from the manufacturer. As for the DNA in solutions, a DNA Clean & Concentrator-5 Kit (Zymo Research, US) was used. The concentration of the purified DNA could be measured with Nano drop 1000 (PeQLab, Erlangen).

DNA samples (200 ng - 1 µg) were digested with restriction endonucleases in corresponding reaction buffers (NEB). Generally, digestions were prepared in 20-50 µl total volume, with 0.2-0.5 µl restriction enzyme and incubated from 1 h to overnight at appropriate temperature provided by the manufacturer. As for double digestion, the recommended reaction conditions are supplied at https://www.neb.com/tools-and-resources/interactive-tools/double-digest-finder.

DNA ligation was performed using T4 ligase (NEB) and the provided reaction buffer at RT (22°C) for 30 min in a volume of 10 µl. Around 50 ng/kb insert was used in one ligation. The molar ratio of vector to insert was 1: 3 for cohesive end ligation, as well as ligation of blunt-end DNA fragments to a pJET1.2/blunt Cloning Vector (Fermentas, St. Leon-Rot).

3.1.4 DNA sequencing

DNA sequencing was done commercially by MWG Biotech (Ebersberg).

3.2 Plasmids extraction from *E. coli* cells

Isolation of plasmid DNA was done with an alkali-lysis method as described in (Sambrook & Russel, 1989). For quick and dirty miniprep of DNA, 2 ml overnight liquid culture was centrifuged for 1 min at 13000 rpm. After re-suspending the pellet in 200 µl Tris-EDTA Buffer, 200 µl of Alkali-lysis buffer was added and gently mixed, followed by addition of 200 µl Neutralization buffer and inversion 6-7 times **(Table 14)**. The mixture was put on ice for 5 min, and then centrifuged for another 5 min (or at 4°C). Afterwards, the supernatant containing the plasmid DNA was transferred to a new tube, followed by adding 0.7 vol. isopropanol and centrifugation for 10 min at 4°C to precipitate the DNA. After washing with 70% ethanol, the dried pellet was re-suspended in TE buffer. To get pure plasmid DNA, a NucleoSpin Plasmid EasyPure kit (MACHEREY-NAGEL, Düren) was used according to the manufacturer's protocols. The plasmids used in this study are listed in **Table 15**.

Table 14. Solutions used for plasmid DNA extraction (miniprep).

Solution	Composition
Tris-EDTA buffer	5 ml 1M Tris-HCl (pH 7.5); 2 ml 0.5M EDTA (pH 8.0); 10 mg RNase in 100 ml
Alkali-lysis buffer	0.2 M NaOH; 1% SDS
Neutralization buffer	1.5 M Potassium Acetate, pH 4.8
TE buffer	10 mM Tris-HCl; 1 mM EDTA; pH 8.0

Table 15. List of plasmids in this work.

Plasmid	Genotype	Source
pJET1.2/blunt	Blunt end cloning vector	Fermentas
pMCB17apx	*alcA(p)*::*GFP*, for N-terminal fusion of GFP to proteins of interest; contains *N. crassa pyr4*	(Efimov *et al.*, 2006)
pAB4-1	Vector with *A. niger pyrG* ORF	(Mattern *et al*., 1987)
pCK17	*pabaA* ORF in pCR2.1-TOPO	Christian Kastner

pGADT7-Rec	Gal4 DNA-activation domain (AD); Amp^r	Clontech
pGBKT7	Gal4 DNA-binding domain (BD); Kan^r	Clontech
pYZ1	*alcA(p)*::*GFP*::*pexC*^{f}, *pyr4* (pMCB17apx with full-length *pexC* ORF)	This study
pYZ6	*alcA(p)*::*GFP*::*apsB*$^{1.0}$, *pyr4* (pMCB17apx with N-1.0 kb *apsB*)	This study
pYZ9	*alcA(p)*::*GFP*::*acuE*^{f}, *pyr4* (pMCB17apx with full-length *acuE* ORF)	This study
pYZ11	pJET1.2/blunt with *apsB*$^{4.7}$ deletion cassette ($LB^{1.0}$::*pyroA*::$RB^{1.0}$)	This study
pYZ13	*alcA(p)*::*pexC*^{f}, *pyr4* (pMCB17apx with full-length *pexC* ORF and without *GFP*)	This study
pYZ14	*alcA(p)*::*apsB*$^{3.2}$, *pyr4* (pMCB17apx with *apsB*$^{3.2}$ and without *GFP*)	This study
pYZ15	*alcA(p)*::*apsB*$^{4.7}$, *pyr4* (pMCB17apx with *apsB*$^{4.7}$ and without *GFP*)	This study
pYZ18	*alcA(p)*::*S-tag*::*apsB*$^{1.0}$, *pyr4* (S-peptide coding sequence fused to *apsB*$^{1.0}$ by oligonucleotides synthesis)	This study
pYZ26	*alcA(p)*::*GFP*::*apsB*$^{4.7}$, *pyroA* (pMCB17apx with *apsB*$^{4.7}$, *pyr4* replaced by *pyroA*)	This study
pYZ27	*alcA(p)*::*mCherry*::*apsB*$^{1.0}$, *pyroA* (pMCB17apx with *apsB*$^{1.0}$, *pyr4* replaced by *pyroA*, *GFP* replaced by *mCherry*)	This study
pYZ28	*alcA(p)*::*GFP*::*apsB*Δ*MASC*Δ*SMB*, *pyroA* (pMCB17apx with *apsB*Δ*MASC*Δ*SMB*, *pyr4* replaced by *pyroA*)	This study
pYZ29	*alcA(p)*::*GFP*::*apsB*Δ*SMB*, *pyroA* (pMCB17apx with *apsB*Δ*SMB*, *pyr4* replaced by *pyroA*)	This study

pYZ47	*alcA(p)*::*YFP*^{C}::*apsB*$^{4.7}$, *pyr4* (pMCB17apx with *apsB*$^{4.7}$, *GFP* replaced by *YFP*^{C})	This study
pYZ51	full-length *SPA18* cDNA in pGBKT7	This study
pYZ56	*alcA(p)*::*YFP*^{N}::*SPA18*^{f}, *pyroA* (pMCB17apx with full-length *SPA18*, *pyr4* replaced by *pyroA*, *GFP* replaced by *YFP*^{N})	This study
pYZ61	full-length *apsB* cDNA in pGADT7-Rec	This study
pYZ65	*alcA(p)*::*mCherry*::*apsB*Δ*CM1*, *pyroA* (pMCB17apx with *apsB*Δ*CM1*, *pyr4* replaced by *pyroA*, *GFP* replaced by *mCherry*)	This study
pYZ66	*alcA(p)*::*GFP*::*SPA18*$^{1.0}$, *pyroA* (pMCB17apx with N-1.0 kb *SPA18*, *pyr4* replaced by *pyroA*)	This study
pYZ67	*alcA(p)*::*GFP*::*apsB*Δ*MASC*, *pyroA* (pMCB17apx with *apsB*Δ*MASC*, *pyr4* replaced by *pyroA*)	This study
pYZ68	*alcA(p)*::*GFP*::*apsB*Δ*SMB*::*SMB-C*, *pyroA* (pMCB17apx with *apsB*Δ*SMB*::*SMB-C*, *pyr4* replaced by *pyroA*)	This study

3.3 Genomic DNA extraction from *A. nidulans* cells

To prepare the genomic DNA from *A. nidulans* cells, spores scratched from an agar plate were inoculated in a plastic Petri dish with liquid medium. After culture overnight at 37°C, the mycelium was harvested with a spatula and dried with miracloth. Approx. 20-100 mg wet mycelium was put in an Eppendorf-tube with slim link (1.5 ml) in addition with 700 µl extraction buffer **(see Table 16)** and one metal bead (3 mm). The mycelium was broken in homogenizer (MM200, Retsch, Haan) for 10-15 min at 30 s frequency. After incubation at 68°C in a Thermo mixer for 1 h, 100 µl 8 M Potassium Acetat (pH 4.2) was added followed by incubation on ice for 30 min with invertion every 5 min. After centrifugation at 13000 rpm for 15 min, 500 µl of the supernatant was transferred to a new Eppendorf-tube (1.5 ml) with 1 ml 100% ethanol and mixed, followed by centrifugation again at 13000 rpm 15 min. The pellet was washed with 70% ethanol and dried in the open air. Afterwards, it was resuspended in 50 µl TE/RNase buffer. 1-2 µl extracted DNA was checked on a gel for integrity.

Table 16. Solutions for genomic DNA extraction.

Solution	Composition
Extraction buffer	1% SDS, 50 mM EDTA, 50 mM pH 7.5 Tris-HCl, dilution 1:1 with 1x TE.
8 M Potassium Acetat (pH 4.2)	Dissolve 29.4 g Potassium Acetat in 50 ml dd H_2O, then add 11.5 ml 100% Acetic Acid and adjust the pH to 4.2 with HCl. Fill up to 100 ml with H_2O.

3.4 Southern blot analysis

DNA-DNA hybridization was performed with DIG labeled DNA probes, amplified by PCR using Taq polymerase and the PCR DIG Probe Synthesis Kit from Roche (Mannheim), according to the distributor's protocol. The probes were diluted in 40 µl ddH_2O and boiled at 100°C for 5 min before putting in hybridization solution and reaching a final concentration of 20-50 ng/ml. 10-30 µg genomic DNA was digested overnight with the appropriate restriction enzyme. Next day DNA samples of candidate strains and wild type were separated at 50 V for 3-4 h through 1% long agarose gel electrophoresis, until the Bromphenole blue band was weakly visible in lower third of the gel. Afterwards, the gel was stained with ethidium bromide and the marker bands were marked by making little holes with a 1 µl pipet tip, then the gel was washed for 10 min in depurination solution and followed by denaturation 2 times for 15 min with denaturation solution at RT. After rinsing briefly in water, the gel was equilibrated 2 times for 15 min in washing with neutralization solution and then 10 min equilibration with 20x SSC. After equilibration, the DNA in gel was transferred overnight at RT through capillary forces to a neutral nitrocellulose membrane (Pall Gelman Laboratories, Dreieich). The transfer was set up (bottom to top) as follows: A bridge of whatman paper (presoaked in 20x SSC and making contact to 20x SSC reservoirs at both ends), gel (upside down), membrane (presoaked in 20x SSC), 3 layers of whatman paper (dry), several layers of tissue, and a glass plate on top with 200 g heavy books or similar device. After blotting the membrane was cross-linked with UV radiation (254 nm, 1.200 x 102 µJ for each side). The membrane was then pre-hybridized in hybridization solution for 1 h at 68°C and then further hybridized for 12 h with the probe at 68°C, which could be stored at -20°C and reused for several times, followed by stringent washing. The membrane was first washed for 5 min with 2x washing solution 2 times at RT, followed by washing in 0.5x washing solution 15 min for 2 times at 68°C. After 5 min at RT in washing buffer, the membrane was incubated for 1 h at RT in blocking buffer followed by 30 min incubation with 2 µl anti-DIG-Antibody-AP (Roche, Manheim) in 20 ml new blocking buffer. Free antibodies were washed away 15 min for 2 times

with washing buffer at RT. Finally the membrane was equilibrated in AP-buffer for 5 min at RT and transferred to a plastic film with AP-Substrate (5 µl Roche CDPStar in 500 µl AP-buffer for a membrane of 10 x 10 cm) distributed evenly above with a second plastic film. Detection was accomplished by Lumi-Imager (PeQLab, Erlangen). If the membrane was reused, stripping was carried out 2 times in stripping buffer for 15 min at 37°C, followed by equilibration for 5 min in 20x SSC. The solutions used for Southern blot were listed in **Table 17.**

Table 17. Solutions used for Southern blot.

Solution	Composition
Hybridization solution	5x SSC; 0.02% SDS; 1% Blocking Reagent (Roche); 0.1% N-Laurylsarcosin
Depurination solution	0.25 M HCl
Denaturation solution	0.5 M NaOH; 1.5 M NaCl
Neutralization solution	1.5 M NaCl; 0.25 M Tris-HCl, pH 7.5
20x SSC	3 M NaCl; 0.3 M NaCitrat, pH 7.0
2x Washing solution	2x SSC; 0.1% SDS
0.5x Washing solution	100 mM Maleic acid; 150 mM NaCl; 0.3 % Tween20
Washing buffer	0.5x SSC; 0.1% SDS
Blocking buffer	100 mM Maleic acid, 150 mM NaCl; 1% Blocking Reagent
AP-buffer	0.1 M Tris-HCl, pH 9.5; 0.1 M NaCl; 50 mM $MgCl_2$
Stripping buffer	0.2 M NaOH; 0.1% SDS

3.5 RNA isolation

Spores scratched from an agar plate were inoculated in a plastic Petri dish with liquid media. After culture overnight at 37°C, the mycelium was harvested with a spatula and dried with miracloth. The mycelium was frozen in liquid nitrogen and stored at -80°C until being used. RNA was isolated with the E. Z. N. A. Fungal RNA Mini Kit (VWR). The isolated RNA was dissolved in RNase-free DEPC water and quantified with Nano drop 1000, followed by removal of the DNA with TURBO DNA-free Kit (Applied Biosystems) under the instructions from the manufacturer.

3.6 First-Strand cDNA Synthesis

The First-Strand cDNA Synthesis was carried out with a SuperScript III Reverse Transcriptase kit (Invitrogen). 500 ng Oligo(dT)$_{12-18}$, 5 µg total RNA and 1 µl 10 mM dNTP Mix were added in a small pcr cup and filled to 13 µl with ddH_2O. The mixture was heated at 65°C for 5 min and incubated on ice for at least 1 min. After collecting the contents of the cup by brief centrifugation, 4 µl 5x First Strand Buffer, 1 µl 0.1 M dTT, 1 µl RNaseOUT Recombinant RNase Inhibitor (40 units/µl) and 1 µl of SuperScript III Reverse Transcriptase (200 units/µl) were added to the reaction and mixed by pipetting gently, followed by incubation at 50°C for 30-60 min. Afterwards, the reaction was inactivated by heating at 70°C for 15 min. To remove RNA complementary to the cDNA, 1 µl (2 units) of *E. coli* RNase H was added and incubated at 37°C for 20 min. The cDNA could be used as a template for amplification in PCR.

4 Biochemical methods

4.1 S-tag affinity purification

1L YAG media in a conical flask was inoculated with 2.5 x 10^6 conidia/ml and incubated with shaking (180 rpm) overnight (~14-16h) at 30°C until grown to a packed cell volume of ~0.3 ml per 10 ml. The mycelia were harvested by filtering through miracloth, and washed with 100 ml cold stop buffer. The miracloth was folded in half to make the mycelia sandwiched inside, followed by gently pressed between paper towels until excess liquid is removed. Afterwards, the mycelial mat was peeled from the miracloth, grinded in a mortar and pestle with liquid mitrogen, or put into a 50 ml falcon and immediately frozen in liquid nitrogen and stored in -80°C. The grinded fine powder (0.7-1.0 g) was added with 1.3 ml of cold HK extraction buffer per 0.1 g dry weight and kept on ice from now on. After vortex 3 times 10 s and placing the tube on ice in between each vortex to keep it cold, the sample was centrifuged at 10000 rpm 4°C for 30 min. Then the supernatant was transferred into a new tube and centrifuged again for 10 min. Afterwards, the protein concentration (~20-25 mg/ml) was measured using the Bradford assay. The supernatant was then transferred to a 50 ml falcon and added with 300 µl of S-Protein Agarose slurry (150 µl packed bead volume) (Novagen) per 100 mg of protein. After incubation the falcon on a rotating platform at 4°C for 1 h, the beads were pelleted by centrifugation (max 500 rpm for 1 min). The beads were washed with an equal volume (e.g. if volume of starting lysate was 10 ml, wash with 10 ml) of HK buffer (containing 0.2% NP-40 and 50 µg/ml PMSF), followed by washing 6 times in an equal volume of wash buffer. Then the beads were transferred to an Eppendorf tube and washed 2 times in 1 ml wash buffer. Afterwards, ¼ the final volume of 4x SDS-PAGE loading buffer was added to the beads (e.g. for 150 µl beads add 50 µl), vortexed and boiled at 95°C for 5 min, followed by centrifugation to pellet the beads. The supernatant with the proteins can be loaded on a SDS-PAGE gel or

stored in -20°C for several months. All the buffers used here are listed in **Table 18**.

Table 18. Solutions used for S-tag affinity purification.

Solution	composition
Stop buffer	0.9% NaCl; 1 mM Na Azide; 10 mM EDTA (pH 8.0); 50 mM Na Fluoride
HK buffer	25 mM TRIS (pH 7.5); 0.5% NP-40; 300 mM NaCl; 5 mM EDTA [pH 8.0]; 15 mM EGTA (pH 8.0); 60 mM Beta Gly. PO_4; 500 µM Na Vanadate; 10 mM Na Fluoride; 15 mM pNPP; 1 µg/ml *Pepstatin A; 10 µg/ml Leupeptin; 10 µg/ml Trypsin ChymoT inhibitor; 10 µg/ml Aprotinin; 10 µg/ml **TPCK; 2 mM TAME; 5 mM Benzamidine; 250 µg/ml ***PMSF#; 1 mM DTT#
Wash buffer	25 mM TRIS [pH 7.5]; 5 mM EDTA [pH 8.0]; 300 mM NaCl; 1 mM DTT#; 50 µg/ml PMSF#
4x SDS-PAGE loading buffer	240 mM Tris/HCl, pH 6.8; 8 % SDS; 40 % Glycerol; 12 % DTT; 0.004 % Bromophenol blue

* Pepstatin A is in 90% EtOH 10% acetic acid.

** TPCK is in EtOH.

*** PMSF is in DMSO.

\# PMSF and DTT are added just before use.

4.2 Bradford assay

Protein concentration was determined according to (Bradford, 1976) using the Roti-Quant Reagent (Roth, Karlsruhe). This measurement is based upon Coomassie Brilliant Blue G-250 dye-binding assay. Acryl-cuvettes (Sarstedt, Nümbrecht) were used here. 200 µl Roti-Quant Reagent were added to samples (1 µl protein sample in 800 µl ddH_2O), after gently mixing and incubation for 5 min, the absorbance was measured with Nano drop 2000c. The standard curve was established with bovine serum albumin (BSA).

4.3 SDS polyacrylamide gel electrophoresis

The SDS polyacrylamide gel consisted of two layers: a resolving gel on the lower layer and a stacking gel on the upper layer. The resolving gel was casted between the glass plates using Bio-Rad Mini Protean II equipment and overlaid with a thin layer of isopropanol. After gel

polymerization, the isopropanol was removed and the gel chamber was filled up with stacking gel. Protein samples with 4x SDS loading buffer were heated at 95°C for 5 min and loaded onto the gel. Electrophoresis was performed at RT, first at 50 V until the sample entered into resolving gel and then 100-120 V until the tracking dye reached the bottom of the gel (for the solutions used, see **Table 19**).

Table 19. Solutions used for SDS-PAGE.

Solution	Composition
5% Stacking gel	0.83 ml 30% Acrylamid-Mix; 0.63 ml 1 M Tris pH 6.8; 0.05 ml 10% SDS; 0.1 ml 10% APS; 0.006 ml TEMED; 4.6 ml ddH_2O.
8% Resolving gel	2.7 ml 30% Acrylamid-Mix; 2.5 ml 1.5 M Tris pH 8.8; 0.1 ml 10% SDS ; 0.1 ml 10% APS; 0.006 ml TEMED; 4.6 ml ddH_2O.
1x SDS gel running buffer	3 g Tris-base; 18.8 g Glycine; 10 ml 10% SDS-solution in 1 liter of ddH_2O

4.4 Western blot

For immunodetection of proteins, Western blot (WB) was performed. After electrophoresis, proteins were transferred from the gel to a Protran® nitrocellulose transfer membrane (Whatman, Dassel). Electroblotting was performed in a “sandwich” assembly in Transfer buffer from 3 h to overnight at 30 mA at 4°C using Mini Trans-Blot® transfer gel apparatus (Bio-Rad, Munich). The membrane was incubated in blocking solution for 1 h at RT, then hybridized with the first antibody diluted in blocking solution for 1-2 h at RT or overnight at 4°C. Afterwards, the membrane was washed 3 x 10 min with TBS-T, incubated for 1 h at RT with the peroxidase conjugated secondary antibody diluted in TBS-T and followed by 3 x 10 min washing with TBS-T (for the solutions and antibodies used, see **Table 20**). The detection was accomplished with Luminol solution as substrate for the horse raddish peroxidase (HRP) and the following Lumi-Imager. If the membrane was reused, stripping was carried out in stripping buffer for 30 min at 50°C.

Table 20. Solutions used for Western blot.

Solution	Composition
10x Transfer buffer	30.3 g Tris; 144 g Glycine in 1 liter of ddH_2O
1x Transfer buffer	100 ml 10x Transfer buffer, 200 ml Methanol, 700 ml ddH_2O

10x TBS	24.2 g Tris, 80 g NaCl in 1 liter of ddH_2O, pH 7.6
1x TBS-T	1x TBS, 0.1% Tween 20 (100%)
Blocking solution	TBS-T with 5% skim milk
Luminol solution	1 ml solution A (50 mg Luminol in 200 ml 0.1 M Tris-HCl pH 8.6); 0.1 ml solution B (11 mg p-Hydroxycoumarin acid in 10 ml DMSO); 0.3 µl 35 % H_2O_2
Stripping buffer	1x TBS; 2 % SDS; 0.1 M beta-Mercaptoethanol

4.5 Commassie staining

Coomassie blue is commonly used to stain proteins in SDS-PAGE gels. The gels were soaked in destaining buffer (40% ethanol; 10% Acetic Acide) with 0.25% SERVA Blue G powder (SERVA FEINBIOCHEMICA, Heidelberg) and shaken for at least 1 h, the excess stain was then eluted with destaining buffer overnight. This treatment allows the visualization of proteins as blue bands on a clear background.

4.6 Silver staining

Silver staining is a highly sensitive method for detecting proteins in polyacrylamide gels, which is 10-50 fold more sensitive than Coomassie staining (detection is ~0.1 ng/mm^2). First the gel was fixed for 1 h (or overnight) in fixer (see **Table 21**), followed by washing with Wash buffer for 30 min. The gel was then sensitized for 1 min and stained in Silver nitrate buffer for 20 min. The following developing step would take several minutes until the bands were visible and not changeable before adding the Stop buffer. In between each step, the gel was washed with water briefly.

Table 21. Solutions used for silver staining.

Solution	Composition
Fixer	50% MeOH; 10% HAc
Wash buffer	30% EtOH
Sensitizing buffer	0.02% $Na_2S_2O_3$
Silver nitrate buffer	0.2% $AgNO_3$; 0.015% Formaldehyde

Developer	6% Na_2CO_3; 0.05% Formaldehyde; 2% $Na_2S_2O_3$
Stop buffer	75% MeOH; 18% HAc

5 Light and fluorescence microscopy

For live-cell imaging, fresh spores were inoculated in 0.5 ml MM (2% glycerol for *alcA* promoter) with appropriate selection markers on 18 x 18 mm cover slip (Roth, Karlsruhe). The samples were incubated at 28°C overnight and following with 2 h at RT before microscopy. VECTASHIELD Mounting Medium with DAPI (Vector Laboratories) was used for staining nuclei in cells. Light and fluorescence images were taken with the Zeiss Microscope "AxioImager Z1" (Carl Zeiss, Jena, Germany) and the software ZEN pro 2012, using the Planapochromatic 63x or 100x oil immersion objective lens, and the Zeiss AxioCam MR camera. UV lamp was the HBO103 mercury arc lamp (Osram). Image and video processing was done with ZEN pro 2012, Adobe Photoshop or ImageJ (National Institutes of Health, MD, USA). The filter setting are listed in **Table 22.**

Table 22. Fluorescence microscopy filters.

Fluorescent dye	Excitation filter Band-pass filter (BP) nm	Beam splitter (BS) nm	Barrier filter Long pass filter (LP) nm
sGFP	450-490	510	520
YFP	D 510/20	530 DCLP	D 560/40
DsRed	546	580	590
DAPI	365	395	397

6 Bimolecular Fluorescence Complementation

Bimolecular fluorescence complementation (BiFC) is a technique to analyze protein-protein interactions *in vivo* (Blumenstein *et al.*, 2005). In the BiFC assay, a fluorescent protein like YFP is split into two halves YFP^N and YFP^C, which are respectively fused to one of the two proteins of interest. If the two proteins interact, the two YFP halves are brought into close contact upon which the fluorescent ability is restored. In our case, using the pMCB17apx backbone, two cassettes *alcA(p)*::*YFP^N*::*gene1 and alcA(p)*::*YFP^C*::*gene2* were constructed and co-transformed into *A. nidulans*. The fluorescence signals could be detected following the

instrutions for microscopy **(VI 5)**.

7 Yeast two Hybrid

Yeast two Hybrid (Y2H) is an advanced GAL4-based two-hybrid system that provides a transcriptional assay for detecting the interactions of proteins or domains *in vivo* in yeast. The Matchmaker™ Gold Yeast Two-Hybrid System (Clontech Laboratories, Inc.) was carried out in this work following the User Manual. The cDNA fragments of two proteins or domains are fused to the GAL4 DNA-binding domain (DNA-BD) and GAL4 activation domain (AD), separately. When the two proteins or domains interact, the DNA-BD and AD are brought into proximity, thus activating transcription of reporter genes (*ADE2*, *HIS3*, *MEL1* and *LacZ*). The *ADE2* reporter alone provides strong nutritional selection. The cDNA fragments of the two proteins of interest were inserted into plasmids pGADT7-Rec and pGBKT7 separately, yielding pGADT7-*cDNA1* and pGBKT7-*cDNA2* **(Figure 36)**, which were transformed into *S. cerevisiae* LiAc competent cells.

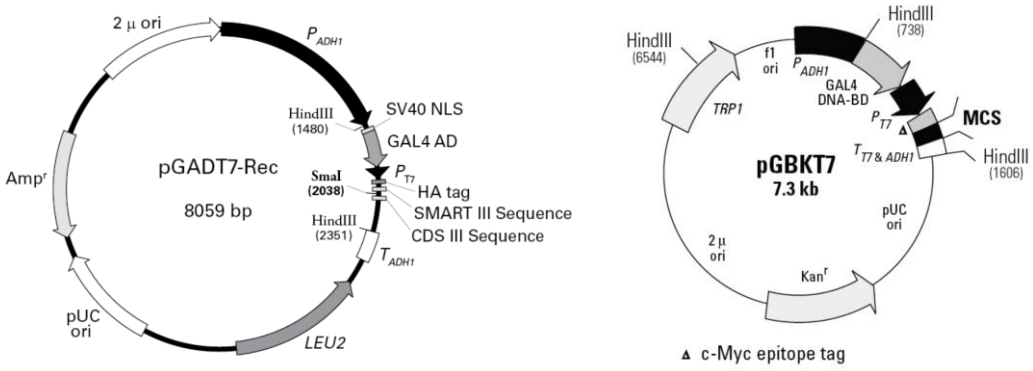

Figure 36. The schemes of plasmids pGADT7-Rec and pGBKT7 for Y2H (from Clontech)**.**

In case of preparation of competent cells, a single colony (<4 weeks old, 2-3 mm in diameter) was picked from YPDA agar plate and inoculated into a conical flask containing 50 ml of YPDA liquid medium. After incubation at 30°C with shaking at 230-250 rpm for 16-20 hr, the OD_{600} should reach >1.5. The overnight culture was then inoculated into 300 ml YPDA, reaching a final OD_{600} of 0.2-0.3 and incubated at 30°C/230rpm until the cells completed one division with an OD_{600} of 0.4-0.7. The cells were collected by centrifugation with 1000 *g* for 5 min at RT. The supernatant was discarded and the cell pellet was resuspended in 50 ml of sterile ddH_2O, followed by centrifugation again for 5 min at 1000 *g* RT. Finally, the cell pellet was resuspended in 1.5 ml of 1.1x TE/LiAc Solution. The yielded competent cells should be used for transformation immediately or stored at RT no more than a few hours.

As for transformation, pGADT7-*cDNA1* and pGBKT7-*cDNA2* were transformed into *S.*

cerevisiae either AH109 or Y187 with different mating types. 5 µl plasmid DNA (~5 µg), 10 µl denatured (100°C for 10 min) Herring Testes Carrier DNA (10 mg/ml), 100 µl competent cells and 600 µl PEG/LiAc Solution were mixed thoroughly by gently vortexing in an 1.5 ml Eppendorf tube. After incubation at 30°C/200 rpm for 30 min, 70 µl of DMSO was added to the EP and mixed well by gentle inversion. Afterwards, the EP was placed in a 42°C waterbath for 15 min with gently inversion every 5 min. The cells were then chilled on ice for 1-2 min, followed by centrifugation at 13000 rpm for 5 sec. The supernatant was removed and the pellet was resuspended in 0.6 ml of 1x TE, which was spread evenly onto 3 SD/-Leu or SD/-Trp agar plates, depending on the nutritional marker carried by the plasmid. The plates were incubated at 30°C (upside down) for 2-4 days, until colonies were visible. The largest grown colonies were re-streaked on the same selection medium and subsequently used for mating.

In case of mating, two fresh single colonies from each type were picked and placed in one tube containing 0.5 ml of 2x YPDA medium in an 1.5 ml Eppendorf tube. After vortexing the tube for 1 min and completely resuspending, the cells were incubated at 30°C overnight (20-24 hr) with 200 rpm shaking, followed by plating cells on 5 SD agar plates. The plates (upside down) were then incubated at 30°C for 3-5 days to allow diploid cells to form visible colonies. The colonies were picked and streaked onto a new SD agar plate. To analyze the interaction of the proteins, a 5 ml overnight culture in SD medium was incubated overnight at 30°C/230 rpm. The culture was diluted to an OD_{600} of 1, as well as a dilution series (1:10, 1:100, 1:1000). Then 5 µl of each suspension (1:1-1:1000) was dropped onto the SD-LW and SD-LWHA agar plates respectively with positive (SRM49) and negative (SRM50) controls. Strains and plamids used for Y2H are listed in **Table 24** and **Table 15**.

Table 23. Solutions or media for Yeast two Hybrid.

Solution or Medium	Composition
10x TE	100 mM Tris-HCl, pH 8.0; 10 mM EDTA
PEG/LiAc Solution (10 ml, fresh prepared)	8 ml of 50% PEG 3350; 1 ml of 10x TE; 1 ml of 1 M LiAc
1.1x TE/LiAc Solution (10 ml, fresh prepared)	1.1 ml of 10x TE; 1.1 ml of 1 M LiAc (10x); 7.8 ml of sterile ddH_2O
YPDA medium	20 g/L Peptone; 10 g/L Yeast extract; 0.03% Adenine hemisulfate; 2% glucose; pH 6.5
SD medium	6.7 g/L Yeast nitrogen base; 20 g/L Glucose; 10x Dropout

	Solution; appropriate 100x amino acid stock solution; pH 5.8
100x L-Adenine stock solution	2 g/L Adenin-Hemisulfat in ddH_2O
100x L-Histidine	2 g/L-Histidin HCl Monohydrat in ddH_2O
100x L-Tryptophane	2 g/L-Tryptophane in ddH_2O
100x L-Leucine	10 g/L-Leucine in ddH_2O
10x Dropout (DO) Solution	200 mg/L L-Arginine HCl; 300 mg/L L-Isoleucine; 300 mg/L L-Lysine HCl; 200 mg/L L-Methionine; 500 mg/L L-Phenylalanine; 2000 mg/L L-Threonine; 300 mg/L L-Tyrosine; 200 mg/L L-Uracil; 1500 mg/L L-Valine

Table 24. *S. cerevisiae* strains in this study.

Strain	Genotype	Source
AH109	MATa; *trp1-901*; *leu2-3*, *112*; *ura3-52*; *his3-200*; *gal4*Δ; *gal80*Δ; *LYS2*::$GAL1_{UAS}$-$GAL1_{TATA}$-*HIS3*; $GAL2_{UAS}$-$GAL2_{TATA}$-*ADE2*; *URA3*::$MEL1_{UAS}$-$MEL1_{TATA}$-*lacZ*	James *et al*., 1996
Y187	*MATα*; *ura3-52*; *his3-200*; *ade2-101*; *trp1-901*; *leu2-3*; *112*; *gal4*Δ; *met-*; *gal80*Δ; *URA3*::$GAL1_{UAS}$-$GAL1_{TATA}$-*lacZ*	Harper *et al*., 1993
YSYZ1	Y187 transformed with pYZ51; Gal4 BD-SPA18	This study
YSYZ2	AH109 transformed with pYZ61; Gal4 AD-ApsB	This study
YSYZ3	YSYZ1 mated with YSYZ2; Gal4 AD-ApsB; Gal4 BD-SPA18	This study
SRM49	AH109 transformed with pGADT7-T and pGBKT7-53; positive control	This study
SRM50	AH109 transformed with pGADT7-T and pGBKT7-Lam; negative control	This study

8 LCM and MS to indentify septal associated proteins

8.1 Collection of septa in *A. nidulans* by laser capture microdissection

Laser capture microdissection (LCM) was performed with a CellCut Plus system (MMI, Molecular Machines and Industries, Zürich, Switzerland) comprising an Olympus IX81 inverted microscope equipped with a UV laser (355 nm), microscope stage and isolation cup holder. Mycelia (from strain FGSC A4) were grown on special membrane slides in YAG medium (the hyphal diameter is 3-4 µm, which is thicker than 2-3 µm in MM medium) and fixed in 100% ethanol for 12 h. After drying the slides, samples were covered with a microscope slide and observed with a 40x objective. Selected regions were cut with a UV laser through the microscope lens. The intensity and speed of the laser were 50%-80% and 40%-60%, respectively. Laser cutting was repeated 3-5 times for each region. To collect the cut regions, the cap of a special collection tube was moved down to the membrane (with the sample attached) and then the membrane with the samples could be collected when the cap was raised again **(Figure 37)** (Teichert *et al.*, 2012). However, single septa of *A. nidulans* turned out to be too small to be collected in the cap. Therefore, we drew irregular shapes including septa but also areas outside the hyphae **(Figure 37, C)**. Around 3000 septa were collected in this way.

8.2 Extraction of proteins from the collected samples by LCM

The collected septa were processed for protein extraction and prepared for mass spectrometry. We used SDC as surfactant, because it is compatible with trypsin and increases the solubility of hydrophobic proteins. Besides, SDC could be successfully removed from the acidified solution by adding a water-immiscible organic solvent (Masuda *et al.*, 2007). Procedures were performed as followed. First, 50 µl 50 mM ammonium bicarbonate solution containing 8 M urea, 1% SDC were added to the tube. The tube was inverted so that the lid was covered with buffer and then incubated 30 min at 42 °C. The solution was sonicated on ice for 3 min (10 s interval every 5 s sonication). After 20 minutes incubation at RT, the solution was vortexed and transfered to a new cup and centrifuged at 13.000 rpm at 4°C for 1 min. Afterwards, DTT (final concentration 10 mM) was added to the supernatant and incubated at 50°C for 30 min, then iodoacetamide (final concentration 55 mM) was added and incubated in the dark for 30 min at RT. After 4-fold dilution of the solution with 50 mM ammonium bicarbonate solution, trypsin (Excision Grade, Bovine Pancreas, Calbiochem) was added to 1 µg/µl, and incubated at 37°C overnight. Afterwards, 100 µl ethyl acetate was added to 100 µl of the digested solution and the mixture was acidified with 0.5% tri-fluor-acetic acid to about pH 2. After centrifugation at 15.700 *g* for 2 min the aqueous phase containing the digested peptides was collected.

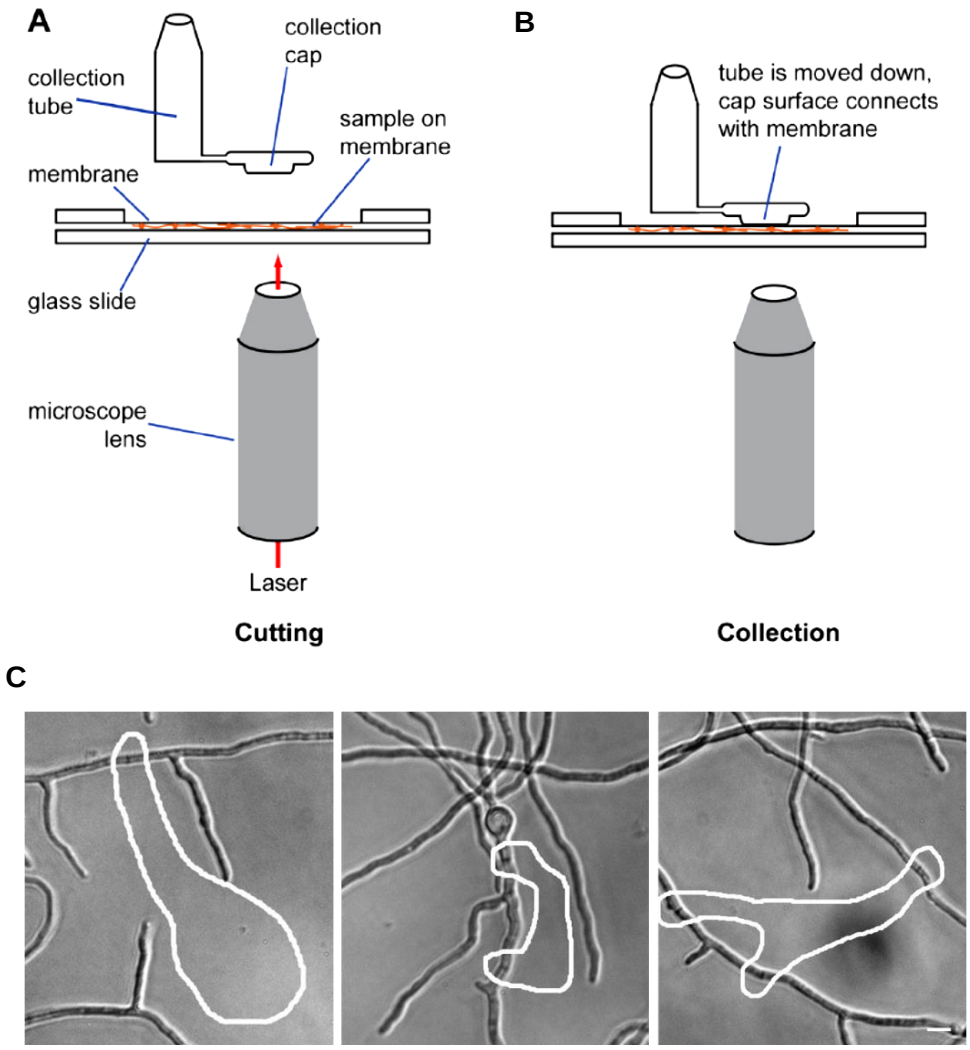

Figure 37. Laser capture microdissection of septa in *A. nidulans*. Mycelia were grown on special membrane slides and fixed in ethanol. After drying of the slides, samples were covered with a glass slide **(A)** and visualized on an inverted microscope **(C)**. Selected regions containing septa were cut with a UV laser through the microscope lens. To collect the cut out regions, the cap of a special collection tube was lowered onto the sample **(B)** where the membrane (with the sample attached) stuck to the cap and could be lifted off when the cap was raised again. Bar, 5 µm. **(A)** and **(B)** are from (Teichert *et al.*, 2012)

8.3 nano-LC-ESI-MS/MS to identify trace amount proteins

The peptide sample was desalted using StageTips C18 (Thermo Scientific) according to the manufacturer's instructions, and eluted with 20 µl 80% acetonitrile containing 5% formic acid. The eluate was concentrated in the SpeedVac to a volume of approximately 5 µl. Afterwards, separation was performed on a Nano-LC Ultra system (Eksigent) using the following columns and chromatographic conditions: Peptides were loaded on a RPC trap column (ReproSil C18, 0.3 x 10 mm) and subsequently separated with an analytical column (C18 PepMap 100, 3 µm bead size, 75µm i.d.; 15 cm length, LC Packings) with a linear gradient (A: 0.1% formic acid in

water, B: 0.1% formic acid in 84% ACN) at a flow rate of 280 nl/min. The gradient used was: 1-60% B in 30 minutes, 100% B for 15 minutes. Mass spectrometry was performed on a linear ion trap mass spectrometer (Thermo LTQ Orbitrap XL, Thermo Electron) online coupled to the nano-LC system. For electrospray ionization a distal coated SilicaTip (FS-360-50-15-D-20) and a needle voltage of 1.4 kV was used. The LTQ Orbitrap was operated in parallel mode performing precursor mass scanning in the Orbitrap (60 000 FWHM resolution at m/z 400) and isochronous acquisition of five data dependent CID MS/MS scans in the LTQ ion trap. Afterwards, the LC-ESI-MS/MS data were used for a database search with the software Mascot (Matrix Science) using the *A. nidulans* protein sequences. Peptide mass tolerance was set to 50 ppm, a significance threshold $p<0.05$ and an ion-score cut-off of 20 was used. The mass-spectrometric analysis was done commercially by TopLab GmbH (Munich).

VII Literature

Adams, I. R. & Kilmartin, J. V. (1999). Localization of core spindle pole body (SPB) components during SPB duplication in *Saccharomyces cerevisiae*. *J Cell Biol* **145**, 809-823.

Anders, A., Lourenco, P. C. & Sawin, K. E. (2006). Noncore components of the fission yeast gamma-tubulin complex. *Mol Biol Cell* **17**, 5075-5093.

Aramayo, R., Adams, T. H. & Timberlake, W. E. (1989). A large cluster of highly expressed genes is dispensable for growth and development in *Aspergillus nidulans*. *Genetics* **122**, 65-71.

Avena, J. S., Burns, S., Yu, Z., Ebmeier, C. C., Old, W. M., Jaspersen, S. L. & Winey, M. (2014). Licensing of yeast centrosome duplication requires phosphoregulation of sfi1. *PLoS Genet* **10**, e1004666.

Azimzadeh, J. & Bornens, M. (2007). Structure and duplication of the centrosome. *J Cell Sci* **120**, 2139-2142.

Azimzadeh, J., Hergert, P., Delouvee, A., Euteneuer, U., Formstecher, E., Khodjakov, A. & Bornens, M. (2009). hPOC5 is a centrin-binding protein required for assembly of full-length centrioles. *J Cell Biol* **185**, 101-114.

Bahtz, R., Seidler, J., Arnold, M., Haselmann-Weiss, U., Antony, C., Lehmann, W. D. & Hoffmann, I. (2012). GCP6 is a substrate of Plk4 and required for centriole duplication. *J Cell Sci* **125**, 486-496.

Ballance, D., Buxton, F. & Turner, G. (1983). Transformation of *Aspergillus nidulans* by the orotidine-5′-phosphate decarboxylase gene of *Neurospora crassa*. *Biochem Biophys Res Commun* **112**, 284-289.

Barrera, J. A., Kao, L., Hammer, R. E., Seemann, J., Fuchs, J. L. & Megraw, T. L. (2010). CDK5RAP2 regulates centriole engagement and cohesion in mice. *Dev Cell* **18**, 913-926.

Batzenschlager, M., Masoud, K., Janski, N., Houlné, G., Herzog, E., Evrard, J., Baumberger, N., Erhardt, M., Nominé, Y. & Kieffer, B. (2013). The GIP gamma-tubulin complex-associated proteins are involved in nuclear architecture in *Arabidopsis thaliana*. *Front Plant Sci* **4**.

Biggins, S. & Rose, M. D. (1994). Direct interaction between yeast spindle pole body components: Kar1p is required for Cdc31p localization to the spindle pole body. *J Cell Biol* **125**, 843-852.

Blumenstein, A., Vienken, K., Tasler, R., Purschwitz, J., Veith, D., Frankenberg-Dinkel, N. & Fischer, R. (2005). The *Aspergillus nidulans* phytochrome FphA represses sexual development in red light. *Curr Biol* **15**, 1833-1838.

Bond, J., Roberts, E., Springell, K., Lizarraga, S., Scott, S., Higgins, J., Hampshire, D. J., Morrison, E. E., Leal, G. F. & Silva, E. O. (2005). A centrosomal mechanism involving CDK5RAP2 and CENPJ controls brain size. *Nat Genet* **37**, 353-355.

Bornens, M. (2012). The centrosome in cells and organisms. *Science* **335**, 422-426.

Bouissou, A., Verollet, C., Sousa, A., Sampaio, P., Wright, M., Sunkel, C. E., Merdes, A. & Raynaud-Messina, B. (2009). Gamma-tubulin ring complexes regulate microtubule plus end dynamics. *J Cell Biol* **187**, 327-334.

Brachat, A., Kilmartin, J. V., Wach, A. & Philippsen, P. (1998). *Saccharomyces cerevisiae* cells with defective spindle pole body outer plaques accomplish nuclear migration via half-bridge-organized microtubules. *Mol Biol Cell* **9**, 977-991.

Bradford, M. M. (1976). A rapid and sensitive method for the quantitation of microgram quantities of protein utilizing the principle of protein-dye binding. *Anal Biochem* **72**, 248-254.

Brugués, J., Nuzzo, V., Mazur, E. & Needleman, D. J. (2012). Nucleation and transport organize microtubules in metaphase spindles. *Cell* **149**, 554-564.

Bugnard, E., Zaal, K. J. & Ralston, E. (2005). Reorganization of microtubule nucleation during muscle differentiation. *Cell Motil Cytoskeleton* **60**, 1-13.

Bullitt, E., Rout, M. P., Kilmartin, J. V. & Akey, C. W. (1997). The yeast spindle pole body is assembled around a central crystal of Spc42p. *Cell* **89**, 1077-1086.

Byers, B. & Goetsch, L. (1975). Behavior of spindles and spindle plaques in the cell cycle and conjugation of *Saccharomyces cerevisiae*. *J Bacteriol* **124**, 511-523.

Byers, B. & Goetsch, L. (1974). Duplication of spindle plaques and integration of the yeast cell cycle. *Cold Spring Harb Symp Quant Biol* **38**, 123-131.

Catalano, A. & O'Day, D. H. (2008). Calmodulin-binding proteins in the model organism

dictyostelium: A complete & critical review. *Cell Signal* **20**, 277-291.

Chabin-Brion, K., Marceiller, J., Perez, F., Settegrana, C., Drechou, A., Durand G. & Pous, C. (2001). The Golgi complex is a microtubule-organizing organelle. *Mol Biol Cell* **12**, 2047-2060.

Chan, J., Sambade, A., Calder, G. & Lloyd, C. (2009). *Arabidopsis* cortical microtubules are initiated along, as well as branching from, existing microtubules. *Plant Cell* **21**, 2298-2306.

Chen, S., Song, Y., Cao, J., Wang, G., Wei, H., Xu, X. & Lu, L. (2010). Localization and function of Calmodulin in live-cells of *Aspergillus nidulans*. *Fungal Genet Biol* **47**, 268-278.

Chen, P., Gao, R., Chen, S., Pu, L., Li, P., Huang, Y. & Lu, L. (2012). A pericentrin-related protein homolog in *Aspergillus nidulans* plays important roles in nucleus positioning and cell polarity by affecting microtubule organization. *Eukaryot Cell* **11**, 1520-1530.

Chen, X. P., Yin, H. & Huffaker, T. C. (1998). The yeast spindle pole body component Spc72p interacts with Stu2p and is required for proper microtubule assembly. *J Cell Biol* **141**, 1169-1179.

Chial, H. J., Rout, M. P., Giddings, T. H. & Winey, M. (1998). *Saccharomyces cerevisiae* Ndc1p is a shared component of nuclear pore complexes and spindle pole bodies. *J Cell Biol* **143**, 1789-1800.

Chrétien, D. & Wade, R. H. (1991). New data on the microtubule surface lattice. *Biol Cell* **71**, 161-174.

Dhani, D. K., Goult B. T., George G. M., Rogerson D. T., Bitton D. A., Miller C. J., Schwabe J. W. & Tanaka K. (2013). Mzt1/Tam4, a fission yeast MOZART1 homologue, is an essential γ-tubulin complex and directly interacts with GCP3 (Alp6). *Mol Biol Cell* **24 (21)**, 3337-49.

Donaldson, A. D. & Kilmartin, J. V. (1996). Spc42p: A phosphorylated component of the S. cerevisiae spindle pole body (SPD) with an essential function during SPB duplication. *J Cell Biol* **132**, 887-901.

Doshi, P., Bossie, C. A., Doonan, J. H., Mays, G. S. & Morris, N. R. (1991). Two α-tubulin genes of *Aspergillus nidulans* encode divergent proteins. *Mol Genet Genomics* **225**, 129-141.

Eckardt, N. A. (2006). Function of γ-tubulin in plants. *Plant Cell* **18**, 1327-1329.

Efimov, A., Kharitonov, A., Efimova, N., Loncarek, J., Miller, P. M., Andreyeva, N., Gleeson, P., Galjart, N., Maia, A. R. & McLeod, I. X. (2007). Asymmetric CLASP-dependent nucleation of noncentrosomal microtubules at the trans-Golgi network. *Dev Cell* **12**, 917-930.

Efimov, V. P., Zhang, J. & Xiang, X. (2006). CLIP-170 homologue and NUDE play overlapping roles in NUDF localization in *Aspergillus nidulans*. *Mol Biol Cell* **17**, 2021-2034.

Elliott, S., Knop, M., Schlenstedt, G. & Schiebel, E. (1999). Spc29p is a component of the Spc110p subcomplex and is essential for spindle pole body duplication. *Proc Natl Acad Sci* **96**, 6205-6210.

Elserafy, M., Šarić, M., Neuner, A., Lin, T., Zhang, W., Seybold, C., Sivashanmugam, L. & Schiebel, E. (2014). Molecular mechanisms that restrict yeast centrosome duplication to one event per cell cycle. *Curr Biol* **24**, 1456-1466.

Emmert-Buck, M. R., Bonner, R. F., Smith, P. D., Chuaqui, R. F., Zhuang, Z., Goldstein, S. R., Weiss, R. A. & Liotta, L. A. (1996). Laser capture microdissection. *Science* **274**, 998-1001.

Enke, C., Zekert, N., Veith, D., Schaaf, C., Konzack, S. & Fischer, R. (2007). *Aspergillus nidulans* Dis1/XMAP215 protein AlpA localizes to spindle pole bodies and microtubule plus ends and contributes to growth directionality. *Eukaryot Cell* **6**, 555-562.

Erhardt, M., Stoppin-Mellet, V., Campagne, S., Canaday, J., Mutterer, J., Fabian, T., Sauter, M., Muller, T., Peter, C., Lambert, A. M. & Schmit, A. C. (2002). The plant Spc98p homologue co-localizes with gamma-tubulin at microtubule nucleation sites and is required for microtubule nucleation. *J Cell Sci* **115**, 2423-2431.

Erickson, H. P. (2000). Gamma-tubulin nucleation: Template or protofilament? *Nat Cell Biol* **2**, E93-E96.

Erickson, H. P. & Stoffler, D. (1996). Protofilaments and rings, two conformations of the tubulin family conserved from bacterial FtsZ to α/β and γ Tubulin. *J Cell Biol* **135**, 5-8.

Evans, L., Mitchison, T. & Kirschner, M. (1985). Influence of the centrosome on the structure of nucleated microtubules. *J Cell Biol* **100**, 1185-1191.

Fant, X., Srsen, V., Espigat-Georger, A. & Merdes, A. (2009). Nuclei of non-muscle

cells bind centrosome proteins upon fusion with differentiating myoblasts. *PLoS One* **4**, e8303.

Fischer, R., Zekert, N. & Takeshita, N. (2008). Polarized growth in fungi–interplay between the cytoskeleton, positional markers and membrane domains. *Mol Microbiol* **68**, 813-826.

Fischer, R. & Timberlake, W. E. (1995). *Aspergillus nidulans apsA* (anucleate primary sterigmata) encodes a coiled-coil protein required for nuclear positioning and completion of asexual development. *J Cell Biol* **128**, 485-498.

Flory, M. R., Morphew, M., Joseph, J. D., Means, A. R. & Davis, T. N. (2002). Pcp1p, an Spc110p-related Calmodulin target at the centrosome of the fission yeast *Schizosaccharomyces pombe*. *Cell Growth Differ* **13**, 47-58.

Flory, M. R., Moser, M. J., Monnat, R. J. Jr. & Davis, T. N. (2000). Identification of a human centrosomal Calmodulin-binding protein that shares homology with pericentrin. *Proc Natl Acad Sci* **97**, 5919-5923.

Fong, K. W., Choi, Y. K., Rattner, J. B. & Qi, R. Z. (2008). CDK5RAP2 is a pericentriolar protein that functions in centrosomal attachment of the gamma-tubulin ring complex. *Mol Biol Cell* **19**, 115-125.

Fujita, A., Vardy, L., Garcia, M. A. & Toda, T. (2002). A fourth component of the fission yeast gamma-tubulin complex, Alp16, is required for cytoplasmic microtubule integrity and becomes indispensable when gamma-tubulin function is compromised. *Mol Biol Cell* **13**, 2360-2373.

Galagan, J. E., Calvo, S. E., Cuomo, C., Ma, L., Wortman, J. R., Batzoglou, S., Lee, S., Başẗurkmen, M., Spevak, C. C. & Clutterbuck, J. (2005). Sequencing of *Aspergillus nidulans* and comparative analysis with *A. fumigatus* and *A. oryzae*. *Nature* **438**, 1105-1115.

Garcia, M. A., Vardy, L., Koonrugsa, N. & Toda, T. (2001). Fission yeast ch-TOG/XMAP215 homologue Alp14 connects mitotic spindles with the kinetochore and is a component of the Mad2-dependent spindle checkpoint. *EMBO J* **20**, 3389-3401.

Geiser, J. R., van Tuinen, D., Brockerhoff, S. E., Neff, M. M. & Davis, T. N. (1991). Can Calmodulin function without binding Calcium? *Cell* **65**, 949-959.

Geiser, J. R., Sundberg, H. A., Chang, B. H., Muller, E. G. & Davis, T. N. (1993). The essential mitotic target of Calmodulin is the 110-kilodalton component of the spindle pole

body in *Saccharomyces cerevisiae*. *Mol Cell Biol* **13**, 7913-7924.

Geissler, S., Pereira, G., Spang, A., Knop, M., Soues, S., Kilmartin, J. & Schiebel, E. (1996). The spindle pole body component Spc98p interacts with the gamma-tubulin-like Tub4p of *Saccharomyces cerevisiae* at the sites of microtubule attachment. *EMBO J* **15**, 3899-3911.

Gillingham, A. K. & Munro, S. (2000). The PACT domain, a conserved centrosomal targeting motif in the coiled-coil proteins AKAP450 and pericentrin. *EMBO Rep* **1**, 524-529.

Girbardt, M. (1957). Der Spitzenkörper von polystictus versicolor (L.). *Planta* **50**, 47-59.

Goshima, G., Mayer, M., Zhang, N., Stuurman, N. & Vale, R. D. (2008). Augmin: A protein complex required for centrosome-independent microtubule generation within the spindle. *J Cell Biol* **181**, 421-429.

Gruneberg, U., Campbell, K., Simpson, C., Grindlay, J. & Schiebel, E. (2000). Nud1p links astral microtubule organization and the control of exit from mitosis. *EMBO J* **19**, 6475-6488.

Gruss, O. J., Wittmann, M., Yokoyama, H., Pepperkok, R., Kufer, T., Silljé, H., Karsenti, E., Mattaj, I. W. & Vernos, I. (2002). Chromosome-induced microtubule assembly mediated by TPX2 is required for spindle formation in HeLa cells. *Nat Cell Biol* **4**, 871-879.

Gunawardane, R. N., Martin, O. C. & Zheng, Y. (2003). Characterization of a new γTuRC subunit with WD repeats. *Mol Biol Cell* **14**, 1017-1026.

Gunawardane, R. N., Martin, O. C., Cao, K., Zhang, L., Dej, K., Iwamatsu, A. & Zheng, Y. (2000). Characterization and reconstitution of *Drosophila* γ-tubulin ring complex subunits. *J Cell Biol* **151**, 1513-1524.

Hagan, I. M. & Petersen, J. (2000). The microtubule organizing centers of *Schizosaccharomyces pombe*. *Curr Top Dev Biol* **49**, 133-159.

Haren, L., Remy, M. H., Bazin, I., Callebaut, I., Wright, M. & Merdes, A. (2006). NEDD1-dependent recruitment of the γ-tubulin ring complex to the centrosome is necessary for centriole duplication and spindle assembly. *J Cell Biol* **172**, 505-515.

Harper, J. W., Adami, G. R., Wei, N., Keyomarsi, K. & Elledge, S. J. (1993). The p21 Cdkinteracting protein Cip1 is a potent inhibitor of G1 cyclin-dependent kinases. *Cell*

75:805–816.

Harris, S. D., Read, N. D., Roberson, R. W., Shaw, B., Seiler, S., Plamann, M. & Momany, M. (2005). Polarisome meets Spitzenkörper: Microscopy, genetics, and genomics converge. *Eukaryot Cell* **4**, 225-229.

Hawkins, T., Mirigian, M., Yasar, M. S. & Ross, J. L. (2010). Mechanics of microtubules. *J Biomech* **43**, 23-30.

Heiland, I. & Erdmann, R. (2005). Biogenesis of peroxisomes. *Febs Journal* **272**, 2362-2372.

Heitz, M. J., Petersen, J., Valovin, S., Hagan & I. M. (2001). MTOC formation during mitotic exit in fission yeast. *J Cell Sci* **114**, 4521-4532.

Herrero, S., Takeshita, N. & Fischer, R. (2011). The *Aspergillus nidulans* CENP-E kinesin motor KipA interacts with the fungal homologue of the centromere-associated protein CENP-H at the kinetochore. *Mol Microbiol* **80**, 981-994.

Ho, C. M., Hotta, T., Kong, Z., Zeng, C. J., Sun, J., Lee, Y. R. & Liu, B. (2011). Augmin plays a critical role in organizing the spindle and phragmoplast microtubule arrays in *Arabidopsis*. *Plant Cell* **23**, 2606-2618.

Höög, J. L., Schwartz, C., Noon, A. T., O'Toole, E. T., Mastronarde, D. N., McIntosh, J. R. & Antony, C. (2007). Organization of interphase microtubules in fission yeast analyzed by electron tomography. *Dev Cell* **12**, 349-361.

Hotta, T., Kong, Z., Ho, C. M., Zeng, C. J., Horio, T., Fong, S., Vuong, T., Lee, Y. R. & Liu, B. (2012). Characterization of the *Arabidopsis* augmin complex uncovers its critical function in the assembly of the acentrosomal spindle and phragmoplast microtubule arrays. *Plant Cell* **24**, 1494-1509.

Hurtado, L., Caballero, C., Gavilan, M. P., Cardenas, J., Bornens, M. & Rios R. M. (2011). Disconnecting the Golgi ribbon from the centrosome prevents directional cell migration and ciliogenesis. *J Cell Biol* **193**, 917-933.

Hutchins, J. R., Toyoda, Y., Hegemann, B., Poser, I., Heriche, J. K., Sykora, M. M., Augsburg, M., Hudecz, O., Buschhorn, B. A. & other authors. (2010). Systematic analysis of human protein complexes identifies chromosome segregation proteins. *Science* **328**, 593-599.

Hynes, M. J., Murray, S. L., Khew, G. S. & Davis, M. A. (2008). Genetic analysis of the

role of peroxisomes in the utilization of acetate and fatty acids in *Aspergillus nidulans*. *Genetics* **178**, 1355-1369.

Izumi, N., Fumoto, K., Izumi, S. & Kikuchi, A. (2008). GSK-3β regulates proper mitotic spindle formation in cooperation with a component of the γ-tubulin ring complex, GCP5. *J Biol Chem* **283**, 12981-12991.

James, P., Haliaday, J. & Craig, E. A. (1996). Genomic libraries and a host strain designed for highly efficient two-hybrid selection in yeast. *Genetics* **144**, 1425–1436.

Janson, M. E., Setty, T. G., Paoletti, A. & Tran, P. T. (2005). Efficient formation of bipolar microtubule bundles requires microtubule-bound γ-tubulin complexes. *J Cell Biol* **169**, 297-308.

Jaspersen, S. L. & Winey, M. (2004). The budding yeast spindle pole body: Structure, duplication, and function. *Annu Rev Cell Dev Biol* **20**, 1-28.

Jaspersen, S. L., Giddings, T. H. Jr. & Winey, M. (2002). Mps3p is a novel component of the yeast spindle pole body that interacts with the yeast centrin homologue Cdc31p. *J Cell Biol* **159**, 945-956.

Jaspersen, S. L., Martin, A. E., Glazko, G., Giddings, T. H. Jr., Morgan, G., Mushegian, A. & Winey, M. (2006). The Sad1-UNC-84 homology domain in Mps3 interacts with Mps2 to connect the spindle pole body with the nuclear envelope. *J Cell Biol* **174**, 665-675.

Job, D., Valiron, O. & Oakley, B. (2003). Microtubule nucleation. *Curr Opin Cell Biol* **15**, 111-117.

Kaláb, P., Pralle, A., Isacoff, E. Y., Heald, R. & Weis, K. (2006). Analysis of a RanGTP-regulated gradient in mitotic somatic cells. *Nature* **440**, 697-701.

Keating, T. J. & Borisy, G. G. (2000). Immunostructural evidence for the template mechanism of microtubule nucleation. *Nat Cell Biol* **2**, 352-357.

Keck, J. M., Jones, M. H., Wong, C. C., Binkley, J., Chen, D., Jaspersen, S. L., Holinger, E. P., Xu, T., Niepel, M. & other authors. (2011). A cell cycle phosphoproteome of the yeast centrosome. *Science* **332**, 1557-1561.

Kilmartin, J. V. (2003). Sfi1p has conserved centrin-binding sites and an essential function in budding yeast spindle pole body duplication. *J Cell Biol* **162**, 1211-1221.

Kilmartin, J. V. (2014). Lessons from yeast: The spindle pole body and the centrosome. *Philos Trans R Soc Lond B Biol Sci* **369**, 10.1098/rstb.2013.0456.

Kilmartin, J. V. & Goh, P. Y. (1996). Spc110p: Assembly properties and role in the connection of nuclear microtubules to the yeast spindle pole body. *EMBO J* **15**, 4592-4602.

Kilmartin, J. V., Dyos, S. L., Kershaw, D. & Finch, J. T. (1993). A spacer protein in the *Saccharomyces cerevisiae* spindle poly body whose transcript is cell cycle-regulated. *J Cell Biol* **123**, 1175-1184.

Kim, H., Takahashi, M., Matsuo, K. & Ono, Y. (2007). Recruitment of CG-NAP to the Golgi apparatus through interaction with dynein–dynactin complex. *Genes to Cells* **12**, 421-434.

Kim, J. & Raines, R. T. (1993). Ribonuclease S-peptide as a carrier in fusion proteins. *Protein Science* **2**, 348-356.

Kim, J. M., Zeng, C. J., Nayak, T., Shao, R., Huang, A. C., Oakley, B. R. & Liu, B. (2009). Timely septation requires SNAD-dependent spindle pole body localization of the septation initiation network components in the filamentous fungus *Aspergillus nidulans*. *Mol Biol Cell* **20**, 2874-2884.

Kirk, K. E. & Morris, N. R. (1993). Either α-tubulin isogene product is sufficient for microtubule function during all stages of growth and differentiation in *Aspergillus nidulans*. *Mol Cell Biol* **13**, 4465-4476.

Kirk, K. E. & Morris, N. R. (1991). The *tubB* α-tubulin gene is essential for sexual development in *Aspergillus nidulans*. *Genes Dev* **5**, 2014-2023.

Kitamura, E., Tanaka, K., Komoto, S., Kitamura, Y., Antony, C. & Tanaka, T. U. (2010). Kinetochores generate microtubules with distal plus ends: Their roles and limited lifetime in mitosis. *Dev Cell* **18**, 248-259.

Knop, M. & Strasser, K. (2000). Role of the spindle pole body of yeast in mediating assembly of the prospore membrane during meiosis. *EMBO J* **19**, 3657-3667.

Knop, M. & Schiebel, E. (1998). Receptors determine the cellular localization of a γ-tubulin complex and thereby the site of microtubule formation. *EMBO J* **17**, 3952-3967.

Knop, M., Pereira, G., Geissler, S., Grein, K. & Schiebel, E. (1997). The spindle pole body component Spc97p interacts with the γ-tubulin of *Saccharomyces cerevisiae* and

functions in microtubule organization and spindle pole body duplication. *EMBO J* **16**, 1550-1564.

Kobe, B. & Deisenhofer, J. (1995). Proteins with leucine-rich repeats. *Curr Opin Struct Biol* **5**, 409-416.

Kollman, J. M., Merdes, A., Mourey, L. & Agard, D. A. (2011). Microtubule nucleation by γ-tubulin complexes. *Nature Reviews Molecular Cell Biology* **12**, 709-721.

Konzack, S., Rischitor, P. E., Enke, C. & Fischer, R. (2005). The role of the kinesin motor KipA in microtubule organization and polarized growth of *Aspergillus nidulans*. *Mol Biol Cell* **16**, 497-506.

Kovacs, W. J. & Krisans, S. (2003). Cholesterol biosynthesis and regulation: role of peroxisomes. In *Peroxisomal Disorders and Regulation of Genes.* pp. 315-327. Springer.

Kubickova, S., Cernohorska, H., Musilova, P. & Rubes, J. (2002). The use of laser microdissection for the preparation of chromosome-specific painting probes in farm animals. *Chromosome Res* **10**, 571-577.

Lai, J., Koh, C. H., Tjota, M., Pieuchot, L., Raman, V., Chandrababu, K. B., Yang, D., Wong, L. & Jedd, G. (2012). Intrinsically disordered proteins aggregate at fungal cell-to-cell channels and regulate intercellular connectivity. *Proc Natl Acad Sci* **109**, 15781-15786.

Lau, C. K., Giddings, T. H. Jr. & Winey, M. (2004). A novel allele of *Saccharomyces cerevisiae* NDC1 reveals a potential role for the spindle pole body component Ndc1p in nuclear pore assembly. *Eukaryot Cell* **3**, 447-458.

Lawo, S., Bashkurov, M., Mullin, M., Ferreria, M. G., Kittler, R., Habermann, B., Tagliaferro, A., Poser, I., Hutchins, J. R. & Hegemann, B. (2009). HAUS, the 8-subunit human augmin complex, regulates centrosome and spindle integrity. *Curr Biol* **19**, 816-826.

Ledbetter, M. C. & Porter, K. R. (1964). Morphology of microtubules of plant cell. *Science* **144**, 872-874.

Lee, I., Coffman, V. C. & Wu, J. (2012). Contractile-ring assembly in fission yeast cytokinesis: Recent advances and new perspectives. *Cytoskeleton* **69**, 751-763.

Li, S., Sandercock, A. M., Conduit, P., Robinson, C. V., Williams, R. L. & Kilmartin, J. V. (2006). Structural role of Sfi1p-centrin filaments in budding yeast spindle pole body

duplication. *J Cell Biol* **173**, 867-877.

Lin, T., Neuner, A. & Schiebel, E. (2015). Targeting of γ-tubulin complexes to microtubule organizing centers: Conservation and divergence. *Trends Cell Biol* **25**, 296-307.

Lin, T. C., Neuner, A., Schlosser, Y. T., Scharf, A. N., Weber, L. & Schiebel, E. (2014). Cell-cycle dependent phosphorylation of yeast pericentrin regulates γ-TuSC-mediated microtubule nucleation. *Elife* **3**, e02208.

Liu, T., Tian, J., Wang, G., Yu, Y., Wang, C., Ma, Y., Zhang, X., Xia, G., Liu, B. & Kong, Z. (2014). Augmin triggers microtubule-dependent microtubule nucleation in interphase plant cells. *Curr Biol* **24**, 2708-2713.

Liu, Y., von Behrens, I., Muthreich, N., Schütz, W., Nordheim, A. & Hochholdinger, F. (2010). Regulation of the pericycle proteome in maize (*Zea mays* L.) primary roots by *RUM1* which is required for lateral root initiation. *Eur J Cell Biol* **89**, 236-241.

Liu, H. L., Osmani, A. H., Ukil, L., Son, S., Markossian, S., Shen, K. F., Govindaraghavan, M., Varadaraj, A., Hashmi, S. B., De Souza, C. P. & Osmani, S. A. (2010). Single-step affinity purification for fungal proteomics. *Eukaryot Cell* **9**, 831-833.

Liu, L. & Wiese, C. (2008). *Xenopus* NEDD1 is required for microtubule organization in *Xenopus* egg extracts. *J Cell Sci* **121**, 578-589.

LU, K. P. & MEANS, A. R. (1993). Regulation of the cell cycle by Calcium and Calmodulin. *Endocr Rev* **14**, 40-58.

Lüders, J., Patel, U. K. & Stearns, T. (2006). GCP-WD is a γ-tubulin targeting factor required for centrosomal and chromatin-mediated microtubule nucleation. *Nat Cell Biol* **8**, 137-147.

Lynch, E. M., Groocock, L. M., Borek, W. E. & Sawin K. E. (2014). Activation of the γ-tubulin complex by the Mto1/2 complex. *Curr Biol* **24**, 896-903.

MacDonald, M. L., Grubisha, M., Arion, D., Yates, N., Lewis, D. A. & Sweet, R. A. (2014). Laser capture microdissection-targeted mass spectrometry for cortical layer specific multiplexed protein quantification in postmortem human brain tissue. *Neuropsychopharmacology* **39**, S448-S449.

Mahoney, N. M., Goshima, G., Douglass, A. D. & Vale, R. D. (2006). Making microtubules and mitotic spindles in cells without functional centrosomes. *Curr Biol* **16**,

564-569.

Manck, R., Ishitsuka, Y., Herrero, S., Takeshita, N., Nienhaus, G. U., Fischer, R. (2015). Genetic evidence for a microtubule-capture mechanism during polarised growth of *Aspergillus nidulans*. *J Cell Sci* **128**, 3569-3582.

Mandel, M. & Higa, A. (1970). Calcium-dependent bacteriophage DNA infection. *J Mol Biol* **53**, 159-162.

Manning, J. A., Shalini, S., Risk, J. M., Day, C. L. & Kumar, S. (2010). A direct interaction with NEDD1 regulates γ-tubulin recruitment to the centrosome. .

Maresca, T. J., Groen, A. C., Gatlin, J. C., Ohi, R., Mitchison, T. J. & Salmon, E. D. (2009). Spindle assembly in the absence of a RanGTP gradient requires localized CPC activity. *Curr Biol* **19**, 1210-1215.

Martin, M. A., Osmani, S. A. & Oakley, B. R. (1997). The role of γ-tubulin in mitotic spindle formation and cell cycle progression in *Aspergillus nidulans*. *J Cell Sci* **110 (Pt 5)**, 623-633.

Martinelli, S. D. & Kinghorn, J. R. (1994). *Aspergillus*: 50 years on. Amsterdam: Elsevier.

Masuda, H., Mori, R., Yukawa, M. & Toda, T. (2013). Fission yeast MOZART1/Mzt1 is an essential γ-tubulin complex component required for complex recruitment to the microtubule organizing center, but not its assembly. *Mol Biol Cell* **24**, 2894-2906.

Mattern, I. E., Unkles, S., Kinghorn, J. R., Pouwels, P. H. & van den Hondel, C. AMJJ. (1987). Transformation of *Aspergillus oryzae* using the *A. niger pyrG* gene. *Mol Gen Genet* **210**, 460-461.

May, G. S., Gambino, J., Weatherbee, J. A. & Morris, N. R. (1985). Identification and functional analysis of β-tubulin genes by site specific integrative transformation in *Aspergillus nidulans*. *J Cell Biol* **101**, 712-719.

Mayorga, M. E. & Timberlake, W. E. (1990). Isolation and molecular characterization of the *Aspergillus nidulans wA* gene. *Genetics* **126**, 73-79.

Miller, P. M., Folkmann, A. W., Maia, A. R., Efimova, N., Efimov, A. & Kaverina, I. (2009). Golgi-derived CLASP-dependent microtubules control Golgi organization and polarized trafficking in motile cells. *Nat Cell Biol* **11**, 1069-1080.

Mishra, R. K., Chakraborty, P., Arnaoutov, A., Fontoura, B. M. & Dasso, M. (2010). The Nup107-160 complex and γ-TuRC regulate microtubule polymerization at kinetochores. *Nat Cell Biol* **12**, 164-169.

Moens, P. B. & Rapport, E. (1971). Spindles, spindle plaques, and meiosis in the yeast *Saccharomyces cerevisiae* (hansen). *J Cell Biol* **50**, 344-361.

Moritz, M., Braunfeld, M. B., Guénebaut, V., Heuser, J. & Agard, D. A. (2000). Structure of the γ-tubulin ring complex: A template for microtubule nucleation. *Nat Cell Biol* **2**, 365-370.

Moritz, M., Zheng, Y., Alberts, B. M. & Oegema, K. (1998). Recruitment of the γ-tubulin ring complex to *Drosophila* salt-stripped centrosome scaffolds. *J Cell Biol* **142**, 775-786.

Morris, N. R., Lai, M. H. & Oakley, C. E. (1979). Identification of a gene for α-tubulin in *Aspergillus nidulans*. *Cell* **16**, 437-442.

Morriswood, B., Havlicek, K., Demmel, L., Yavuz, S., Sealey-Cardona, M., Vidilaseris, K., Anrather, D., Kostan, J., Djinovic-Carugo, K., Roux, K. J. & Warren, G. (2013). Novel bilobe components in *Trypanosoma brucei* identified using proximity-dependent biotinylation. *Eukaryot Cell* **12**, 356-367.

Munoz-Centeno, M. C., McBratney, S., Monterrosa, A., Byers, B., Mann, C. & Winey, M. (1999). *Saccharomyces cerevisiae* MPS2 encodes a membrane protein localized at the spindle pole body and the nuclear envelope. *Mol Biol Cell* **10**, 2393-2406.

Murata, T., Sonobe, S., Baskin, T. I., Hyodo, S., Hasezawa, S., Nagata, T., Horio, T. & Hasebe, M. (2005). Microtubule-dependent microtubule nucleation based on recruitment of γ-tubulin in higher plants. *Nat Cell Biol* **7**, 961-968.

Murphy, S. M., Urbani, L. & Stearns, T. (1998). The mammalian γ-tubulin complex contains homologues of the yeast spindle pole body components Spc97p and Spc98p. *J Cell Biol* **141**, 663-674.

Murphy, S. M., Preble, A. M., Patel, U. K., O'Connell, K. L., Dias, D. P., Moritz, M., Agard, D., Stults, J. T. & Stearns, T. (2001). GCP5 and GCP6: Two new members of the human γ-tubulin complex. *Mol Biol Cell* **12**, 3340-3352.

Nakaoka, Y., Miki, T., Fujioka, R., Uehara, R., Tomioka, A., Obuse, C., Kubo, M., Hiwatashi, Y. & Goshima G. (2012). An inducible RNA interference system in *Physcomitrella patens* reveals a dominant role of augmin in phragmoplast microtubule generation. *Plant Cell* **24**, 1478-1493.

Nayak, T., Szewczyk, E., Oakley, C. E., Osmani, A., Ukil, L., Murray, S. L., Hynes, M. J., Osmani, S. A. & Oakley, B. R. (2006). A versatile and efficient gene-targeting system for *Aspergillus nidulans*. *Genetics* **172**, 1557-1566.

Nguyen, T., Vinh, D. B., Crawford, D. K. & Davis, T. N. (1998). A genetic analysis of interactions with Spc110p reveals distinct functions of Spc97p and Spc98p, components of the yeast γ-tubulin complex. *Mol Biol Cell* **9**, 2201-2216.

Nierman, W., May, G., Kim, H., Anderson, M., Chen, D. & Denning, D. (2005). What the *Aspergillus* genomes have told us. *Med Mycol* **43**, 3-5.

Nogales, E., Wolf, S. G., Downing & K. H. (1998). Structure of the αβ tubulin dimer by electron crystallography. *Nature* **391**, 199-203.

Nogales, E., Whittaker, M., Milligan, R. A. & Downing, K. H. (1999). High-resolution model of the microtubule. *Cell* **96**, 79-88.

Oakley, B. R. (1992). γ-Tubulin: The microtubule organizer? *Trends Cell Biol* **2**, 1-5.

Oakley, B. R., Oakley, C. E. & Rinehart, J. E. (1987). Conditionally lethal *tubA* α-tubulin mutations in *Aspergillus nidulans*. *Mol Gen Genet* **208**, 135-144.

Oakley, B. R., Oakley, C. E., Yoon, Y. & Jung, M. K. (1990). γ-Tubulin is a component of the spindle pole body that is essential for microtubule function in *Aspergillus nidulans*. *Cell* **61**, 1289-1301.

Oakley, C. E. & Oakley, B. R. (1989). Identification of γ-tubulin, a new member of the tubulin superfamily encoded by *mipA* gene of *Aspergillus nidulans*. *Nature* **338**, 662-664.

Oegema, K., Wiese, C., Martin, O. C., Milligan, R. A., Iwamatsu, A., Mitchison, T. J. & Zheng, Y. (1999). Characterization of two related Drosophila γ-tubulin complexes that differ in their ability to nucleate microtubules. *J Cell Biol* **144**, 721-733.

Ohkura, H., Garcia, M. A. & Toda, T. (2001). Dis1/TOG universal microtubule adaptors - one MAP for all? *J Cell Sci* **114**, 3805-3812.

Okada, N., Toda, T., Yamamoto, M. & Sato, M. (2014). CDK-dependent phosphorylation of Alp7-Alp14 (TACC-TOG) promotes its nuclear accumulation and spindle microtubule assembly. *Mol Biol Cell* **25**, 1969-1982.

Oriolo, A. S., Wald, F. A., Canessa, G. & Salas, P. J. (2007). GCP6 binds to intermediate filaments: A novel function of keratins in the organization of microtubules in

epithelial cells. *Mol Biol Cell* **18**, 781-794.

Osmani, S. A. & Mirabito, P. M. (2004). The early impact of genetics on our understanding of cell cycle regulation in *Aspergillus nidulans*. *Fungal Genet Biol* **41**, 401-410.

Osmani, A. H., Davies, J., Liu, H. L., Nile, A. & Osmani, S. A. (2006). Systematic deletion and mitotic localization of the nuclear pore complex proteins of *Aspergillus nidulans*. *Mol Biol Cell* **17**, 4946-4961.

O'Toole, E. T., Winey, M. & McIntosh, J. R. (1999). High-voltage electron tomography of spindle pole bodies and early mitotic spindles in the yeast *Saccharomyces cerevisiae*. *Mol Biol Cell* **10**, 2017-2031.

Pavelk, M. & Mironov, A. (2008). The Golgi apparatus: State of the art 110 years after camillo Golgi's discovery. 3-211.

Pereira, G., Grueneberg, U., Knop, M. & Schiebel, E. (1999). Interaction of the yeast γ-tubulin complex-binding protein Spc72p with Kar1p is essential for microtubule function during karyogamy. *EMBO J* **18**, 4180-4195.

Peterson, J. B., Gray, R. H. & Ris, H. (1972). Meiotic spindle plaques in *Saccharomyces cerevisiae*. *J Cell Biol* **53**, 837-841.

Petry, S. & Vale, R. D. (2015). Microtubule nucleation at the centrosome and beyond. *Nat Cell Biol* **17**, 1089-1093.

Petry, S., Groen, A. C., Ishihara, K., Mitchison, T. J. & Vale, R. D. (2013). Branching microtubule nucleation in *Xenopus* egg extracts mediated by augmin and TPX2. *Cell* **152**, 768-777.

Pinyol, R., Scrofani, J. & Vernos, I. (2013). The role of NEDD1 phosphorylation by aurora A in chromosomal microtubule nucleation and spindle function. *Curr Biol* **23**, 143-149.

Pontecorvo, G., Roper, J. A., Hemmons, L. M., Macdonald, K. D. & Bufton, A. W. (1953). The genetics of *Aspergillus nidulans*. *Adv Genet* **5**, 141-238.

Prigozhina, N. L., Oakley, C. E., Lewis, A. M., Nayak, T., Osmani, S. A. & Oakley, B. R. (2004). γ-tubulin plays an essential role in the coordination of mitotic events. *Mol Biol Cell* **15**, 1374-1386.

Pringle, J. R., Bi, E., Harkins, H. A., Zahner, J. E., De Virgilio, C., Chant, J., Corrado, K. & Fares, H. (1995). Establishment of cell polarity in yeast. *Cold Spring Harb Symp Quant Biol* **60**, 729-744.

Rasmussen, C., Lu, K., Means, R. & Means, A. (1992). Calmodulin and cell cycle control. *J Physiol Paris* **86**, 83-88.

Ravindran, A., Lao, Q. Z., Harry, J. B., Abrahimi, P., Kobrinsky, E. & Soldatov, N. M. (2008). Calmodulin-dependent gating of $Ca_v1.2$ Calcium channels in the absence of $Ca_v\beta$ subunits. *Proc Natl Acad Sci* **105**, 8154-8159.

Riquelme, M., Fischer, R. & Bartnicki-Garcia, S. (2003). Apical growth and mitosis are independent processes in *Aspergillus nidulans*. *Protoplasma* **222**, 211-215.

Rivero, S., Cardenas, J., Bornens, M. & Rios, R. M. (2009). Microtubule nucleation at the cis-side of the Golgi apparatus requires AKAP450 and GM130. *EMBO J* **28**, 1016-1028.

Robinow, C. F. & Marak, J. (1966). A fiber apparatus in the nucleus of the yeast cell. *J Cell Biol* **29**, 129-151.

Rose, M. D. & Fink, G. R. (1987). KAR1, a gene required for function of both intranuclear and extranuclear microtubules in yeast. *Cell* **48**, 1047-1060.

Roubin, R., Acquaviva, C., Chevrier, V., Sedjai, F., Zyss, D., Birnbaum, D. & Rosnet, O. (2013). Myomegalin is necessary for the formation of centrosomal and Golgi-derived microtubules. *Biol Open* **2**, 238-250.

Sambrook, J. & Russell David, W. (1989). Molecular cloning: a laboratory manual. Harbor, New York: Cold Spring Harbor Laboratory Press.

Samejima, I., Miller, V. J., Rincon, S. A. & Sawin, K. E. (2010). Fission yeast Mto1 regulates diversity of cytoplasmic microtubule organizing centers. *Curr Biol* **20**, 1959-1965.

Samejima, I., Miller, V. J., Groocock, L. M. & Sawin, K. E. (2008). Two distinct regions of Mto1 are required for normal microtubule nucleation and efficient association with the γ-tubulin complex in vivo. *J Cell Sci* **121**, 3971-3980.

Samejima, I., Lourenco, P. C., Snaith, H. A. & Sawin, K. E. (2005). Fission yeast mto2p regulates microtubule nucleation by the centrosomin-related protein mto1p. *Mol Biol Cell* **16**, 3040-3051.

Sato, M. & Toda, T. (2007). Alp7/TACC is a crucial target in ran-GTPase-dependent spindle formation in fission yeast. *Nature* **447**, 334-337.

Sawin, K. E. & Tran, P. (2006). Cytoplasmic microtubule organization in fission yeast. *Yeast* **23**, 1001-1014.

Sawin, K. E., Lourenco, P. C. & Snaith, H. A. (2004). Microtubule nucleation at non-spindle pole body microtubule-organizing centers requires fission yeast centrosomin-related protein mod20p. *Curr Biol* **14**, 763-775.

Schaerer, F., Morgan, G., Winey, M. & Philippsen, P. (2001). Cnm67p is a spacer protein of the *Saccharomyces cerevisiae* spindle pole body outer plaque. *Mol Biol Cell* **12**, 2519-2533.

Schoustra, S. E., Slakhorst, M., Debets, A. J. & Hoekstra, R. F. (2005). Comparing artificial and natural selection in rate of adaptation to genetic stress in *Aspergillus nidulans*. *J Evol Biol* **18**, 771-778.

Schramm, C., Elliott, S., Shevchenko, A. & Schiebel, E. (2000). The Bbp1p-Mps2p complex connects the SPB to the nuclear envelope and is essential for SPB duplication. *EMBO J* **19**, 421-433.

Sdelci, S., Schütz, M., Pinyol, R., Bertran, M. T., Regué, L., Caelles, C., Vernos, I. & Roig, J. (2012). Nek9 phosphorylation of NEDD1/GCP-WD contributes to Plk1 control of γ-tubulin recruitment to the mitotic centrosome. *Curr Biol* **22**, 1516-1523.

Seiler, S. & Justa-Schuch, D. (2010). Conserved components, but distinct mechanisms for the placement and assembly of the cell division machinery in unicellular and filamentous Ascomycetes. *Mol Microbiol* **78**, 1058-1076.

Seltzer, V., Janski, N., Canaday, J., Herzog, E., Erhardt, M., Evrard, J. & Schmit, A. (2007). *Arabidopsis* GCP2 and GCP3 are part of a soluble γ-tubulin complex and have nuclear envelope targeting domains. *The Plant Journal* **52**, 322-331.

Seybold, C., Elserafy, M., Ruthnick, D., Ozboyaci, M., Neuner, A., Flottmann, B., Heilemann, M., Wade, R. C. & Schiebel, E. (2015). Kar1 binding to Sfi1 C-terminal regions anchors the SPB bridge to the nuclear envelope. *J Cell Biol* **209**, 843-861.

Shaw, S. L., Kamyar, R. & Ehrhardt, D. W. (2003). Sustained microtubule treadmilling in *Arabidopsis* cortical arrays. *Science* **300**, 1715-1718.

Sheir-Neiss, G., Nardi, R., Gealt, M. & Morris, N. (1976). Tubulin-like protein from

Aspergillus nidulans. *Biochem Biophys Res Commun* **69**, 285-290.

Sheir-Neiss, G., Lai, M. H. & Morris, N. R. (1978). Identification of a gene for β-tubulin in *Aspergillus nidulans*. *Cell* **15**, 639-647.

Shen, K. F., Osmani, A. H., Govindaraghavan, M. & Osmani, S. A. (2014). Mitotic regulation of fungal cell-to-cell connectivity through septal pores involves the NIMA kinase. *Mol Biol Cell* **25**, 763-775.

Sievers, N., Krüger, M. & Fischer, R. (1997). Kreuzung von *Aspergillus nidulans*. *Biologie in Unserer Zeit* **27**, 383-388.

Snell, V. & Nurse, P. (1994). Genetic analysis of cell morphogenesis in fission yeast - a role for casein kinase II in the establishment of polarized growth. *EMBO J* **13**, 2066-2074.

Snyder, M. (1994). The spindle pole body of yeast. *Chromosoma* **103**, 369-380.

Soues, S. & Adams, I. R. (1998). SPC72: A spindle pole component required for spindle orientation in the yeast *Saccharomyces cerevisiae*. *J Cell Sci* **111 (Pt 18)**, 2809-2818.

Spang, A., Grein, K. & Schiebel, E. (1996). The spacer protein Spc110p targets Calmodulin to the central plaque of the yeast spindle pole body. *J Cell Sci* **109**, 2229-2237.

Spang, A., Courtney, I., Grein, K., Matzner, M. & Schiebel, E. (1995). The Cdc31p-binding protein Kar1p is a component of the half-bridge of the yeast spindle pole body. *J Cell Biol* **128**, 863-877.

Spang, A., Courtney, I., Fackler, U., Matzner, M. & Schiebel, E. (1993). The Calcium-binding protein cell division cycle 31 of *Saccharomyces cerevisiae* is a component of the half-bridge of the spindle pole body. *J Cell Biol* **123**, 405-416.

Stavru, F., Hulsmann, B. B., Spang, A., Hartmann, E., Cordes, V. C. & Gorlich, D. (2006). NDC1: A crucial membrane-integral nucleoporin of metazoan nuclear pore complexes. *J Cell Biol* **173**, 509-519.

Stirling, D. A., Welch, K. A. & Stark, M. J. (1994). Interaction with Calmodulin is required for the function of Spc110p, an essential component of the yeast spindle pole body. *EMBO J* **13**, 4329-4342.

Stringer, M. A., Dean, R. A., Sewall, T. C. & Timberlake, W. E. (1991). *Rodletless*, a new *Aspergillus* developmental mutant induced by directed gene inactivation. *Genes Dev*

5, 1161-1171.

Suelmann, R., Sievers, N., Galetzka, D., Robertson, L., Timberlake, W. E. & Fischer, R. (1998). Increased nuclear traffic chaos in hyphae of *Aspergillus nidulans*: Molecular characterization of *apsB* and *in vivo* observation of nuclear behaviour. *Mol Microbiol* **30**, 831-842.

Sui, H. & Downing, K. H. (2010). Structural basis of interprotofilament interaction and lateral deformation of microtubules. *Structure* **18**, 1022-1031.

Sundberg, H. A. & Davis, T. N. (1997). A mutational analysis identifies three functional regions of the spindle pole component Spc110p in *Saccharomyces cerevisiae*. *Mol Biol Cell* **8**, 2575-2590.

Sundberg, H. A., Goetsch, L., Byers, B. & Davis, T. N. (1996). Role of Calmodulin and Spc110p interaction in the proper assembly of spindle pole body compenents. *J Cell Biol* **133**, 111-124.

Swart, K. (1996). Mapping and breeding strategies. *Mycology Series* **13**, 235-246.

Szewczyk, E., Andrianopoulos, A., Davis, M. A. & Hynes, M. J. (2001). A single gene produces mitochondrial, cytoplasmic, and peroxisomal NADP-dependent isocitrate dehydrogenase in *Aspergillus nidulans*. *J Biol Chem* **276**, 37722-37729.

Tadross, M. R., Dick, I. E. & Yue, D. T. (2008). Mechanism of local and global Ca^{2+} sensing by Calmodulin in complex with a ca^{2+} channel. *Cell* **133**, 1228-1240.

Takahashi, M., Yamagiwa, A., Nishimura, T., Mukai, H. & Ono, Y. (2002). Centrosomal proteins CG-NAP and kendrin provide microtubule nucleation sites by anchoring gamma-tubulin ring complex. *Mol Biol Cell* **13**, 3235-3245.

Takahashi, M., Shibata, H., Shimakawa, M., Miyamoto, M., Mukai, H. & Ono, Y. (1999). Characterization of a novel giant scaffolding protein, CG-NAP, that anchors multiple signaling enzymes to centrosome and the Golgi apparatus. *J Biol Chem* **274**, 17267-17274.

Takeshita, N., Manck, R., Grün, N., de Vega, S. H. & Fischer, R. (2014). Interdependence of the actin and the microtubule cytoskeleton during fungal growth. *Curr Opin Microbiol* **20**, 34-41.

Takeshita, N., Higashitsuji, Y., Konzack, S. & Fischer, R. (2008). Apical sterol-rich membranes are essential for localizing cell end markers that determine growth

directionality in the filamentous fungus *Aspergillus nidulans*. *Mol Biol Cell* **19**, 339-351.

Tamura, K., Peterson, D., Peterson, N., Stecher, G., Nei, M. & Kumar, S. (2011). MEGA5: Molecular evolutionary genetics analysis using maximum likelihood, evolutionary distance, and maximum parsimony methods. *Mol Biol Evol* **28**, 2731-2739.

Tang, N. H., Takada, H., Hsu, K. S. & Toda, T. (2013). The internal loop of fission yeast Ndc80 binds Alp7/TACC-Alp14/TOG and ensures proper chromosome attachment. *Mol Biol Cell* **24**, 1122-1133.

Teichert, I., Wolff, G., Kück, U. & Nowrousian, M. (2012). Combining laser microdissection and RNA-seq to chart the transcriptional landscape of fungal development. *BMC Genomics* **13**, 511-2164-13-511.

Teixido-Travesa, N., Villen, J., Lacasa, C., Bertran, M. T., Archinti, M., Gygi, S. P., Caelles, C., Roig, J. & Luders, J. (2010). The γTuRC revisited: A comparative analysis of interphase and mitotic human γTuRC redefines the set of core components and identifies the novel subunit GCP8. *Mol Biol Cell* **21**, 3963-3972.

Tilney, L. G., Bryan, J., Bush, D. J., Fujiwara, K., Mooseker, M. S., Murphy, D. B. & Snyder, D. H. (1973). Microtubules: Evidence for 13 protofilaments. *J Cell Biol* **59**, 267-275.

Tomlin, G. C., Morrell, J. L. & Gould, K. L. (2002). The spindle pole body protein Cdc11p links Sid4p to the fission yeast septation initiation network. *Mol Biol Cell* **13**, 1203-1214.

Tulu, U. S., Fagerstrom, C., Ferenz, N. P. & Wadsworth, P. (2006). Molecular requirements for kinetochore-associated microtubule formation in mammalian cells. *Curr Biol* **16**, 536-541.

Uehara, R., Nozawa, R. S., Tomioka, A., Petry, S., Vale, R. D., Obuse, C. & Goshima, G. (2009). The augmin complex plays a critical role in spindle microtubule generation for mitotic progression and cytokinesis in human cells. *Proc Natl Acad Sci* **106**, 6998-7003.

Upshall, A., Gilbert, T., Saari, G., O'Hara, P., Weglenski, P., Berse, B., Miller, K. & Timberlake, W. (1986). Molecular analysis of the *argB* gene of *Aspergillus nidulans*. *Mol Gen Genet* **204**, 349-354.

Usui, T., Maekawa, H., Pereira, G. & Schiebel, E. (2003). The XMAP215 homologue Stu2 at yeast spindle pole bodies regulates microtubule dynamics and anchorage. *EMBO J* **22**, 4779-4793.

van Driel, K. G., Boekhout, T., Wösten, H. A., Verkleij, A. J. & Müller, W. H. (2007). Laser microdissection of fungal septa as visualised by scanning electron microscopy. *Fungal Genet Biol* **44**, 466-473.

Veith, D., Scherr, N., Efimov, V. P. & Fischer, R. (2005). Role of the spindle-pole-body protein ApsB and the cortex protein ApsA in microtubule organization and nuclear migration in *Aspergillus nidulans*. *J Cell Sci* **118**, 3705-3716.

Venkatram, S., Jennings, J. L., Link, A. & Gould, K. L. (2005). Mto2p, a novel fission yeast protein required for cytoplasmic microtubule organization and anchoring of the cytokinetic actin ring. *Mol Biol Cell* **16**, 3052-3063.

Venkatram, S., Tasto, J. J., Feoktistova, A., Jennings, J. L., Link, A. J. & Gould, K. L. (2004). Identification and characterization of two novel proteins affecting fission yeast γ-tubulin complex function. *Mol Biol Cell* **15**, 2287-2301.

Verollet, C., Colombie, N., Daubon, T., Bourbon, H. M., Wright, M. & Raynaud-Messina, B. (2006). *Drosophila melanogaster* γ-TuRC is dispensable for targeting γ-tubulin to the centrosome and microtubule nucleation. *J Cell Biol* **172**, 517-528.

Vinh, D. B., Kern, J. W., Hancock, W. O., Howard, J. & Davis, T. N. (2002). Reconstitution and characterization of budding yeast γ-tubulin complex. *Mol Biol Cell* **13**, 1144-1157.

Vogt, N., Koch, I., Schwarz, H., Schnorrer, F. & Nusslein-Volhard, C. (2006). The γTuRC components Grip75 and Grip128 have an essential microtubule-anchoring function in the *Drosophila* germline. *Development* **133**, 3963-3972.

Wanders, R. J. (2004). Metabolic and molecular basis of peroxisomal disorders: A review. *Am J Med Genet A* **126**, 355-375.

Wang, Z., Zhang, C. & Qi, R. Z. (2014). A newly identified myomegalin isoform functions in Golgi microtubule organization and ER-Golgi transport. *J Cell Sci* **127**, 4904-4917.

Wang, Z., Wu, T., Shi, L., Zhang, L., Zheng, W., Qu, J. Y., Niu, R. & Qi, R. Z. (2010). Conserved motif of CDK5RAP2 mediates its localization to centrosomes and the Golgi complex. *J Biol Chem* **285**, 22658-22665.

Wasteneys, G. O. & Ambrose, J. C. (2009). Spatial organization of plant cortical microtubules: Close encounters of the 2D kind. *Trends Cell Biol* **19**, 62-71.

Wasteneys, G. O. (2002). Microtubule organization in the green kingdom: Chaos or self-order? *J Cell Sci* **115**, 1345-1354.

Weatherbee, J. A., May, G. S., Gambino, J. & Morris, N. R. (1985). Involvement of a particular species of beta-tubulin (beta 3) in conidial development in *Aspergillus nidulans*. *J Cell Biol* **101**, 706-711.

West, R. R., Vaisberg, E. V., Ding, R., Nurse, P. & McIntosh, J. R. (1998). *cut11*$^{+}$: A gene required for cell cycle-dependent spindle pole body anchoring in the nuclear envelope and bipolar spindle formation in *Schizosaccharomyces pombe*. *Mol Biol Cell* **9**, 2839-2855.

Wiech, H., Geier, B. M., Paschke, T., Spang, A., Grein, K., Steinkotter, J., Melkonian, M. & Schiebel E. (1996). Characterization of green alga, yeast, and human centrins. specific subdomain features determine functional diversity. *J Biol Chem* **271**, 22453-22461.

Wiese, C. & Zheng, Y. (2000). A new function for the γ-tubulin ring complex as a microtubule minus-end cap. *Nat Cell Biol* **2**, 358-364.

Wigge, P. A., Jensen, O. N., Holmes, S., Soues, S., Mann, M. & Kilmartin, J. V. (1998). Analysis of the *Saccharomyces* spindle pole by matrix-assisted laser desorption/ionization (MALDI) mass spectrometry. *J Cell Biol* **141**, 967-977.

Wilson, E. B. (1925). Cell in development and heredity, 3rd. rev.

Winey, M., Hoyt, M. A., Chan, C., Goetsch, L., Botstein, D. & Byers, B. (1993). NDC1: A nuclear periphery component required for yeast spindle pole body duplication. *J Cell Biol* **122**, 743-751.

Xiang, X. & Plamann, M. (2003). Cytoskeleton and motor proteins in filamentous fungi. *Curr Opin Microbiol* **6**, 628-633.

Xiong, Y. & Oakley, B. R. (2009). In vivo analysis of the functions of γ-tubulin-complex proteins. *J Cell Sci* **122**, 4218-4227.

Yelton, M. M., Hamer, J. E. & Timberlake, W. E. (1984). Transformation of *Aspergillus nidulans* by using a *trpC* plasmid. *Proc Natl Acad Sci* **81**, 1470-1474.

Yoder, T. J., Pearson, C. G., Bloom, K. & Davis, T. N. (2003). The *Saccharomyces cerevisiae* spindle pole body is a dynamic structure. *Mol Biol Cell* **14**, 3494-3505.

Yokoyama, H., Koch, B., Walczak, R., Ciray-Duygu, F., González-Sánchez, J. C., Devos, D. P., Mattaj, I. W. & Gruss, O. J. (2014). The nucleoporin MEL-28 promotes RanGTP-dependent γ-tubulin recruitment and microtubule nucleation in mitotic spindle formation. *Nat Commun* **5**.

Zekert, N., Veith, D. & Fischer, R. (2010). Interaction of the *Aspergillus nidulans* microtubule-organizing center (MTOC) component ApsB with γ-tubulin and evidence for a role of a subclass of peroxisomes in the formation of septal MTOCs. *Eukaryot Cell* **9**, 795-805.

Zheng, Y., Wong, M. L., Alberts, B. & Mitchison T. (1995). Nucleation of microtubule assembly by a γ-tubulin-containing ring complex. *Nature* **378**, 578-583.

Zhu, X. & Kaverina, I. (2013). Golgi as an MTOC: Making microtubules for its own good. *Histochem Cell Biol* **140**, 361-367.

Zickler, D. & Olson, L. W. (1975). The synaptonemal complex and the spindle plaque during meiosis in yeast. *Chromosoma* **50**, 1-23.

Zimmerman, W. C., Sillibourne, J., Rosa, J. & Doxsey, S. J. (2004). Mitosis-specific anchoring of γ tubulin complexes by pericentrin controls spindle organization and mitotic entry. *Mol Biol Cell* **15**, 3642-3657.

VIII Appendix

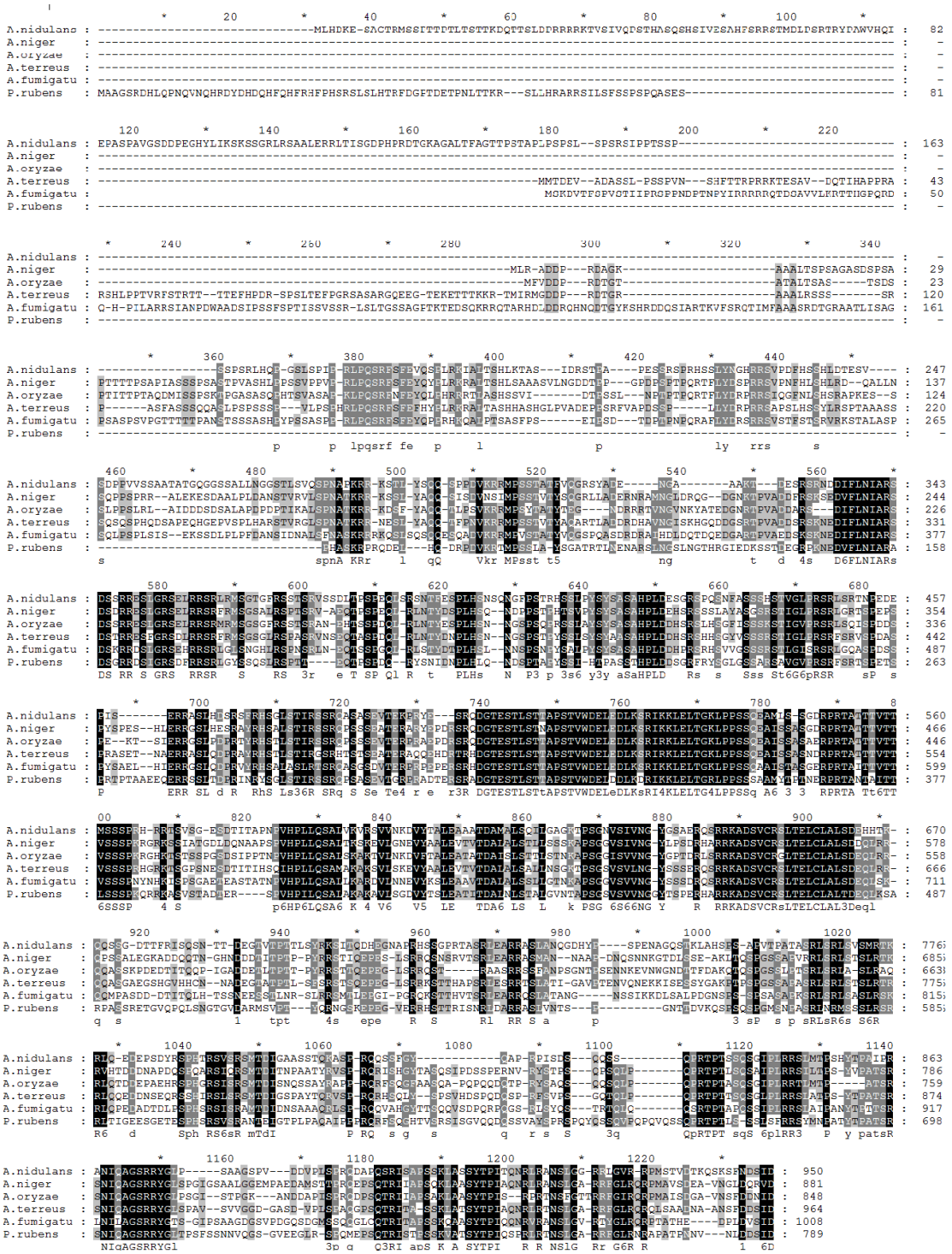

Figure S1. Sequence alignment of SPA18 homologs in different organisms. Proteins listed here are *A. nidulans* SPA18 (AN4545), *A. niger* EHA24150, *A. oryzae* EIT82140, *A. terreus* XP_001218235, *A. fumigates* KEY76871 and *P. rubens* XP_002562312. The alignment was done by GeneDoc.

Acknowledgement

First of all, I would like to thank Prof. Dr. Reinhard Fischer, for the chance he gave me to work in his group. He offered me many opportunities for conferences and working experiences in other labs. Because of that I have learned not only the knowledge, but also how to become a real scientist. His knowledge and enthusiasm in science gave me a deep impression, and I am sure they will encourage me in the rest of my research life. His patience and sense of humor make him such a nice person. I am so lucky to have a supervisor like him.

I also want to give my thanks to Prof. Dr. Jörg Kämper and Prof. Dr. Natalia Requena. They are always so kind and gave me very good suggestions in the seminar. Thanks to all my colleagues in IAB, especially to Dr. Andreas Herr, Dr. Claudia Kempf and Dr. Maren Hedtke, for their helps when I was new in the lab and in Germany. Dr. Norio Takeshita gave me many good suggestions for my work. Maren helped me with correcting the summary, as well as with the complicated procedures for submitting the thesis. Thank you so much Maren. I also want to thank my bachelor student Marjorie Schmid, my Chinese colleague Zhenzhong Yu, Dr. Saturnino Herrero de Vega and Nathalie Grün who also offered me many helps in the lab. It's so good to know you all.

Many thanks to Prof. Dr. Stephen Osmani from Ohio University, who provided me many strains I need, as well as very good advices. Prof. Dr. Ulrich Kück and Dr. Ines Teichert from Ruhr-Universität Bochum helped me with laser capture microdissection in their lab. I really enjoyed the time I spent in Bochum. And I also want to give my thanks to China Scholarship Council (CSC) who financially supported me in the first three years of my Ph.D..

Finally, I do want to thank my parents for their unconditional support and love to me. I want to thank my boyfriend Kai and my friends in Karlsruhe. We shared our life together in this beautiful city. It would be one of the best experiences in my life.